UNIVERSIDAD DEL PAÍS VASCO/EUSKAL HERRIKO UNIBERTSITATEA

Escuela de Ingeniería de Bilbao

Departamento de Ingeniería Química y del Medio Ambiente

Levulinic acid conversion to 2-methyltetrahydrofuran over Ni-Cu/Al_2O_3 catalysts

Dissertation summited to fulfil the final requirements to obtain the degree of

Ph.D. in Chemical Engineering

by:

Mr. Iker Obregón Bengoa

Thesis advisors:

Prof. Dr. Pedro L. Arias Ergueta

Dr. Iñaki Gandarias Goikoetxea

Bilbao, 2017

Agradecimientos

Durante los últimos cuatro años esta tesis ha ocupado buena parte de mi tiempo y, ahora que ha llegado la mejor parte, el final, es momento de echar la vista atrás y acordarme de la gente que, en mayor o menor medida, ha contribuido en esta fase de mi vida.

En primer lugar, expresar mi agradecimiento a mis directores Pedro e Iñaki por todo su trabajo y ayuda. Habéis sido unos guías inmejorables durante la tesis y por eso, por la beca que conseguí con vuestra ayuda, por lo mucho que he aprendido de y con vosotros y por los buenos momentos que hemos pasado estoy en deuda con vosotros.

No puedo olvidarme del apoyo de los compañeros del grupo de investigación SuPrEn que siempre se han mostrado dispuestos para echar una mano. Quisiera hacer énfasis en Marifeli; somos afortunados de tenerte con nosotros y no quiero ni pensar cómo nos arreglaríamos sin ti. Asimismo, merecen una especial mención los compañeros de fatigas más cercanos: Kepa, Sara, Iker, Naia, Jon y Aitziber; además del apoyo con los problemas me habéis aportado también la necesaria dosis de amistad y desconexión, muchas gracias.

Mi estancia de seis meses en la RWTH Aachen University fue una experiencia enriquecedora que no olvidaré. Mi gratitud a la Prof. Regina Palkovits por acogerme en su grupo de investigación y tratarme como a uno de los suyos. Igualmente agradecer la cálida acogida de los compañeros del grupo que amenizaron las jornadas de trabajo y con los que disfruté de comidas muy internacionales, helados preparados con nitrógeno líquido, partidas de Laser-Tag y más de una cerveza.

No podría dejarme en el tintero a Eriz, David, Christian y Nerea, que trabajaron conmigo durante sus respectivos proyectos de fin de carrera o máster y con quienes compartí los altibajos de la investigación. Todos me aportasteis vuestra alegría, trabajo y amistad y espero que yo os aportara algo de mí en justa correspondencia.

Como bien es sabido que *no sólo de ciencia vive el hombre*, no podía faltar en esta sección un agradecimiento expreso a mi cuadrilla del pueblo quienes, pese a haberlos

tenido desatendidos en ocasiones, estuvieron, están y estarán ahí para lo que haga falta, siempre dispuestos a pasar un buen rato.

Naturalmente, mi familia merece un agradecimiento mucho más que especial. Ama, aita y Adrián, es por vosotros que he llegado a ser quien soy. Vuestro apoyo y dedicación no conocen límites y así es también mi agradecimiento. No podría haber llegado hasta aquí sin vosotros y, por eso, mis logros son tan vuestros como míos.

Finalmente, Ainhoa, eres la razón de mi felicidad. Siempre te alegras con mis pequeñas victorias y me aguantas y consuelas cuando éstas se resisten. Me haces mejor y quiero ser mejor para ti y por eso, por lo vivido y lo que nos queda por delante, te quiero.

A mis padres, por su apoyo incondicional.

A Ainhoa, por hacerme feliz.

Table of contents

Resumen 3

Summary 8

Chapter 1. Introduction 13

Chapter 2. State of the art 39

Chapter 3. Objective and scope of the thesis 63

Chapter 4. Experimental 67

Chapter 5. Levulinic acid hydrogenolysis on Al_2O_3 supported Ni-Cu bimetallic catalysts 79

Chapter 6. One pot 2-methyltetrahydrofu-ran production from levulinic acid in green solvents over Ni-Cu/Al_2O_3 catalysts 95

Chapter 7. The role of the hydrogen source on the selective production of γ-valerolactone and 2-methyltetrahydrofuran from levulinic acid 113

Chapter 8. Structure-activity relationships of Ni-Cu/Al_2O_3 catalysts for γ-valerolactone conversion to 2-methyltetrahydrofuran 135

Chapter 9. Global conclusions and future work 163

List of acronyms 169

Appendix. Publications derived from the Ph.D. Thesis 171

Resumen

El actual modelo económico basado principalmente en recursos fósiles presenta serios problemas tanto en el corto plazo como para un futuro más lejano. Entre ellos cabe destacar el calentamiento global, la dependencia energética, las inestabilidades geopolíticas y el agotamiento de estos recursos. Para superar estos problemas las sociedades deben evolucionar hacia modelos energéticos basados en recursos renovables. En el caso de la generación eléctrica la solución parece residir en el aprovechamiento de fuentes renovables de energía como la eólica, la solar o las marinas. La transición hacia la sostenibilidad del sector del transporte, sin embargo, se espera que se lleve a cabo, en parte, sustituyendo los hidrocarburos de origen fósil por biocombustibles derivados de biomasa no comestible producida de forma sostenible.

El aprovechamiento de la biomasa, sin embargo, es un proceso complejo que suele consistir en la reducción de la funcionalización de sus moléculas originales para incrementar su densidad energética, su hidrofobicidad y su estabilidad. Por tanto, el éxito en el tránsito hacia un modelo económico basado en la biomasa está supeditado al desarrollo y la implementación industrial de nuevos y efectivos procesos catalíticos para su valorización hasta productos comercializables, en definitiva, al desarrollo de biorefinerías.

Esta tesis aborda uno de estos posibles procesos de biorefinería: la conversión del ácido levulínico (LA) en 2-metiltetrahidrofurano por medio de catalizadores heterogéneos basados en Ni-Cu/Al_2O_3. Esta conversión se considera muy interesante, dado que parte de uno de los 10 compuestos más importantes para los procesos de biorefinería, para producir un biocombustible de uso directo, ya que puede ser mezclado en proporciones de hasta el 70% en volumen con gasolina y ser utilizado en los motores actuales sin necesidad de modificaciones en éstos.

A pesar del interés de este proceso, la literatura científica al respecto es escasa. Se ha documentado la activación de esta reacción por catalizadores basados tanto en metales nobles como de transición en condiciones de reacción muy diversas: fase gas y medios líquidos, disolventes orgánicos y medios acuosos y en un amplio rango de temperaturas. No obstante, no existen estudios detallados sobre la influencia en la

actividad del disolvente, del tipo de metal y los posibles efectos de promoción en presencia de dopantes o de la acidez del catalizador.

Por ello, esta tesis se planteó con el propósito de aportar una comprensión más profunda de los factores que determinan el curso de las reacciones involucradas mediante el estudio del sistema catalítico Ni-Cu/Al_2O_3, de su actividad y de sus características estructurales y superficiales.

En primer lugar se estudió la actividad de este sistema en medio acuoso, hallándose que, mientras que la primera etapa de la reacción (hidrogenólisis del LA a GVL) se produce con altos rendimientos (> 90%), la posterior conversión de la GVL en PDO y MTHF se ve claramente inhibida por la reacción de deshidrogenación de la GVL a AL y la consecuente deposición de carbono sobre el catalizador.

Para resolver estas limitaciones se estudió el uso de bio-alcoholes como medio de reacción con un catalizador Ni/Al_2O_3. Los resultados en etanol fueron similares a los obtenidos en medio acuoso. Al usar 1-butanol como disolvente el rendimiento a MTHF aumentó hasta un 10% y, en 2-propanol, llegó al 46%. A la vista de estos resultados se ensayaron catalizadores con igual contenido metálico y distintos ratios Ni-Cu para la reacción, encontrando importantes efectos de promoción.

La actividad del Cu fue notablemente inferior a la del Ni, llegando sólo a un 23% de rendimiento a MTHF tras 5 h de reacción. La adición de pequeñas proporciones de Ni mejoró la actividad del catalizador, permitiendo llegar a rendimientos del 35%. Por otro lado, los catalizadores con altos contenidos de Ni (y bajos de Cu) llegaron a rendimientos del 46%. En este barrido se halló un máximo en el rendimiento a MTHF de 56% para la proporción Ni-Cu 2:1. Las especiales características de este catalizador proporcionan una alta actividad para la costosa conversión de la GVL sin que ello implique una alta actividad para la degradación del MTHF, como es el caso del catalizador Ni/Al_2O_3. La caracterización llevada a cabo mediante TPR y XRD apuntó a la formación de una fase mixta Ni-Cu como la responsable de las diferencia de actividad observadas.

Las diferencias de actividad relacionadas con el disolvente se asociaron a la mayor capacidad donadora de hidrógeno del 2-propanol. Para comprobarlo se llevaron a cabo una serie de ensayos tanto en atmósfera inerte (N_2) como reactiva (H_2) con tres

catalizadores (Ru(5%)/C, Ni(35%)/Al_2O_3 and Ni(23%)-Cu(12%)/Al_2O_3) con distintas actividades para reacciones de hidrogenación catalítica por transferencia (CTH) en tres disolventes (1,4-dioxano, 1-butanol y 2-propanol) con distintas capacidades para donar hidrógeno. Los resultados mostraron consistentemente mayores rendimientos a MTHF en disolventes con mayor capacidad donadora y en presencia de catalizadores más activos para el mecanismo CTH. Además, la comparación de los resultados en atmósfera inerte y reactiva evidenció la importancia del mecanismo CTH incluso en presencia de altas presiones de H_2 y la necesidad de la cooperación de ambas fuentes de hidrógeno para la conversión de la GVL.

Así mismo, en las condiciones de reacción empleadas se observaron importantes diferencias de actividad entre los tres catalizadores. El catalizador de Ru/C, debido a su baja acidez, mostró la esperable baja actividad para la CTH comparado con los más activos Ni/Al_2O_3 y Ni-Cu/Al_2O_3. En atmósfera de H_2 y en presencia de 2-propanol, un buen donador de hidrógeno, la actividad del Ru/C para la conversión de la GVL aumentó drásticamente hasta valores cercanos a los de los otros dos catalizadores. Sin embargo, y en contra de lo mostrado por los otros dos catalizadores, la selectividad de esta reacción se vio limitada tanto por la tendencia a formar subproductos a partir de la GVL como por la gran actividad para la degradación del MTHF. La alta actividad del catalizador Ni-Cu/Al_2O_3 junto con su selectividad a MTHF y la baja actividad para su degradación dieron como resultado el rendimiento más alto a MTHF documentado en disolventes “verdes” y usando catalizadores no-nobles (80%).

Adicionalmente se comprobó que el mecanismo de CTH, que comprende la hidrogenación-deshidrogenación del disolvente, no perjudica la velocidad de reacción de la GVL y, en atmósfera de H_2, esta reacción del disolvente alcanza rápidamente el equilibrio. Este hecho es interesante porque permitiría la recirculación directa del disolvente, tras la separación de los productos de reacción, al proceso sin necesidad de una hidrogenación (regeneración). La posibilidad de emplear alimentaciones más concentradas en LA se puso de manifiesto al obtener el mismo rendimiento con alimentaciones entre el 5 y el 30% en peso de LA, manteniendo la relación catalizador a LA.

Curiosamente, a pesar de las grandes diferencias en contenido metálico de los catalizadores, la muestra Ni-Cu/Al_2O_3 mostró la menor concentración de centros

metálicos, seguido por el Ru/C, siendo el Ni/Al_2O_3 el catalizador con mayor concentración de centros metálicos. Se estimó que los centros activos de Ru mostraron un rendimiento por centro y unidad de tiempo (STY) entre 1.4 y 2 veces superior a los centros de Ni, mientras que los centros activos del catalizador $Ni\text{-}Cu/Al_2O_3$ mostraron STY entre 2 y 4 veces mayores a los de Ni usando 2-propanol como disolvente y en atmósferas de N_2 y H_2. Una parte de los centros activos de este catalizador bimetálico se corresponden con una fase metálica mixta Ni-Cu que presentan una actividad muy superior a los derivados de fases monometálicas.

El último capítulo de esta tesis se centró en la elucidación del efecto de las características del catalizador sobre la actividad del paso limitante de la reacción, la conversión de la GVL en los precursores (PDO) del MTHF. Para ello se preparó por impregnación húmeda una serie de catalizadores con la proporción Ni-Cu optimizada (2:1) y distintos contenidos metálicos, y se caracterizó su actividad y sus propiedades. Los resultados destacaron la gran importancia de la fase mixta Ni-Cu, al mostrar mayor actividad los catalizadores con menor concentración de centros activos pero con mayores proporciones de esta fase.

La importancia de la acidez también quedó patente al mostrar similar actividad y STY catalizadores con menor acidez pero mayor concentración de centros metálicos y proporción de la fase Ni-Cu. Considerando, además, que sólo se detectaron trazas de PDO entre los productos de reacción se deduce que la acidez es suficiente para la deshidratación del PDO a MTHF y que éste no es el paso limitante de la reacción. De ello se concluye que la acidez también interviene en la conversión de la GVL y se especula que su mecanismo de reacción pueda comenzar con la adsorción de la GVL en un centro ácido y, debido a dicha interacción, la estabilidad de la molécula se ve reducida facilitando la adición del hidrógeno adsorbido sobre los centros metálicos adyacentes. Un experimento, en el que se añadió Al_2O_3 como co-catalizador ácido no mostró ninguna diferencia respecto al mismo experimento sin co-catalizador, confirmó la necesidad de que los centros activos (ácidos y metálicos) se encuentren próximos y que la actividad global resultante no depende tanto del número total de centros ácidos disponibles.

Usando un método de co-precipitación para la preparación de los catalizadores se obtuvo una mejora sustancial de la actividad de los mismos, debido al incremento de la

acidez y de la dispersión de las partículas metálicas con similares proporciones de la fase Ni-Cu. Sin embargo, la reutilización directa de los catalizadores más prometedores mostró una continua desactivación por depósitos carbonosos. Ésta pudo ser mitigada mediante regeneración térmica (calcinación y reducción) entre cada dos ensayos, obteniéndose rendimientos estables a MTHF del 36% con el mejor catalizador preparado por impregnación y del 54% para el mejor catalizador por co-precipitación tras tres usos.

Summary

The current oil based economy presents serious present and future challenges, such as global warming, energy dependency and geo-political and economical instabilities, along with their forecasted depletion. In order to overcome those problems, the energy sector needs to evolve from the non-renewable fossil fuel based model towards more sustainable feedstocks. While power supply is expected to be fulfilled by renewable resources, such as solar, wind or tide energy, the most straightforward alternative for the huge transportation sector lies on biofuels derived from sustainably produced non-edible biomass feedstocks.

Biomass utilization, however, is a challenging process. Biomass derived molecules are highly functionalized, therefore, their upgrading often involves the reduction of several functionalities in order to increase its energy density, make them more hydrophobic and more stable. The successful switch from the current oil based economy to a biomass based sustainable model requires, hence, the development and industrial implementation of new and effective catalytic processes for the upgrading of biomass feedstocks *i.e.* the development of biorefineries.

This thesis is focused on one of those biorefinery processes, the conversion of levulinic acid (LA) into 2-methyltetrahydrofuran (MTHF) using Ni-Cu/Al_2O_3 heterogeneous catalysts. This particular reaction is considered very interesting owing to the fact that LA is ranked amongst the “top 10” biomass derived building block molecules- MTHF is also reported to be a suitable gasoline additive that can be blended up to 70 vol% with conventional gasoline and used without any modifications on current internal combustion engines.

Despite the interest of this reaction, only a handful of references can be found in the scientific literature dealing with this topic. Both noble and transition metals were effective for this reaction under very different reaction conditions, *i.e.* vapor and liquid phases, aqueous and organic solvents and within a quite large temperature range. Nevertheless, there is no comprehensive research concerning the influence of the different solvents on the activity, the role of the metal and acid active sites or the explanation of the activity promotion observed when different metals or oxides are added to the catalyst formulation.

For that reason, the scope of the present thesis was the understanding of the different factors that determine the yield of this reaction. In order to do so, the Ni-Cu/Al_2O_3 catalyst system was selected, its activity thoroughly studied and its structural and surface properties characterized.

First, the activity of the selected catalyst system (Ni-Cu/Al_2O_3) for the reaction was tested on aqueous phase reaction. The first step of the reaction (LA hydrogenolysis to GVL) was found to be readily achievable under the applied reaction conditions; nevertheless, GVL hydrogenation to PDO and MTHF was limited by the reverse reaction (GVL dehydrogenation to AL) and the observed carbon deposition on the catalyst.

In order to overcome these issues, a solvent screening was conducted over a Ni/Al_2O_3 catalyst with alcohols which could be derived from biological processes. In ethanol the reaction showed similar results to those in water; interestingly using 1-butanol MTHF yields improved up to 10% and, in 2-propanol, they increased up to 46%. After this findings, different catalyst compositions, with equal total metal contents, were tested for the reaction in 2-propanol and important bimetallic promotion effects were found.

Cu was found to be significantly less active than Ni, showing only 23% MTHF yield after 5 h of reaction. The addition of low Ni amounts enhanced the activity achieving up to 35% MTHF. On the other hand, high Ni loadings facilitated up to 46% MTHF yields. In this screening an optimal Ni-Cu ratio (2:1) was found to achieve 56% MTHF yield. This catalyst, in addition to high activity for the challenging GVL conversion, showed significantly lower activity for MTHF degradation than the Ni/Al_2O_3 catalyst, affording greater selectivities. XRD and TPR characterization pointed to the formation and abundance of a mixed Ni-Cu phase as the cause of the observed catalyst activity differences.

The previously explained solvent related activity differences were attributed to the hydrogen donation capacity of 2-propanol. In order to prove it, a series of experiments was carried out using three catalysts (Ru(5%)/C, Ni(35%)/Al_2O_3 and Ni(23%)-Cu(12%)/Al_2O_3) with different activities towards catalytic transfer hydrogenation (CTH) and three solvents with different hydrogen donation potential under inert (N_2) and reacting (H_2) atmospheres. These results consistently showed higher MTHF yields

for better hydrogen donors and for catalysts with higher CTH activity. Furthermore, a comparison of the results under strict CTH conditions (N_2 atmosphere) and under H_2 atmosphere showed that the cooperation of both mechanisms is required for the conversion of GVL.

Under these reaction conditions vast activity differences were observed for the used catalysts. The Ru/C catalyst, as expected due to the low acidity of the support, showed very poor activity under CTH conditions compared to the Ni/Al_2O_3 and the $Ni-Cu/Al_2O_3$, which was the most CTH active catalyst. However, under H_2 atmosphere, and in the presence of a good hydrogen donor molecule (2-propanol), the activity of the Ru/C catalyst was sharply enhanced, matching the activity of the other two catalysts. Nevertheless, and opposite to the transition metal based catalysts, the Ru/C catalyst showed a low selectivity in the GVL to MTHF conversion in addition to high activity for MTHF degradation. Using the bimetallic catalyst the highest reported MTHF yield using transition metal heterogeneous catalysts and green solvents (80%) was achieved operating at 250 ºC and under 100 bar H_2. Besides, the solvent hydrogenation-dehydrogenation mechanism, which is part of the CTH mechanism and it is close to the chemical equilibrium conditions under H_2 atmosphere, showed not to interfere with the GVL conversion over the $Ni-Cu/Al_2O_3$ catalyst. This is interesting since no external solvent hydrogenation (regeneration) would be required for its recirculation to the reactor (after product separation). Furthermore, similar reaction rates were achieved using 5 to 30 wt% LA feeds keeping the catalyst – LA weight ratio constant, proving the applicability of the system to more concentrated solutions.

Interestingly, despite of the important metal load differences, the catalyst with the lowest amount of metal active sites was the $Ni-Cu/Al_2O_3$ catalyst, followed by the Ru/C and the Ni/Al_2O_3 showed the largest concentration of metal sites. Considering the explained activities and the metal sites concentration, the Ru sites allowed 1.4 – 2 times higher site time yields (STY) than the Ni sites and, the metal sites on the $Ni-Cu/Al_2O_3$ catalyst, facilitated 2 - 4 times higher STY than the Ni ones when 2-propanol was the solvent under N_2 and H_2 atmospheres. It is worth noting that part of the active sites on the bimetallic catalyst is associated with a Ni-Cu mixed phase which showed a significantly higher activity than the monometallic sites.

Finally, the origin of the catalysts activity differences was studied for the rate limiting step of the reaction (GVL to PDO). A series of impregnated catalysts with the optimized Ni-Cu ratio (2:1) and different total metal loadings were prepared, characterized and their activities tested. The results showed the great importance of the Ni-Cu phase on the catalyst activity; the catalysts with lower metal active site concentration achieved higher MTHF yields than the catalysts with low particle sizes (and higher metal sites concentration) due to the higher amounts of the Ni-Cu phase present on the large particle containing catalysts.

In addition, the acidity showed to play a determinant role on the reaction. The fact that catalysts with high Ni-Cu phase contents and the highest metal sites concentrations did not show higher STYs suggested that their lower acidities became the limiting factor. Besides, considering that only trace amounts of PDO were detected among the reaction products suggested that the acidity was sufficient for the PDO to MTHF dehydration and that this reaction was not the rate limiting step. Thus, it was pointed out that the acidity also played a role on the GVL conversion to PDO aside from its dehydration activity. In view of these evidences, it was suggested that GVL conversion might start with its adsorption over an acid site and, due to this interaction, the GVL molecule may loss some stability becoming easier the addition of hydrogen from the adjacent metal sites. The need for close proximity between the metal and acid sites was highlighted in an experiment where bare Al_2O_3 was added as a co-catalyst and the results were identical to those without the co-catalyst addition.

Improved activities and STYs were achieved by using a co-precipitation method, due to the metal dispersion improvement, with similar Ni-Cu proportions, and the higher acidity of the catalyst. However, carbon deposition on the catalyst surface led to a steady decrease of the activity upon direct recycling. This deactivation could be mitigated by catalyst regeneration (calcination and reduction) between runs, achieving stable 36% MTHF yields over the best impregnated catalyst and 54% MTHF yields over the best co-precipitated catalyst after 3 runs.

Chapter 1

Introduction

Table of contents

1.1. Abstract 17

1.2. The current and future energy systems 17

1.3. Fuels from biomass 21

1.3.1. Biofuels from edible biomass (first generation biofuels) 22

1.3.2. Biofuels from non-edible biomass (second generation biofuels) 24

1.4. The Biofine Process 27

1.5. The 5-chloromethylfurfural (CMF) process 28

1.6. Other processes for levulinic acid (LA) production 30

1.7. Levulinic acid (LA) 32

1.8. γ-Valerolactone (GVL) 34

1.9. 2-Methyltetrahydrofuran (MTHF) 35

1.10. References 37

1.1. Abstract

This chapter is devoted to provide a general overview of the present energetic sector, the challenges it is expected to face in the near future and, connected to them, explain the process selected for this thesis.

This thesis, as it belongs to the areas of green chemistry and sustainability, is oriented towards the improvement of the knowledge of biomass transformation processes for biofuel production. Such processes are widely considered by both the academia and industry to be necessary in order to reduce fossil resources consumption and decrease the environmental problems that come along with their use.

1.2. The current and future energy systems

Before fossil fuels were broadly available, the society relied on plant biomass to fulfill its energy requirements. The discovery and massive exploitation of fossil resources, coal and crude oil, led to the first and second industrial revolutions respectively, which rapidly enhanced the living standards, increased farming and industrial productivity and, hence, allowed a demographic explosion in the so-called developed countries[1]. Nowadays, fossil feedstocks (oil, natural gas and coal) account for 86% of the worlds energy consumption and crude oil still remains as the leading fuel covering 33% of the global energy demand[2]. This energy resource, however, possess some major drawbacks.

First of all, even if small quantities of petroleum are continuously generated[3], crude oil is a non-renewable source of energy and chemicals due to its overwhelming consumption rate. Furthermore, this rate is expected to rise by 30% in the next years, reaching a consumption rate of 111 million barrels per day in 2035[4]. The origin of crude oil is the anaerobic decomposition of organic matter (microorganisms, algae, *etc.*) under certain temperature and pressure conditions[3,5], a process that takes thousands of years to be accomplished. The total quantity of oil is, thus, limited and cannot be increased; leading to the oil depletion predicted by the geophysicist M. King Hubbert in 1956 for the United States (U.S.) oil production[6]. Hubbert´s analysis forecasts a peak

in the national oil production followed by a continuous decline to the total depletion of the reserves.

While this point is widely accepted, there is a great deal of controversy related to the depletion point. Whereas some forecast that oil will only last for some decades[6], the proved oil reserves have steadily grown in the last two decades[2], as it is depicted in Figure 1.1.

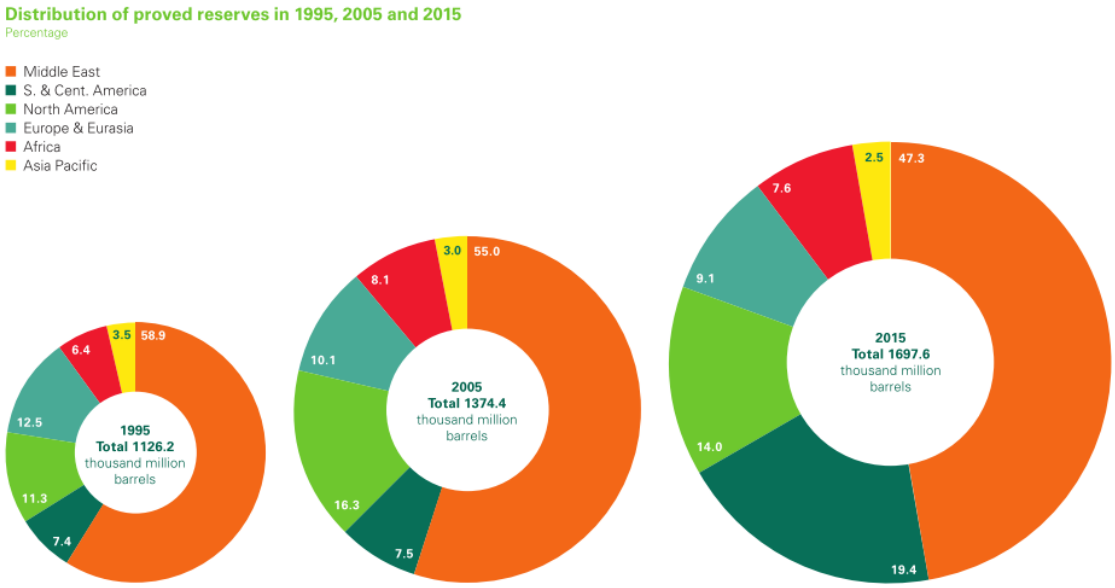

Figure 1.1. Proved oil reserves by region[2].

Another important issue related to conventional oil production is that very few countries have petroleum reserves[2]. For instance, Middle-East countries control 47% of world conventional oil reserves and 43% of those of natural gas, and only three countries (U.S., China and Russia) account for 57% of the world recoverable coal reserves[2,4]. This fact leads to a situation of massive energy dependence of the consumer countries on the producer ones which, most of them, suffer geopolitically unstable situations.

Clear examples of the mentioned instabilities are the Libyan war (2010, that lead to an outage in their exportations), the Syrian war (from 2011 and ongoing) or the decision of Saudi Arabia to increase oil production (2016) that drop the price of the Brent barrel from 110 $ in Jun 2015 to below 40 $ in January 2016.

The rise in the crude oil price stimulated the discovery and enhanced the recovery of conventional and non-conventional oil and gas sources such as tar sands, extra-heavy oil or oil shale[6]. Furthermore, new extraction and production technologies were developed for the production of liquid fuels, for instance, *gas-to-oil* and *coal-to-oil* processes or *fracking* (high-volume, slick-water hydraulic fracturing). All these new technologies present lower energy (and, hence, economic) balances (higher amounts of energy are required for the production/extraction of lower energy quantities), and that is the reason why they have not been fully developed and exploited until recent times[6,7]. The implementation of these techniques, however, is only profitable provided a high enough oil price. During the aforementioned time-lapse of record-high oil price these technologies flourish; as of this writing, however, with the oil price in the range of 50 $, the investments and projects stopped.

The increase in the use of the above mentioned techniques, together with the discovery of new oil reservoirs, are responsible for the increase in the proved oil reserves that can be observed in Figure 1.1. In addition to lower energy balances and production yields, there is a lack of information about the environmental impact of these techniques. For instance, the pollution of underground water reserves and the release of strong greenhouse gases such as methane, together with benzene and other hazardous compounds, have been reported in *fracking* areas[7].

Last but not least, there is clear scientific evidence that the accumulation of greenhouse gases, such as carbon dioxide (CO_2) or methane (CH_4), as a result of the fossil fuels combustion are perturbing the climate on Earth. The effect of the greenhouse gases build up is made evident by the continuous increase of the Earth's surface and sea temperature, the decrease in the snow and ice cover both in land and in the oceans, the rise in sea levels, the growth in the atmospheric moisture content, the variations in the precipitation pattern within the latitudes (increase in northern latitudes and decrease in subtropical areas) and the variations reported in wind and sea circulation patterns[8].

To overcome these important challenges, great efforts are being devoted to the research, development and exploitation of sustainable energy sources and vectors. An important part of the fossil fuel requirements (electricity and heating account for around 42% of global CO_2 emissions[9]) are expected to be replaced by means of electricity-producing renewable technologies such as solar, tides, waves or wind energy. Some of

these technologies, however, are not currently effective and their required development may take longer than forecasted[10]. Besides, a major drawback of these technologies is the instable energy production, related to the availability of the natural energy source (day and night for solar, calm days for wind energy, *etc.*). Moreover, the short term replacement of the petroleum-derived liquid fuels for the transportation sector by hydrogen cells or fully electrical vehicles is unlikely to become viable, technically and economically, on a massive scale within the next decade at least[11]. Additionally, the development and implementation of a supporting infrastructure for the distribution of those energy vectors is required, and it would take a long time to modify current market habits based on the widespread availability of hydrocarbon fuels[12].

In this regard, biomass-derived liquid fuels are unique in their similarity to the currently used fuels. As such, their implementation does not require extensive changes of the transportation infrastructure and the internal combustion engine. Thus, the use of biomass as a renewable source of carbon for the production of transportation fuels is a promising alternative that could be put into practice on short time scales. For instance, bioethanol and biodiesel are currently used as commercial blending agents for petroleum-derived gasoline and diesel fuels[12].

Biofuels have also the capacity to overcome most of the issues associated with fossil fuels. As plants grow on atmospheric CO_2, the use of biomass-derived fuels generates far lower impact on greenhouse gases build up. This impact could theoretically be close to neutral if efficient technologies and integrated processes are developed[1,13].

Provided that the feedstock for the production of those fuels, biomass, is a renewable source and more evenly distributed than oil, it has the potential to make each country less dependent, eventually energetically independent, from foreign suppliers. Recent researches by the U.S. Department of Agriculture and Oak Ridge National Laboratory estimated that the U.S. could sustainably produce $1.3\ x10^9$ metric tons of dry biomass per year using its agricultural (72% of total) and forest (28% of total) resources and still meet its food, animal feed, and export demands[14]. This amount of biomass contains $3.8\ x10^9$ barrels of oil equivalent (boe) energy, what is an important amount considering that the U.S. consumes $7\ x10^9$ barrels of oil per year. Calculations on the European Union's biomass production potential based on "surplus" land (food-first

paradigm) estimated a maximum of 27.7 $x10^{18}$ J/year by 2030[15]. Furthermore, several studies indicate that the use of liquid biofuels produced domestically would strengthen local economies by reducing the dependence on foreign oil or gas and by creating new well-paid jobs in different sectors such as agriculture and forest management[4,16].

Additionally, biomass is a more flexible feedstock than crude oil. The diversity of building block compounds from biomass offers a great opportunity for the production of a range of chemicals as wide as that available from non-renewable resources. Besides, with the progresses in genetic engineering, the tailoring of certain plants to produce high levels of specific chemicals is also possible[17]. Unlike the building blocks obtained from crude oil, biomass derived materials are often highly oxygenated. That is an advantage considering that many of the final products of the (petro-)chemical industry are oxygenated and that there are few general and efficient procedures to incorporate oxygen to hydrocarbons, and many of them require the use of toxic reagents (chromium, lead, *etc.*) resulting in severe waste disposal problems[17]. However, the high functionalization of biomass often needs to be reduced in order to produce molecules with higher energy density or easily usable building blocks[18–20].

Nevertheless, there are issues related to biofuels that must be carefully taken into account. For instance, greenhouse-gas neutrality must be carefully considered since detailed *life cycle assessments* of the production of certain products from biomass could show worse environmental impacts than those generated by petroleum derived ones[17,21]. Besides, biomass transformations into useful products, such as fine chemicals or transportation fuels, represent a serious challenge. The reason for that lies on the mentioned high functionality of biomass derived molecules and the lack of knowledge about the involved chemical processes as compared to those of the well-developed petrochemical industry[22,23].

In order to illustrate the complexity of biomass transformations, the next section provides an insight in the corresponding processes.

1.3. Fuels from biomass

In analogy with the common oil refineries, the *biorefinery* concept was postulated as an integrated factory where biomass feedstocks are sustainably processed into a

variety of marketable products and energy[24]. Similar to oil refining, the biorefinery is expected to be based on a handful of molecules (10 - 12) with a rich chemistry[20], which will allow the production of the final valuable products *i.e.* fuels, polymers, value-added chemicals, *etc*.

In order to better understand the upgrading strategies to be discussed, the basic composition of biomass will be described in the next paragraphs. Biomass is a complex mixture of several components among which edible, starches and triglycerides, and non-edible or lignocellulosic components can be distinguished.

1.3.1. Biofuels from edible biomass (first generation biofuels)

Starch is a biopolymer, composed of a mixture of two polysaccharides, amylose and amylopectin, and it is produced by green plants for energy storage over long periods[25]. Amylose consists on repeating maltose units, which are α-(1→4) linked disaccharides of D-glucopyranose units. This bonding, named glycosidic, presents an axial geometry which limits the strength and abundance of intermolecular hydrogen bonds, thus, facilitating hydrolysis processes[11,26].

Amylopectin, which is the mayor constituent of most starches, also contains glucose units linked via α-(1→4) bonds; however, there are also α-(1→6) branches that occur in plants every 24 – 30 glucose units (see Figure 1.2), about 5% of the bonds[11,25]. These branches prevent the polymer from coiling into a helix so that no compact intermolecular alignment occurs and, hence, preventing the appearance of significant hydrogen bonding. The weak nature of the starchy linkages makes their hydrolysis efficient using inexpensive enzymes, and under moderate reaction conditions[11].

Bioethanol production from starchy biomass is achieved by fermentation of the sugars that make up the starch. However, and attending to the nature of the biomass and the selected microorganisms, several reaction set-ups can be used. While *separate hydrolysis and fermentation* approach allows for optimal reaction conditions in each step of the reaction[11,27], process integration resulted in *simultaneous saccharification and fermentation* processes. In these processes the compatibility of reaction parameters (*e.g.* pH and temperature) is of capital importance but, it allows for greater lignocellulosic biomass hydrolysis rate due to the limited end product inhibition[27]. Further improvements of this method are provided by genetically engineered

microorganisms, which allow for *simultaneous saccharification and co-fermentation* of hexoses and pentoses to produce higher ethanol yields[27].

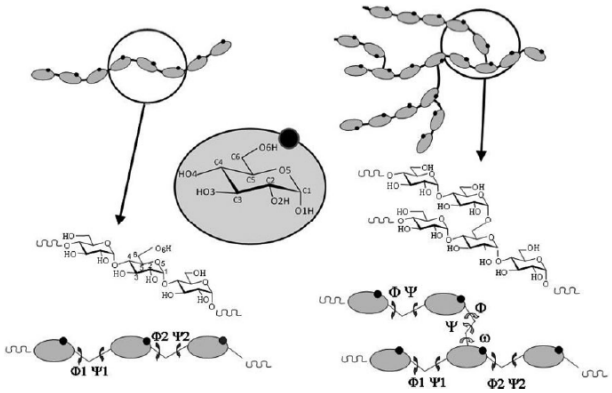

Figure 1.2. Molecular structures of amylose and amylopectin[25].

Triglycerides, which can be derived from both plant and animal sources, are composed of fatty acids linked to a glycerol unit. They can be converted into biodiesel by means of transesterification reactions with alcohols such as methanol or ethanol[12,13]. In this process, for every 10 kg of biodiesel 1 kg of glycerol is produced, building up an important surplus of this chemical with interesting valorization routes[28].

An alternative use of vegetable oils for biofuel production is their hydroprocessing in existing petroleum refinery infrastructures, alone or mixed with heavy gas-oil[1,29]. This process is typically run at 350 – 450 ºC under 40 to 150 bar pressure and 0.5 to 5.0 h^{-1} *Weight Hour Space Velocity* (WHSV) using sulfided Ni-Mo/Al_2O_3 catalysts for alkane production and zeolite or molecular sieve catalysts for isomerization[1].

Oil hydrotreating presents several advantages over esterification[30] *e.g. i)* lower processing costs (50% of esterification) *ii)* feedstock flexibility *iii)* compatibility with current infrastructure and existing internal combustion engines. Furthermore, a 10 month on-road test with postal delivery vans showed a greatly improved fuel economy using a blend of petroleum derived diesel with hydrotreated vegetable oil products[1].

The aforementioned materials are the so-called *First Generation Biofules*. They were the first produced biofuels because the required transformation processes are

comparatively easy. For instance, bioethanol production is achieved by biological fermentation of sugars obtained *via* hydrolysis of starches[11,12].

Despite showing chemical and processing advantages, the first generation biofuels present several mayor drawbacks. Starches, sucrose and triglycerides are present only in minor proportions, even in first generation feedstock plants[11–13]; thus, their cost can be high particularly in Europe[1]. In addition their net energy balance is low[11]. Furthermore, the utilization of high-quality arable land for their production resulted in a clear competition between fuel and food-requirements (the fuel-versus-food issue).

Nevertheless, nowadays the biofuel market is monopolized by the first generation biofuels. Its current production is about 75 million tons of oil equivalent (toe) in 2015 and it is expected to grow up to 5.9 million barrel per day (294 million toe) by 2030, reaching 6.3% of the conventional oil production[2,4]. The greatest biofuels producer countries in 2015 were the U.S. (41% of the total) and Brazil (24%). Spain shared a 1.3% of the global biofuel production with 1 million toe in 2015, which amounted for a 1.7% increase from 2014 figures[2].

1.3.2. Biofuels from non-edible biomass (second generation biofuels)

The economical and ethical disadvantages of the currently used biofuels lead to further research on fuel production from the non-edible lignocellulosic fraction of biomass, which is the most abundant and inexpensive. Lignocellulosic material is always present in plants because it is the component that contributes to their structural integrity[12]. Furthermore, cellulosic feedstocks are usually more productive and require less energy to be processed than starch does[31]. This non-edible biomass fraction is made of three main components: cellulose, hemicelluloses and lignin, as it is illustrated in Figure 1.3.

Lignin usually represents 15 to 20% of the biomass weight[1,26]. It is an amorphous polymer composed of methoxylated phenylpropane structures which provide plants with structural rigidity and a hydrophobic vascular system for the transportation of water and solutes[12,19,32]. Lignin surrounds the hemicellulose and cellulose fractions and, although it can be isolated, nowadays it is not readily amenable to upgrading strategies even if some promising technologies are being developed for its conversion into biofuels and biochemicals[33].

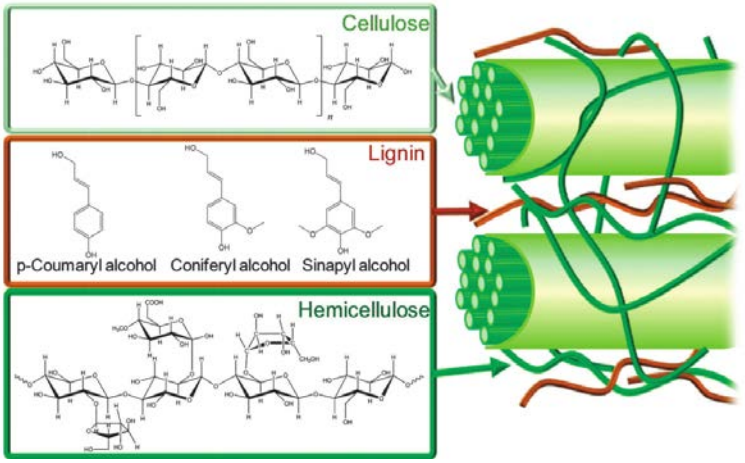

Figure 1.3. Components of the lingo-cellulosic biomass[19].

As such, one option for lignin utilization is to burn it directly for heat and electricity production[34,35]. This valorization path takes advantage of the fact that the char obtained from biomass treating processes (such as the *Biofine* process described in the next section) may have significantly higher heating value than the original feedstock (25.6 *vs.* 18.6 MJ/kg for the Biofine process treating paper sludge residues)[31]. A report on the Biofine commercial scale plant in Caserta, Italy, estimates that thermal valorization of the lignin and residual solids from the process exceeds the energy requirements to run the process provided a production scale greater than 270 metric tons of dry biomass per day[31].

Additionally, lignin residues can be submitted to pyrolysis or gasification processes for its upgrading. Fast pyrolysis processes lead to high bio-oil yields, a product that can be further upgraded to biodiesel or reformed to produce hydrogen[11]. When low temperatures (300 - 550 ºC) are used high yields of biochar can be obtained. On the contrary, when harsher conditions are used (> 700 ºC) the main product is a gas mixture of H_2, CH_4, CO_2 and CO with potential uses as syngas (after a purification step) or further treated via *Water-Gas-Shift* reaction to produce more H_2 from CO and steam[11,31].

Cellulose is the most abundant polymer in the world with estimated $3.24\ x10^{11}$ m^3 available globally and an annual production of 10^{11} tones[11,17,26]. This component, which represents between 40 and 50% of the biomass weight, is a high molecular weight polymer of glucose units connected linearly via β-(1→4) glycoside bonds (see Figure 1.3)[4]. This arrangement allows strong hydrogen bonding among cellulosic

chains, conferring the material with rigid crystallinity and, hence, high resistance to deconstruction. As a result of all these characteristics cellulose is about 100 times more difficult to hydrolyze than starch[11]. This fact is the responsible for more expensive products; for example, the cost of cellulosic ethanol is approximately double of that of corn ethanol due to the complexity of the isolation of sugars from lignocellulosic biomass[36].

Cellulose strands are interlaced by hemicellulose, which is an amorphous and branched (see Figure 1.3) – thus more readily hydrolysable – polymer. Hemicellulose is composed of five different C5 and C6 sugars, said D-xylose with smaller amounts of the L-arabinose pentose and D-glucose, D-mannose and D-galactose hexoses[4,11].

The key to upgrade lignocellulosic feedstocks lies on the depolymerization of their matrixes in order to obtain readily useful molecules, or molecules that can be converted into platform chemicals and biofuels[11]. Pretreatments such as milling and other physical/chemical treatments serve to permeate lignin and extract hemicelluloses, which are not extractable by hot water or chelating agents but, unlike cellulose, are extractable in aqueous alkali[11]. That way the subsequent hydrolysis steps to isolate the glucose monomers of cellulose are more effective[12].

Cellulose, owing to its rigid crystallinity, is largely inaccessible to hydrolysis in untreated biomass. Once isolated, its hydrolysis for glucose production is considered more difficult than the analogous production of xylose from hemicellulose. High glucose yields (> 90% of theoretical maximum) can be achieved *via* enzymatic hydrolysis of cellulose[12,31]. Chemical hydrolysis of cellulose can also be carried out, but harsher reaction conditions, higher temperature and mineral acid media (H_2SO_4) are required. Nevertheless, these reaction conditions promote the formation of sugar dehydration products such as hydroxymethylfurfural (HMF), levulinic acid (LA), and insoluble humins[12,37].

The following sections describe raw biomass hydrolysis methods for the production of the aforementioned platform chemicals (HMF and LA). Those processes were selected according to the industrial applicability, high yields and simplicity.

1.4. The Biofine Process

The Biofine process[38,39] is a near commercial biorefining technology that does not require any biotic activity for the conversion of biomass to the final product. Instead, it uses diluted H_2SO_4 in a two-reactor system optimized to obtain high yields of the building block chemicals LA and furfural from the degradation of the hexoses and pentoses isolated from the lignocellulosic biomass[11].

The advantage of this technology over previous ones is that the yields are 70 – 80% of the theoretical maximum (71.6% by mass of cellulose)[38,39]. This translates to the conversion of approximately 50% of C6 sugars mass to LA, with a 20% being converted to formic acid (FA) and 30% being incorporated to the residual char material which also contains all of the *Klason* lignin and a 50% mass fraction of the C5 sugars that do not convert to furfural[11,38,39].

The Biofine yield data result from trials at two pilot plants: in a 1 ton per day facility in the U.S. (South Glens Falls, NY) various feedstocks, including agricultural residues, paper sludge, and the organic fraction of municipal waste, have been processed; in a 50 metric ton per day commercial facility in Caserta, Italy, waste paper, municipal wastes and agricultural residues have been processed[11,31].

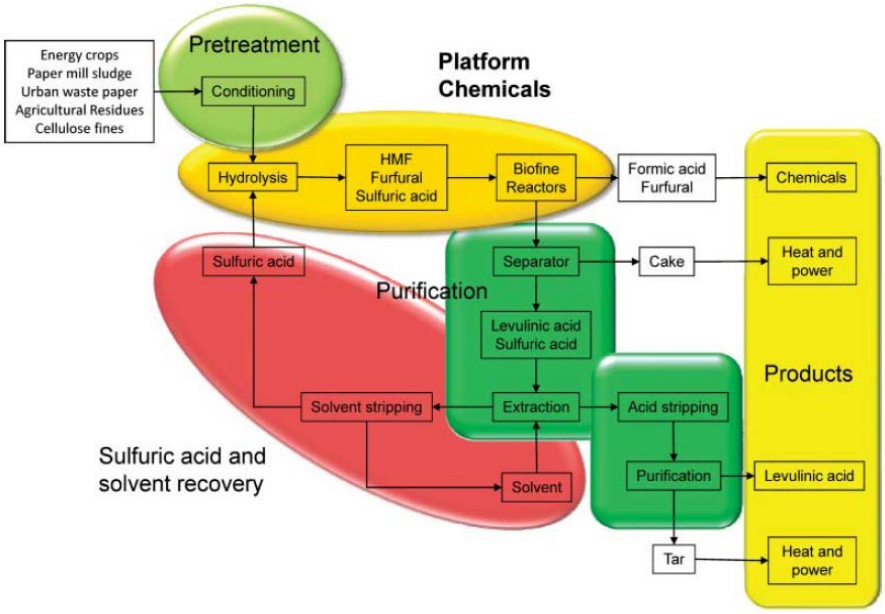

Figure 1.4. Scheme of the Biofine process[12].

The Biofine process is schematically represented in Figure 1.4. The biomass feedstocks, with particle sizes between 0.5 and 1 cm, are fed to a reactor operating at 210 to 230 °C under 25 bar pressure where carbohydrates are hydrolyzed for 13 to 25 s in the presence of 1 to 5 wt% aqueous solutions of a mineral acid, usually H_2SO_4. This initial hydrolysis produces HMF, which is continuously removed and fed to a second reactor. There, the HMF is further hydrolyzed for 15 to 30 min at 195 to 215 °C and under 14 bar pressure to produce LA and FA. Furfural and other volatile products tend to be removed at this stage while the tarry mixture of LA and residues are fed to a gravity separator.

From there, the insoluble mixture goes to a dehydration unit where water and other volatiles are boiled off. The crude LA obtained is 75% pure, and can be further purified up to 98%. H_2SO_4 is recovered in the final recycle stage, allowing it to be reused in the process. The LA yield of this process is 60%, based on the hexose content of the starting material, one of the highest reported in the literature[12,31,40].

Economic projections indicate that an optimized Biofine process could produce LA at 0.06 to 0.18 €/kg depending on the scale of the operation, increasing, thus, the interest and applicability of this chemical for the production of liquid fuels and fine chemicals. Furthermore, the impact on waste reduction and domestic energy use would also be remarkable[12,40,41].

1.5. The 5-chloromethylfurfural (CMF) process

Recently, a new efficient approach to the production of fuels and value added chemicals from biomass has been reported by Mascal and co-workers. Their work opens a new route for the hydrolysis of sugars, starches, cellulose and even raw biomass under mild conditions with outstanding yields.

This new approach is based on biomass hydrolysis using concentrated hydrochloric acid (HCl) in a biphasic reactor to produce a new platform chemical: 5-(chloromethyl) furfural (CMF). The experimental setup is as simple as an open continuous stirred tank reactor fed with a mixture of water, biomass, HCl, a chloride donor and an organic solvent. The first experiments were carried out using a chloride donor (LiCl) and 1,2-dichloro ethylene as the solvent, which is denser than water, in

order to extract the reaction products from the bottom of the reactor. These experiments require about 30 h to reach high conversions, less time than the fermentation but still a slow reaction. The process, however, achieved 85 to 91% carbon based yields and 70% yields to the desired product CMF together with small amounts of other chemicals (LA, HMF, *etc.*)[42].

Later developments provided an impressive improvement on the process by using a closed reactor operated under pressure. These modifications avoid the loss of HCl in the reaction system and allow higher reaction temperatures (above 100 ºC) and, therefore, reaching 80% CMF yields in just 3 h of reaction. The new setting did not require the addition of any special chloride donor and has been reported to obtain high yield for saccharide concentrations up to 10%(w/v)[43]. Besides, these new operation conditions proved to effectively hydrolyze chitin (1,4-β linked *N*-acethyl-2-amino-2-deoxy-D-glucan), the second most abundant biopolymer in nature of which the exoskeletons of crustaceans and insects are made. This material possess high crystallinity and is, hence, very insoluble and resistant to hydrolysis. The results showed 45% yield of CMF and 29% yield of LA, very interesting results considering the nature of the feed material[43].

Additionally, this process has been applied to the production of a hybrid lipidic/cellulosic biodiesel via hydrolysis of oil seed feedstocks. At 80 ºC the cellulosic matrix is fully dissolved and converted to CMF in high yields while leaving the fatty acids intact. An additional step, heating the mixture of CMF and triglycerides in ethanol, renders ethyl levulinates and ethyl esters, gaining an extra 24% of biofuel precursors if compared to the common, base catalyzed, transesterification of triglycerides[44].

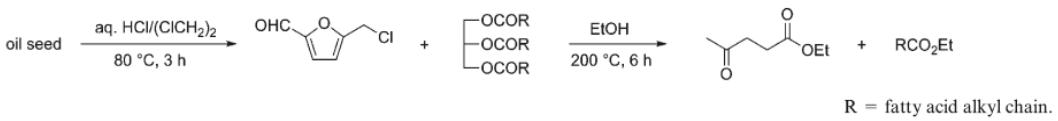

Figure 1.5. Production of hybrid lipidic/cellulosic biodiesel[44].

Further research of this group focused on finding applications for the CMF as a platform chemical. They have recently demonstrated the suitability of this compound to be converted into a biodegradable herbicide (δ-amino levulinic acid)[45] and the antiulcer drug *Zantc* (ranitidine)[46] in high yields (over 50% overall yield) and from a

renewable source of chemicals. They also studied the conversion of CMF to other building block molecules, such as HMF or LA, by heating the compound in water at 100 ºC (for 30 s) and 190 ºC (for 20 s) respectively, obtaining HMF yields up to 86% and LA yields up to 91%. Considering the overall process, depending on the saccharide source employed the process enables LA yields as high as 78% (from glucose), 87% (from sucrose), 81% (from cellulose or corn stover)[47].

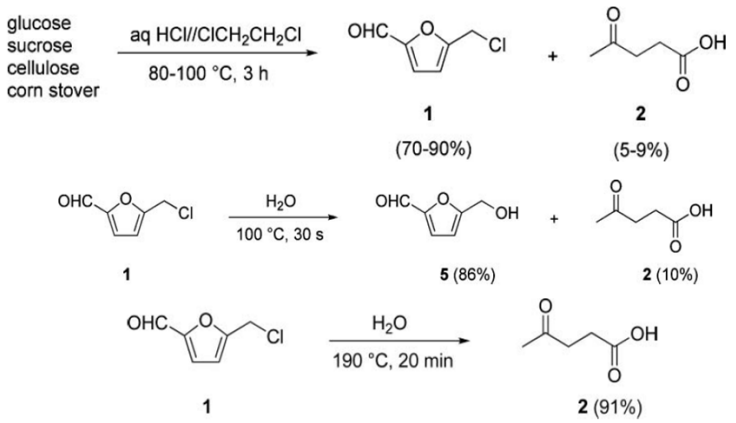

Figure 1.6. Conversion of biomass to CMF, HMF and LA. Adapted from[47].

This process shows higher yields than the Biofine process (overall 80% versus 60%)[31,47], requires milder conditions and it is more flexible since it can be optimized to produce a range of useful chemicals. On the other hand, it has been very recently developed so there is no experience in industrial scale approaching operation. Contrary to the Biofine process, it is focused only on the C6 fraction, leaving all the C5 sugars from hemicellulose unused. Finally, HCl is more expensive than H_2SO_4 and it tends to evaporate, generating an environmental problem if not carefully handled and recycled[48].

1.6. Other processes for levulinic acid (LA) production

Other examples of biomass utilization for LA production can also be found in the scientific literature. Here a brief summary is presented.

Shen and co-workers proposed a hydrochloric acid mediated cellulose decomposition to LA and FA[49]. After a thorough kinetic analysis, operation variables were optimized for a batch system resulting in 60% LA yields (from the theoretical

maximum) using 0.1 mol/L cellulose solutions in 0.93 mol/L HCl medium at 180 – 200 ºC.

The group of Dumesic proposed, in addition to the cellulose deconstruction process, two viable LA extraction procedures. The cellulose processing approach consisted on the use of 0.5 mol/L H_2SO_4 at 150 ºC. Cellulose (1:2.3 weight ratio referred to the acid solution) was added to the solution in five steps (1/5 of the weight at a time) with 6 h intervals[36]. This procedure allowed a 57% LA yield (from the theoretical maximum) and a 20 wt% LA content in the batch reactor after the five cycles[36]. Regarding LA (and FA) separation for upgrading, and in order to recycle the acid solution, liquid-liquid extractions were proposed considering the high boiling point of LA (245 ºC) and the typically low concentrations achieved during its industrial production[50].

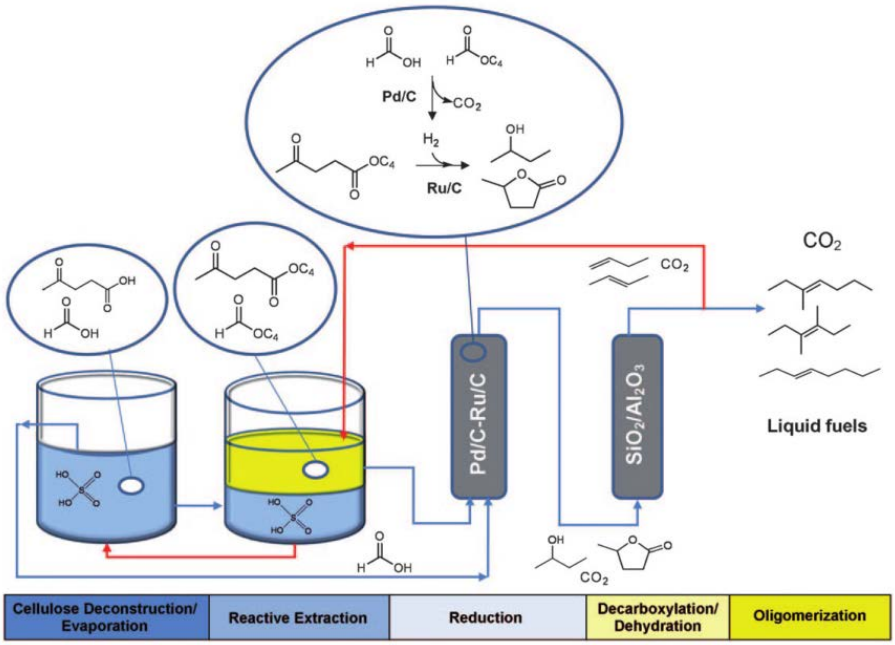

Figure 1.7. Process integration for LA extraction through hydrophobic LA esters production[51].

Alkylphenol solvents were found to selectively extract LA and FA from the H_2SO_4 solution, at temperatures near the hydrolysis reaction temperature, and to be stable to downstream LA upgrading processes, which also allows for solvent recycling[50]. The extraction technique was further improved into an integrated process by using butene (which is produced from LA derivatives conversion) to produce hydrophobic levulinic acid esters which spontaneously separate from the aqueous

phase[51]. This system, showed in Figure 1.7, reduced the need for an external solvent and allows for the recycle of the aqueous solution.

Huber and co-workers reported LA production from biomass in the absence of a homogeneous acid catalyst. This approach required an initial cellulose non-catalytic hydrothermal treatment at 220 ºC for 30 min in order to produce water soluble molecules such as glucose or HMF. In a second step, those molecules are hydrolyzed to LA over a solid acid catalyst at 260 ºC for 8 h[52]. This procedure allowed up to 28% yield of LA (from the theoretical maximum).

Table 1.1. Summary of the main processes for LA production from biomass. All figures are given in kg.

Process	Input	Output	Yield
Biofine	100 Cellulose 5455 H_2O 191 H_2SO_4	54 LA + 22 FA 5455 H_2O[a] 191 H_2SO_4[a] 24 Humins	76% of theoretical maximum
Mascal	100 Cellulose 2157 H_2O 11004 HCl 24806 CH_2Cl_2	58 LA + 23 FA 2157 H_2O[a] 11004 HCl[a] 24806 CH_2Cl_2 19 Humins	81% of theoretical maximum
Sheen & Wyman	100 Cellulose 6198 H_2O 209 HCl (230 NaOH)[b]	43 LA + 17 FA 6301 H_2O 40 Humins (336 NaCl)[b]	60% of theoretical maximum
Dumesic	100 Cellulose 380 H_2O 19 H_2SO_4 400 Solvent[d]	10 (+29)[c] LA 14 (+2)[c] FA 380 H_2O 400 Solvent[d] 45 Humins	55% of theoretical maximum
Huber	100 Cellulose 482 H_2O	20 LA + 10 FA 400 H_2O 7 Others 15 Humins	28% of theoretical maximum

[a] Acid streams for recycling. [b] Neutralization materials. [c] In the organic phase. [d] 2-sec-butylphenol.

The above explained processes for producing LA at low cost, together with its high functionality and reactivity[11,41,53,54], have focused the researchers´ attention on this interesting building block molecule. In the next section a detailed description of LA chemistry and applications is provided to further illustrate its importance.

1.7. Levulinic acid (LA)

LA is a useful platform chemical whose value comes from its particular chemical structure: its two highly reactive functional groups, a carboxylic acid (pK_a 4.5)[54] and a ketone, allow a great number of reactions[11]. This fact, together with its suitable,

sustainable and economical production methods made the U.S. Department of Energy consider this chemical as one of the "Top 10" building blocks for biorefinery processes[23,41].

As depicted in Figure 1.8, LA is the starting point for a number of chemicals from fields as diverse as solvents and fuels, polymers and plasticizers, food additives, pharmaceuticals, *etc.*

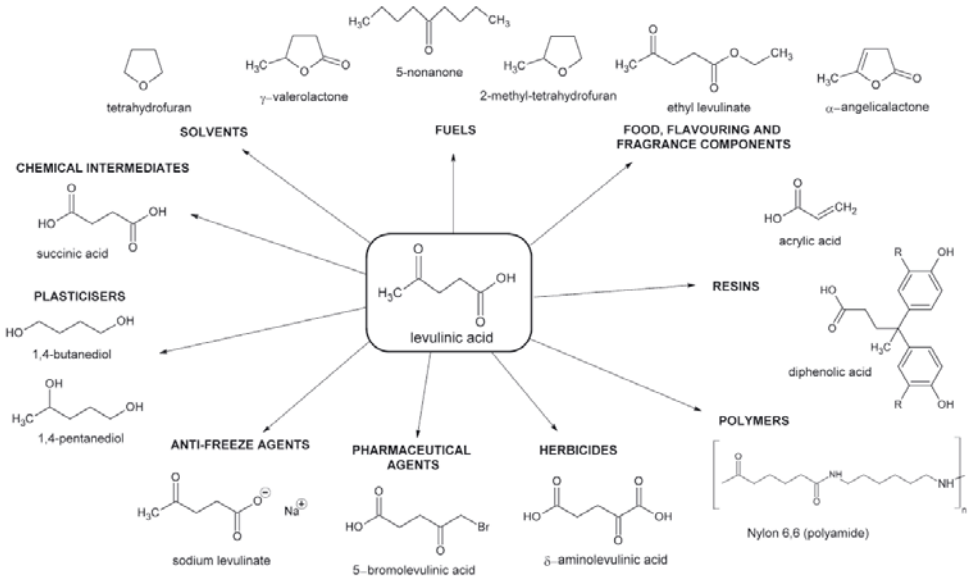

Figure 1.8. Useful chemicals derived from LA[55].

In the pharmaceutical industry calcium levulinate is used as a calcium supplement, it enhances bone formation and muscular excitability[54]; in agriculture, its derivate δ-aminolevulinic acid is a biodegradable herbicide[45], levulinate potash can be used as a highly effective fertilizer[54]. Levulinic acid and its esters can be used as fuel additives[56], precursors for diphenolic acid (a monomer, substitute for bisphenol A), plasticizers, surfactants, *etc.*[40,54]

LA can also be used for the production of gasoline additives and blenders[23]. A promising reaction path is the one leading to the production of γ-valerolactone (GVL) and 2-methyl tetrahydrofuran (MTHF), due to the interesting properties of this chemical to be used in gasoline engines. This conversion, showed in Figure 1.9, consists of two hydrogenolysis steps; each of them involving one hydrogenation and one dehydration.

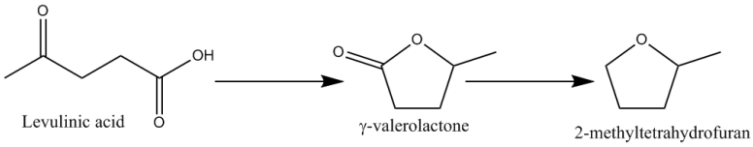

Figure 1.9. Reaction sequence from LA to MTHF.

The next sections summarize some of the most important properties and applications of GVL and MTHF.

1.8. γ-Valerolactone (GVL)

GVL is a natural compound present in some fruits and a commonly used additive in food, tobacco and perfume industries[10,54]. It can be used in cutting oils and braking fluids and, furthermore, it is a useful solvent for lacquers, adhesives and insecticides[13].

It has some very interesting physicochemical properties to be a sustainable liquid. It has a low melting point (-31 ºC), a high boiling point (207 ºC) and open cup flash point (96 ºC) and it has been reported that GVL does not form measurable amounts of peroxides when exposed to air for 35 days[10,57]. These properties, along with an intense but not disgusting smell for easily noticing leaks and spills and low toxicity (LD50 Oral-rat = 8,800 mg/kg)[10,58] makes it safe to store and transport in large scales[10].

In addition, both GVL and ethanol show similar characteristics when blended (10 vol%) with 95 octane gasoline. GVL, however, has a lower vapor pressure which leads to better performances[10,41]. GVL is miscible with water (and does not form azeotropes), a good environmental property since it assists biodegradation but it is a drawback similar to that of ethanol to be used as fuel blender[10,58].

Finally, GVL can react to form a number of compounds among which monomers (such as α-methylene-γ-pentanoate, which gives a polymer with similar properties to those of methyl methacrylate), ionic liquids (tetraalkylammonium 4-hydroxyvalerate for instance) and fuels additives (like 5-nonanone, alkanes or MTHF), and can be mentioned[58,59]. Some of these reactions are shown in Figure 1.10.

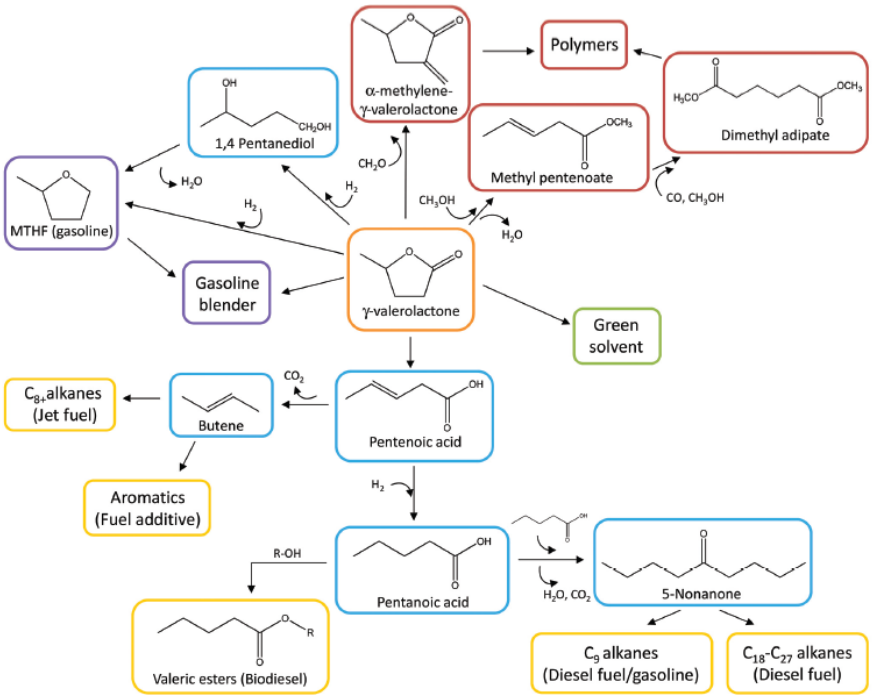

Figure 1.10. GVL reaction products[58].

1.9. 2-Methyltetrahydrofuran (MTHF)

Despite the fact that the reduction of LA to MTHF was first reported as a by-product in 1947[60], this process has gained remarkable attention only in view of recent researches. The most important could be the one performed by Paul[61], which provides a new and renewable fuel formulation, the *P-Series Fuels*[62], which can be used alone or mixed with gasoline in any proportion[31].

P- Series Fuels are composed of ethanol, *pentanes plus* (hydrocarbons from natural gas with more than 4 carbon atoms), and MTHF, which significantly reduces the vapor pressure of ethanol acting as a co-solvent[31]. These fuel formulations contain from 64 to 70% renewable chemicals, provided that both ethanol and MTHF can be derived from renewable sources. *Pure Energy Corporation* claims that this alternative fuels require less production energy and have a process efficiency between 1.75 and 2.25 (kJ produced/kJ spent)[62]. Additionally, exhaust gas tests performed by the *U.S. Environmental Protection Agency* (U.S. EPA) showed a significant reduction in ozone formation potential due to lower non-methane hydrocarbon, nitrogen oxides and carbon monoxide emissions compared to those of currently used conventional fuels[11,61,62].

However, these new blends are only applicable to the so-called *flexible-fuel engines* because of the slightly corrosive behavior of ethanol. The energy density of ethanol is less than that of gasoline leading, thus, to lower fuel economy. Moreover, the addition of oxygenated compounds to gasoline increases water solubility and, hence, the risk of phase separation and removal of ethanol from the mixture[4,41].

One way to overcome the above mentioned drawbacks is exploiting the potential of MTHF to be blended with conventional gasoline in proportions up to 70 vol% without modification of current engines[1,12]. MTHF has a lower energy density compared to conventional gasoline but, due to its higher specific gravity, renders a similar mileage. Nevertheless, MTHF presents the drawback of peroxide formation which could be a security issue for its storage and transportation if the necessary safety measures are not taken[54].

Apart from its use as a fuel blender, MTHF has a number of potential uses such as general solvent[31] being a green substitute of tetrahydrofuran (THF)[63] with more suitable physicochemical properties[64], a reagent in biphasic reactions[65], a substitute for the increasingly regulated chlorinated solvents. In addition, MTHF is increasingly used as a solvent in the pharmaceutical industry[64,66–69]. Its use in such a delicate sector as pharmaceutical is possible because it has been established that MTHF possess no mutagenicity nor genotoxicity characteristics and the human permitted daily exposure limit is 6.2 mg/day[64]. Anyway, the biggest market potential is expected to be as fuel blender with a projected market greater than 4500 metric tons per year[70].

In the next Chapter, an overview of the reported catalytic processes for the conversion of LA to MTHF is provided.

1.10. References

[1] G. W. Huber, S. Iborra, A. Corma, *Chem. Rev.* **2006**, *106*, 4044–4098.
[2] British Petroleum, *BP Statistical Review of World Energy About This Review Contents*, **2016**.
[3] K. Bjørlykke, P. Avseth, *Petroleum Geoscience*, Springer, **2010**.
[4] J. C. Serrano-Ruiz, J. A. Dumesic, *Energy Environ. Sci.* **2011**, *4*, 83–99.
[5] J. Lluch, *Tecnología Y Margen de Refino Del Petróleo*, Díaz De Santos, **2011**.
[6] S. Sorrell, J. Speirs, R. Bentley, A. Brandt, R. Miller, *Global Oil Depletion, an Assessment of the Evidence for a near-Term Peak in Global Oil Production*, UK ENERGY RESEARCH CENTRE, London, United Kingdom, **2009**.
[7] R. W. Howarth, A. Ingraffea, T. Engelder, *Nature* **2011**, *477*, 271.
[8] IPCC, 2001, *Climate Change 2001: The Scientific Basis. Contribution of Working Group I to the Third Assessment Report of the Intergovernmental Panel on Climate Change*, Cambridge University Press, Cambridge, United Kingdom, **2001**.
[9] International Energy Agency, *CO2 EMISSIONS FROM FUEL COMBUSTION Highlights*, **2015**.
[10] I. T. Horváth, H. Mehdi, V. Fabos, L. Boda, L. T. Mika, *Green Chem.* **2008**, *10*, 238.
[11] D. J. Hayes, *Catal. Today* **2009**, *145*, 138–151.
[12] D. M. Alonso, J. Q. Bond, J. a. Dumesic, *Green Chem.* **2010**, *12*, 1493–1513.
[13] A. Corma, S. Iborra, A. Velty, *Chem. Rev.* **2007**, *107*, 2411–2502.
[14] R. D. Perlack, L. L. Wright, A. F. Turhollow, R. L. Graham, B. J. Stokes, D. C. Erbach, *BIOMASS AS FEEDSTOCK FOR A BIOENERGY AND BIOPRODUCTS INDUSTRY: THE TECHNICAL FEASIBILITY OF A BILLION-TON ANNUAL SUPPLY*, US DOE, US DOA, **2005**.
[15] M. de Wit, A. Faaij, *Biomass and Bioenergy* **2010**, *34*, 188–202.
[16] C. Flavin, J. L. Sawin, L. Mastny, *American Energy, The Renewable Path to Energy Security*, Washington DC, **2006**.
[17] J. J. Bozell, in *Chem. Mater. from Renew. Resour.*, American Chemical Society, **2001**, p. 1.
[18] M. J. Gilkey, B. Xu, *ACS Catal.* **2016**, *5*, 1420–1436.
[19] D. M. Alonso, S. G. Wettstein, J. a. Dumesic, *Chem. Soc. Rev.* **2012**, *41*, 8075.
[20] J. C. Serrano-Ruiz, R. M. West, J. A. Dumesic, *Annu. Rev. Chem. Biomol. Eng.* **2010**, *1*, 79–100.
[21] R. B. Gupta, A. Demirbas, *Gasoline, Diesel, and Ethanol Biofuels from Grasses and Plants*, Cambridge University Press, Cambridge, **2010**.
[22] J. N. Chheda, G. W. Huber, J. a. Dumesic, *Angew. Chemie Int. Ed.* **2007**, *46*, 7164–7183.
[23] J. J. Bozell, G. R. Petersen, *Green Chem.* **2010**, *12*, 539–554.
[24] F. Cherubini, *Energy Convers. Manag.* **2010**, *51*, 1412–1421.
[25] S. Pérez, E. Bertoft, *Starch - Stärke* **2010**, *62*, 389–420.
[26] C.-H. Zhou, X. Xia, C.-X. Lin, D.-S. Tong, J. Beltramini, *Chem. Soc. Rev.* **2011**, *40*, 5588.
[27] V. Menon, M. Rao, *Prog. Energy Combust. Sci.* **2012**, *38*, 522–550.
[28] C.-H. (Clayton) Zhou, ab N. Jorge Beltramini, Y.-X. Fan, G. Q. (Max) Lu, J. N. Beltramini, Y.-X. Fan, G. Q. (Max) Lu, *Chem. Soc. Rev.* **2008**, *37*, 527–549.
[29] S. Bezergianni, A. Kalogianni, I. A. Vasalos, *Bioresour. Technol.* **2009**, *100*, 3036–3042.
[30] M. Stumborg, A. Wong, E. Hogan, *A Collect. Pap. Present. An Altern. Energy Conf. - Liq. Fuels, Lubr. Addit. from Biomass* **1996**, *56*, 13–18.
[31] D. J. Hayes, S. W. Fitzpatrick, M. H. B. Hayes, J. R. H. Ross, in *Biorefineries-Industrial Process. Prod.* (Eds.: B. Kamm, P.R. Gruber), Wiley-VCH Verlag GmbH, **2006**, pp. 139–164.
[32] R. Vanholme, K. Morreel, J. Ralph, W. Boerjan, *Physiol. Metab. - Ed. by Markus Pauly Kenneth Keegstra* **2008**, *11*, 278–285.
[33] R. Rinaldi, R. Jastrzebski, M. T. Clough, J. Ralph, M. Kennema, P. C. A. Bruijnincx, B. M. Weckhuysen, *Angew. Chemie Int. Ed.* **2016**, *55*, 8164–8215.
[34] D. J. Braden, C. a. Henao, J. Heltzel, C. C. Maravelias, J. a. Dumesic, *Green Chem.* **2011**, *13*, 1755.
[35] A. Aden, T. Foust, *Cellulose* **2009**, *16*, 535–545.
[36] J. C. Serrano-Ruiz, D. J. Braden, R. M. West, J. A. Dumesic, *Appl. Catal. B Environ.* **2010**, *100*, 184–189.
[37] R. Rinaldi, F. Schüth, *ChemSusChem* **2009**, *2*, 1096–1107.
[38] S. W. Fitzpatrick, *Lignocellulose Degradation to to Furfural and Levulinic Acid.*, **1990**.
[39] S. W. Fitzpatrick, *Production of Levulinic Acid from Carbohydrate-Containing Materials.*, **1997**, WO 9640609.
[40] J. J. Bozell, L. Moens, D. C. Elliott, Y. Wang, G. G. Neuenscwander, S. W. Fitzpatrick, R. J.

Bilski, J. L. Jarnefeld, P. Northwest, P. O. Box, et al., **2000**, *28*, 227–239.
[41] J. C. Serrano-Ruiz, A. Pineda, A. M. Balu, R. Luque, J. M. Campelo, A. A. Romero, J. M. Ramos-Fernández, *Catal. Biorefineries* **2012**, *195*, 162–168.
[42] M. Mascal, E. B. Nikitin, *Angew. Chemie* **2008**, *120*, 8042–8044.
[43] M. Mascal, E. B. Nikitin, *ChemSusChem* **2009**, *2*, 859–861.
[44] M. Mascal, E. B. Nikitin, *Energy & Fuels* **2010**, *24*, 2170–2171.
[45] M. Mascal, S. Dutta, *Green Chem.* **2011**, *13*, 40–41.
[46] M. Mascal, S. Dutta, *Green Chem.* **2011**, *13*, 3101–3102.
[47] M. Mascal, E. B. Nikitin, *Green Chem.* **2010**, *12*, 370–373.
[48] US EPA, *EMERGENCY PLANNING AND COMMUNITY RIGHT-TO-KNOW ACT -SECTION 313 Guidance for Reporting Hydrochloric Acid (Acid Aerosols Including Mists, Vapors, Gas, Fog, and Other Airborne Forms of Any Particle Size)*, **1999**.
[49] J. Shen, C. E. Wyman, *Am. Inst. Chem. Eng. J.* **2012**, *58*, 236–246.
[50] D. M. Alonso, S. G. Wettstein, J. Q. Bond, T. W. Root, J. A. Dumesic, *ChemSusChem* **2011**, *4*, 1078–1081.
[51] E. I. Gürbüz, D. M. Alonso, J. Q. Bond, J. a. Dumesic, *ChemSusChem* **2011**, *4*, 357–361.
[52] R. Weingarten, W. C. Conner, G. W. Huber, *Energy Environ. Sci.* **2012**, *5*, 7559–7574.
[53] B. V Timokhin, V. a Baransky, G. D. Eliseeva, *Russ. Chem. Rev.* **1999**, *68*, 73–84.
[54] J. Zhang, S. Wu, B. Li, H. Zhang, *ChemCatChem* **2012**, *4*, 1230–1237.
[55] D. W. Rackemann, W. O. Doherty, *Biofuels, Bioprod. Biorefining* **2011**, *5*, 198–214.
[56] A. Démolis, N. Essayem, F. Rataboul, *ACS Sustain. Chem. Eng.* **2014**, *2*, 1338–1352.
[57] M. Vasiliu, K. Guynn, D. A. Dixon, *J. Phys. Chem. C* **2011**, *115*, 15686–15702.
[58] D. M. Alonso, S. G. Wettstein, J. a. Dumesic, *Green Chem.* **2013**, *15*, 584.
[59] I. T. Horváth, *Green Chem.* **2008**, *10*, 1024.
[60] R. V. J. Christian, H. D. Brown, R. M. Hixon, *J. Am. Chem. Soc.* **1947**, *69*, 1961–1963.
[61] S. F. Paul, *Alternative Fuel.*, **1997**, WO 9743356 A1.
[62] U. S. D. of Energy, in (Ed.: F. Register), U.S. Government Printing Office, Washington, NW, **1999**, pp. 26822–26829.
[63] B. Comanita, S. Chemicals, **2006**, 1–2.
[64] V. Antonucci, J. Coleman, J. B. Ferry, N. Johnson, M. Mathe, J. P. Scott, J. Xu, *Org. Process Res. Dev.* **2011**, *15*, 939.
[65] D. F. Aycock, *Org. Process Res. Dev.* **2007**, *11*, 156–159.
[66] J. T. Kuethe, K. G. Childers, G. R. Humphrey, M. Journet, Z. Peng, *Org. Process Res. Dev.* **2008**, *12*, 1201–1208.
[67] I. N. Houpis, D. Shilds, U. Nettekoven, A. Schnyder, E. Bappert, K. Weerts, M. Canters, W. Vermuelen, *Org. Process Res. Dev.* **2009**, *13*, 598–606.
[68] X.-L. Du, Q.-Y. Bi, Y.-M. Liu, Y. Cao, H.-Y. He, K.-N. Fan, *Green Chem.* **2012**, *14*, 935.
[69] V. Pace, P. Hoyos, L. Castoldi, P. Domínguez De María, A. R. Alcántara, *ChemSusChem* **2012**, *5*, 1369–1379.
[70] J. J. Bozell, L. Moens, D. C. Elliott, Y. Wang, G. G. Neuenscwander, S. W. Fitzpatrick, R. J. Bilski, J. L. Jarnefeld, *Resour. Conserv. Recycl.* **2000**, *28*, 227–239.

Chapter 2

State of the art

Table of contents

2.1. Abstract 43

2.2. MTHF production through GVL 43

2.2.1. GVL production from LA 43

2.2.1.1. Ru as hydrogenation active phase 44

2.2.1.2. Other noble metals as hydrogenating active phase 46

2.2.1.3. Effect of the catalyst acidity 47

2.2.1.4. Non noble metals as the hydrogenating phase 49

2.2.1.5. Biomass conversion to LA and GVL 51

2.2.1.6. Formic acid as the hydrogen source 52

2.2.1.7. Catalytic transfer hydrogenation (CTH) 53

2.2.2. MTHF production from GVL 55

2.3. Direct production of MTHF from LA 57

2.4. General conclusions 59

2.5. References 61

2.1. Abstract

The objective of this chapter is to provide an overview of the reported heterogeneous catalytic processes used for the transformation of levulinic acid (LA) into 2-methyltetrahydrofuran (MTHF). In this chapter, the attention is focused on solid catalysts since they are more suitable for industrial application rather than homogeneous catalysts, usually employed for very high value added products in batch operations. This state of the art is meant to be more than a mere list of the references in the field, by providing a critical review of the literature on the topic of this thesis.

Two different approaches are considered in this review: *i)* the conversion of LA to γ-valerolactone (GVL) followed by the reaction of GVL to yield MTHF and *ii)* the direct conversion of LA to MTHF. It is noteworthy the fact that, while a number of papers focus on the production of GVL, very few authors reported the production of MTHF.

2.2. MTHF production through GVL

This approach takes advantage of the fact that GVL is relatively easy to obtain in good yields. Most of the authors focus on GVL production as the goal of the process while not so many report its production as an intermediate for the production of more suitable fuels such as alkanes or MTHF.

2.2.1. GVL production from LA

The production of GVL from LA is the most studied process among the ones presented in this *state of the art* section. The commercial Ru(5%)/C catalyst has been widely used for this reaction, demonstrating the particular activity and selectivity of Ru for this hydrogenation process[1].

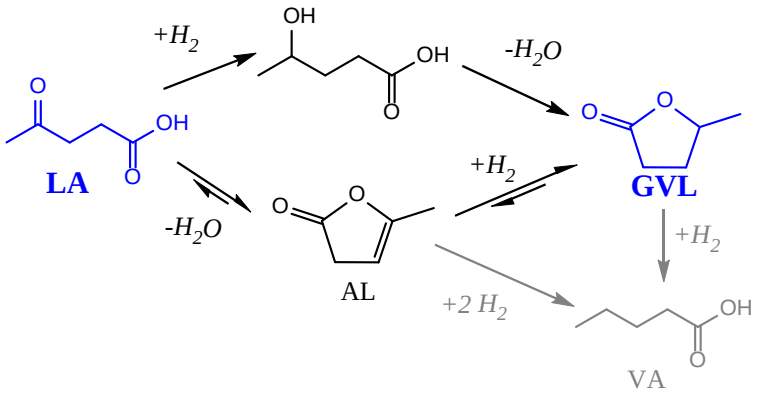

Figure 2.1. LA to GVL reaction mechanism.

2.2.1.1. Ru as hydrogenation active phase

A series of publications screened the catalytic activity of a number of noble metals (Ru, Rh, Pd, Pt, Ir, Re and Ni) supported on inert materials (C, carbon) with a 50 wt% LA solution in 1,4-dioxane feed[2–4]. The highest yields (97%) were obtained with Ru under operation conditions ranging from 150 to 215 ºC, 55 bar H_2 pressure and 2 to 4 h reaction time. Another set of catalysts (Ru/C, Pd/C, Raney Ni and Urushibara Ni) was tested for the reduction of a 5 wt% LA solution in methanol. Consistent results were achieved, with Ru/C showing the best performance at 130 ºC and 12 bar H_2: > 90% yield with Ru/C versus < 10% yield for all the other catalysts[5,6].

In a continuous reaction system the activity of three noble metal based catalyst (5 wt% Ru, Pd and Pt supported on C) for the reduction of a 10 wt% LA feed in 1,4-dioxane was studied. Experiments at 265 ºC over a range of H_2 pressures, 1 to 25 bar, showed vast differences among the three metals. Under 1 bar, Ru was the most active and selective (98.6% yield to GVL) metal compared to Pd (90%) and Pt (30%); and the dissimilarities increased with increasing pressures: Ru maintained over 90% yield whereas for Pd decreased from 90 to 60% at 10 bar. On the contrary, the yield with the Pt based catalyst increased from 30 to 60% at 25 bar[7].

The effect of different alcohols as solvents was studied in the presence of a commercial Ru(5%)/C catalyst. 160 min tests were carried out at 130 ºC under 12 bar H_2 with 5 wt% LA in different solvents feed. This research showed that the best solvent for this reaction was 1,4-dioxane (96% yield) followed by water (86%), methanol (84%), ethanol (61%) and 1-butanol (31%)[8]. GVL yields showed to be improved in two ways: *i)* increasing H_2 pressure led to 98% yields in 1-butanol but reduced to 78%

that obtained in methanol or *ii)* adding water (10 vol%) to the solvent did not alter the yield when methanol was used but substantially increased the yield when 1-butanol was used (from 31% to 75%). These results were also confirmed by the activity increase of a Ru/ZrO_2 catalyst for LA to GVL reaction when up to 10% water was added to 1,4-dioxane[9]. These experimental results were theoretically supported *via* density functional theory calculations, showing that the hydrogenation of ketones proceed through an energetically more favored path in the presence of water over Ru surfaces[10].

Additionally, the activity of different supported 5% Ru catalysts (Ru/C, Ru/SiO_2, Ru/Al_2O_3 and Ru/TiO_2) was compared[8]. The first demonstrated to be superior (89% versus 75%, 76% and 71% respectively) dealing with a water-ethanol (10 vol% water) solution of LA (5 wt%) at 130 ºC. Further evidence of the outstanding activity of this catalyst was provided when setting the reaction temperature at 25 ºC under 12 bar H_2; Ru(5%)/C catalyst enabled 97% GVL yield in 50 h while $Ru(5\%)/SiO_2$ and $Ru(5\%)/Al_2O_3$ only led to 1.7% and 6.3% yields[8]. Another research paper reported similar activities at 150 ºC under 30 bar H_2 in 1,4-dioxane solution for Ru catalysts supported on C, TiO_2 and ZrO_2; nevertheless, vast stability differences were found between them[9]. While Ru/ZrO_2 showed no deactivations signs operating at 50% LA conversion for 5 cycles, the activity of both Ru/C and Ru/TiO_2 sharply decreased in the second run. In this case, the instability of the TiO_2 support was responsible for the activity loss; TiO_2 was partially reduced during the reaction and strong metal support interactions led to Ru encapsulation.

The effect of different solvents on the reaction was further investigated using unsupported Ru nanoparticles as catalyst. These trials, carried out at 130 ºC for 24 h, showed that no solvent is needed for high yields (95%) towards GVL under 12 bar H_2[11]. However, the reaction yield was improved using THF as solvent (96% yield) under the same reaction conditions, and even 100% GVL yields were achieved in water solutions for H_2 pressures from 5 to 12 bar.

The commercial Ru(5%)/C catalyst was also reported to be active in aqueous media, achieving quantitative LA conversion with high selectivity (96%) to GVL with a 50 wt% LA solution fed at 150 ºC and 35 bar H_2[12]. This continuous system operated at 32 h^{-1} WHSV and suffered a slow deactivation falling from 96% to 68% after 106 h operation.

Two more publications can be found studying the combined effect of the solvent and the catalyst on the reaction yield. On the one hand, LA, GVL and solvent competition for the adsorption sites on a zeolite supported Ru catalysts was shown by the higher pentanoic acid yield (produced by GVL hydrogenation) achieved in 1,4-dioxane compared to 2-ethylethanoic acid[13]. This point was confirmed by the lower reaction times required for over 90% GVL yield when the reaction was performed in 1,4-dioxane or in solvent free LA rather than in 2-ethylethanoic acid (4 *vs.* 10 h). On the other hand, a solvent screening for GVL production using Ir(4.5%)/CNT (carbon nanotubes) catalyst at 50 ºC and 20 bar of H_2 showed water to be the best reaction solvent achieving 99% yield followed by pure LA (97%), $CHCl_3$ (91%), far higher than those obtained with toluene (66%), methanol (18%), acetone (7%) or 1,4-dioxane (2%)[14]. The reported screening results seem to be discrepant; nevertheless the very different reaction conditions and catalysts used can be responsible for the inconsistent results.

A special solvent application in a triphasic system (aqueous - ionic liquid - organic) can be found in the literature. The reaction was set with 4.4 mL of water containing 7.9 mmol LA, 4.4 mL of isooctane and 0.53 mmol of the ionic liquid *trioctylmethylammonium bis(trifluoromethylsulfonyl)imide* ($[N_{8,8,8,1}][NTf_2]$) using a Ru(5%)/C catalyst and the reaction proceed at 100 ºC under 35 bar H_2 to 100% GVL yield in 2 h. The organic phase was important in this set-up to improve phase separation and the segregation of the catalyst to the ionic liquid, thus stabilizing the catalyst and facilitating its recovery[15], and allowing over 75% GVL yields in 8 consecutive runs. Supercritical CO_2 was also found to be a suitable media for this reaction. The reaction, at 200 ºC and 100 bar, proceed towards > 99% GVL yield with a commercial Ru(5%)/SiO_2 catalyst and a 75 wt% LA aqueous solution feed (H_2/LA molar ratio of 3.0)[16]. The main benefit of using this reaction media is that it allows a very selective GVL extraction (< 0.4 wt% H_2O), thus eliminating downstream purification steps.

2.2.1.2. Other noble metals as hydrogenating active phase

Other noble metal catalysts have also been the object of research for this reaction. Pt was reported to be one of the best hydrogenation metals over inorganic supports, nonetheless, requiring higher temperatures than Ru. Two thorough catalyst screenings, conducted at 200 ºC under 40 bar H_2, reducing 89 wt% LA solution in GVL, concluded that Pt(1%)/TiO_2 and Pt(1%)/ZrO_2 were the most active catalysts amongst a number of

metals (1% Re, Au, Pd, Ru, Pt and some 1:1 alloys of them) and supports (TiO_2, ZrO_2, C, SiO_2), achieving up to 99.5% yields with little deactivation over 100 h continuous operation[17,18]. A previous report showed that Pt(0.4%)/SiO_2 reached high GVL yields (99%) at the same reaction conditions as the above mentioned but the feed was 13 wt% LA in GVL and the WHSV 0.25 h^{-1} instead of 9 h^{-1}[19].

Further studies on bimetallic, alloyed, catalysts yielded interesting conclusions. Strong electronic interactions between two inactive metals (Pd and Au) supported on TiO_2 produced an active bimetallic catalyst for the production of GVL at 200 ºC in 1,4-dioxane[20]. On the other hand, when the active metal Ru was alloyed with Pd (using the same catalyst preparation method) no activity differences were noticed. Nevertheless, metal alloying greatly improved the catalysts stability in both cases, hampering particle sintering and allowing for constant activity in three consecutive runs[20].

A report focused on Ir as the hydrogenating metal was also published[14]. A number of supports were tested for the hydrogenation of LA to GVL in water (0.4 mol/L LA) at 50 ºC under 20 bar H_2 for 1 h. The best results were obtained when CNTs were used (99% yield), followed by activated carbon (76%), CeO_2 (55%), Al_2O_3 and ZnO (51%), SiO_2 (37%) and MgO (20%). Interestingly, the displayed series of supports does not follow an acidity based order of activity as previously reported[13]. The activity of Ir catalysts, however, is known to be critically dependent on the support and the interactions amongst both materials[14].

2.2.1.3. Effect of the catalyst acidity

The reaction sequence displayed in Figure 2.1 shows that GVL production from LA is achieved *via* a hydrogenation and a dehydration (or *vice versa*) steps. Therefore, some articles explored the influence of the catalyst acidity on the reaction. Acid-functionalized *Ordered Mesoporous Carbons* (OMC) as support for Ru catalysts provided significant activity differences according to the functionality[21]. Phosphoric acid functionality was found to be the most active/promoting one, achieving stable 93% GVL yield in 9 h at 70 ºC for five consecutive runs in aqueous medium under 7 bar H_2. Interestingly, and despite its lack of acidity, the unfunctionalized OMC as support facilitated higher activity than the sulfonic groups containing OMC, which only reached 18% GVL yield. This fact, however, was not due to mechanistic reasons, but to the

instability of the sulfonic groups: they were found to be reduced under the reaction conditions producing sulfide species which anchored on the Ru sites and blocked them.

Further studies tested commercial Ru catalysts in aqueous phase under mild reaction conditions finding Ru/C to be twice as active as Ru/Al_2O_3[22,23]. Despite the fact that the most acidic catalyst (Ru/Al_2O_3) was less active, the addition of solid acid co-catalysts facilitated higher activities in all cases. The influence of several acidic solids ($NbOPO_4$, $Nb_2O_5 \cdot nH_2O$, *Amberlyst A15 dry* and *Amberlyst A70 wet*) was checked and found that a 4.6 wt% LA aqueous solution can be reduced under mild conditions (70 ºC and 30 bar H_2) yielding 90% GVL in 30 min (*vs.* 15% with only Ru/C) and 100% in 3 h (*vs.* 47%)[22]. Other research papers explored the union of both catalyst and co-catalysts in a single one, by impregnating Ru over an ion exchange resin (*DOWEX*)[24]. The aqueous phase hydrogenation of LA to GVL was carried out at 70 ºC under 10 bar H_2 for 4 h, achieving 98% LA conversion.

The fact that an acidic co-catalyst enhanced the activity for both catalysts (Ru/C and Ru/Al_2O_3) does not fit with the lower activity of Ru/Al_2O_3 compared to Ru/C considering their acidity differences. In this case, it should be noted that the surface area of Ru/Al_2O_3 is ten times lower than that of Ru/C, which may be detrimental for the dispersion of Ru particles. In fact, Ru is known not to be homogeneously dispersed over γ-Al_2O_3 which, in addition, is prone to rehydration into bohemite in the presence of water due to its abundant surface –OH groups[25]. The activity and stability of a Ru/Al_2O_3 catalyst was reported to be enhanced by surface modification of the surface –OH groups of Al_2O_3 by silylation reaction with 2-aminopropyltriethoxysilane. This modified catalyst showed high stability against boehmite formation under hydrothermal conditions, and a significantly lower average Ru particle size with a much narrower distribution. All these facts produced a catalyst with up to 7 times higher *Turnover Frequency* (TOF), high activity even at 25 ºC and an activity decrease from 100 to 90% after 10 runs (*vs.* 100 to 60% for the unmodified Ru/Al_2O_3)[25].

These activity-acidity relating results contrast with literature reports[26–28] claiming that lower yields GVL are expected when acidic catalyst are employed due to coke formation. In order to identify the mechanism responsible for the activity increase by the addition of an acidic co-catalyst, the reaction mechanism should be considered. In a thorough kinetic paper it was stated that LA hydrogenation over Ru/C proceeds

exclusively through 4-hydroxyvaleric acid (HVA) at temperatures below 150 ºC in the presence of H_2[29]. Under N_2 atmosphere, the main product of the reaction was α-angelica lactone (AL), but with a *site time yield* (STY) lower by 4 orders of magnitude. The results also indicate that, under the applied reaction conditions, the rate limiting step of the reaction was the intramolecular esterification of HVA to GVL, most presumably due to the low acidity of the Ru/C catalyst. The enhanced activity of the system when an acidic co-catalyst is added can then be attributed to a double effect. On the one hand, the acid catalyst would increase the total acidity and its strength, increasing the rate of the limiting step (HVA to GVL). On the other hand, the presence of an acid would also accelerate the slower reaction path (through AL), which would increase the turnover frequency of the less occupied sites, the hydrogenating ones, because an additional reaction (AL to GVL) would also take place in them.

The role of the supports acidity on the reaction performance was further investigated in a methodical paper in which four 1% Ru catalysts supported on H-ZSM5, H-β, TiO_2 and Nb_2O_5 were used. Consistently with the previously presented results, higher activity (and TOF) was observed for the most acidic supports. In addition, deep hydrogenation products (mainly MTHF and valeric acid, VA) were more abundant in the presence of those catalysts since strong acidity favors GVL ring opening[13,21]. Higher and stronger acidity also favored coke formation, being AL its main precursor, as indicated by mass spectrometer coupled thermogravimetric analysis (TGS-MS).

2.2.1.4. Non noble metals as the hydrogenating phase

The use of supported non-noble metal catalysts for the production of GVL is scarce compared to the use of noble metals. Copper containing hydrotalcite derived catalysts have been applied for the reduction of a 16 wt% aqueous LA solution to GVL with up to 91% yield at 200 ºC under 70 bar H_2[30]. The best activity was provided by a Cu-Cr catalyst followed by Cu-Al (86%) and Cu-Fe (81%) (molar ratio Cu/metal = 2 in every case) after 10 h of reaction. Besides, a correlation was found between the electronegativity of the cations on the catalysts support and the MTHF yield. It was suggested that the higher electronegativity of the Fe^{3+} enhanced GVL electron attraction and promoted its further hydrogenolysis to MTHF[30]. Despite the interest of this finding, the results must be carefully considered, since the maximum MTHF yield in this paper was only 3.5% and Cu^0, the active metal phase in all those catalysts, is more

electronegative than Al^{3+} or Cr^{3+}, which makes the discussion not very clear. Another Ni-Cu-Mg-Al-Fe containing hydrotalcite derived catalysts showed up to 98% GVL yields at 142 ºC in methanol solutions from LA in 3 h under 20 bar H_2[31]. The optimized catalyst composition showed slow deactivation when a regeneration procedure was applied between runs (from 98% to 90% in five runs) whereas direct reuse of the catalyst led to severe deactivation (from 98% to 60% in the second run). Interestingly, when the reaction solvent was water instead of methanol, the activity of the catalyst decreased and so did the selectivity (from 98% to 67%).

Another Cu based catalyst series was used for the reduction of a 5 wt% LA aqueous solution at 200 ºC under 34 bar H_2 in 5 h[32]. In contrast with the previously displayed results, 100% GVL yield was reported using Cu/Al_2O_3 and Cu/ZrO_2 catalysts while the Cu/Cr_2O_3 catalyst only achieved 9% yield. This activity discrepancy may be assigned to the different catalyst preparation method rather than to the two times higher H_2 pressure used in[30], which should favor the conversion of all chemicals. Another example of Cu based catalyst ($Cu(35\%)\text{-}Ni(4\%)/SiO_2$) was reported to achieve stable > 95% GVL yields from both LA and EtLA at 230 ºC under 30 bar H_2[33]. This paper showed the improved stability of the catalyst when Ni was present in the catalyst and, also, the switch in the products selectivity with increasing temperatures: below 180 ºC GVL was the main reaction product (< 91%) and it decreased to 5% at 260 ºC, where a 67 % MTHF yield was achieved.

Vapor phase reactions were also reported for GVL production. In 1957 a process was patented by Dunlop in which a feed containing 0.09 to 0.24 g LA per liter H_2 (at 180 ºC and atmospheric pressure) claimed to produce GVL with 95 to 100% yield using a $Cu(50\%)/Cr_2O_3$ catalyst at 175 to 225 ºC and 1 to 5 psig, to overcome the pressure drop in the reactor[34]. Recently a $Cu(5\%)/SiO_2$ catalyst was found to be active for the reduction of LA with H_2 at 265 ºC and 10 bar pressure (H_2/LA = 80 molar ratio)[7]. Operating at a WHSV of 0.513 h^{-1} the system enabled stable 99% GVL yields along 100 h operation.

Finally, as a curiosity, the 316 stainless steel walls of a reactor were found to have catalytic activity in the presence of trifluoromethylsulfonic acid (HTOf). At temperatures ranging from 75 to 100 ºC the system achieved 100% GVL yield in 24 h

from a 0.5 mol/L LA and 0.04 mol/L HOTf water solution under 55 bar H_2[35]. Even more, at 250 ºC the sole reactor wall enabled 68% GVL yield in 24 h.

2.2.1.5. Biomass conversion to LA and GVL

The aim for straight utilization of the raw products of acid hydrolysis made researchers include H_2SO_4 in the feed to the reactors. Ru(5%)/C was successfully employed to reduce a 15.2 wt% LA, 6.6 wt% FA and 0.5 mol/L H_2SO_4 aqueous solution to GVL in quantitative yields. The reaction, 2 h long, was performed at 150 ºC under 35 bar H_2 despite of the addition of FA[36]. As no control experiments were reported without molecular H_2 addition, it is not possible to determine if the H_2 produced from this FA solution was sufficient (*e.g.* pressure) for the production of GVL. On the other hand, this catalyst proved to be unstable in the presence of H_2SO_4 containing feeds, as evidenced by a tenfold decrease in the TOF when feeding acid containing solutions[37]. A Ru(4%)-Re(11%)/C catalyst was proposed to enhance the reaction rate with a feed similar to that obtained from cellulose deconstruction (*i.e.* 2.2 mol/L LA and FA containing 0.5 mol/L H_2SO_4 aqueous solution). This enhanced activity could be attributed to the improved properties of the alloy as well as to the threefold higher metal content of the catalyst; since the authors did not compare the Ru-Re/C catalyst with Ru(15%)/C or Re(11%)/C catalysts. The reported catalyst showed a remarkable stability (150 h on stream) in an acidic medium. This was an unexpected result considering the well-known solubility of Re in water[38].

Further research focused on the use of real biomass deconstruction streams. In order to do so, a two-step process was developed in which *i)* biomass was hydrolyzed to produce LA (and FA) using 0.5 mol/L H_2SO_4 at 170 ºC for 1 h and *ii)* the produced LA was hydrogenated to GVL using the byproduct FA at 150 ºC in 8 h. The process required partial neutralization of the H_2SO_4 (to pH = 2) and solid residue filtration prior to feed the solution to the second reactor[39]. The hydrogenation step proceeded with remarkable > 95% yield for all the employed hydrocarbon sources (*i.e.* glucose, fructose, sucrose, starch and cellulose) while the overall yield ranged from 33% (for cellulose) to 60% (for fructose), due to the limited yields of the first hydrolysis step.

Another two-step process was reported in which *i)* biomass hydrolysis with 0.5 mol/L H_2SO_4 at 180 ºC under 5 bar N_2 for 1 h and *ii)* neutralization, filtration and reduction of the obtained LA under 40 bar H_2 with an Ir(4.5%)/CNT catalyst at 50 ºC

was carried out[14]. In this case, the mild reaction temperature did not allow FA decomposition; therefore, molecular hydrogen addition was necessary. This process achieved a similar 94% GVL yield on the second step for all feedings and, in good agreement with the previously presented results, the overall GVL yield was maximum when starting from fructose (60%) and minimum when using cellulose (32%). These two studies clearly indicated that biomass hydrolysis is the yield limiting step of the reaction while LA hydrogenation can be carried out to quantitative yields using real feeds over a wide range of catalysts and reaction conditions.

Using a combination of a heterogeneous acid catalyst (Al-$NbOPO_4$) and Ru(5%)/C, a two-steps one-pot cellulose hydrolysis to LA and subsequent conversion to GVL was carried out[40]. The first step of the reaction was carried out under N_2 atmosphere at 180 ºC for 24 h with a 53% LA yield. After changing the atmosphere to 30 bar H_2, the produced LA was fully converted into GVL at 180 ºC in 12 h, with an overall 57% GVL yield. The fact that the GVL yield is higher than that of LA is a consequence of strong LA adsorption on the catalyst acid catalyst, as explained in the article.

A different cellulose deconstruction approach was repotted using methanol and H_2SO_4 to produce methyl levulinate (MeLA) at 200 ºC in 4 h. This reaction produced a 2.5 wt% MeLA solution (49% yield) which, after H_2SO_4 neutralization with CaO, was converted into GVL over Cu nanoparticles at 240 ºC with 69% yield (34% overall GVL yield) in 4 h using the methanol solvent as the hydrogen source[41]. The Cu nanoparticles, which were generated *in-situ* from CuO by reduction with the methanol solvent, proved to be recyclable showing > 72% GVL selectivity with up to 98% MeLA conversion over 3 runs with calcination at 500 ºC between runs.

2.2.1.6. Formic acid as the hydrogen source

As previously explained, FA is a byproduct of the manufacture of LA by acid hydrolysis of biomass, that can be used as a hydrogen source; by this means, the dependence on external H_2 could be reduced and savings made in separation steps, obtaining a more competitive product[42,43].

The capacity of a series of noble metals (Au, Pd, Pt and Ru) supported on different materials (TiO_2, SiO_2 and ZrO_2, C) to promote the hydrogenation of LA to GVL with equimolar amounts of FA as the only source of hydrogen was explored[39].

Au(0.8%)/ZrO_2 was found to be the most active catalyst for the selective decomposition of FA to H_2 and CO_2 and, at the same time, the most suitable for the reduction of LA to GVL, achieving 99% yields in 6 h at 150 ºC or in 3 h at 180 ºC, under 5 bar N_2.

A two-step process was reported using Ru based catalysts where *i)* an aqueous FA solution (8 mol/L) was decomposed over a Ru(1.43%)PPh_2-SiO_2 ($RuCl_2$ anchored on functionalized silica) catalyst at 170 ºC for 1 h and then *ii)* use the generated H_2 to reduce the aqueous LA solution (8 mol/L) to GVL over a Ru(0.55%)/TiO_2 catalyst at 170 ºC for 2 h with 88 to 92% yields[44].

Unsupported Ru nanoparticles were also effectively applied to the reaction, reaching 100% yields in GVL in 24 h. The reaction was carried out at 130 ºC but required the addition of triethylamine (Et_3N) and a considerable excess of FA (LA - Et_3N - FA molar ratios 1.0 - 0.4 - 4.0)[11]. Further studies on unsupported nanoparticles showed transition metals to be active for GVL conversion. Using FA (6 equivalents, eq.) and Et_3N (1 eq.) in aqueous solution at 175 ºC Co nanoparticles enabled 89% GVL yield in 48 h[45]. Under microwave irradiation, polymer stabilized Co nanoparticles allowed 85% GVL yield for five consecutive runs in ethanol solution with 2 eq. KOH in 30 min[45].

In addition, the use of FA as hydrogen donor in the gas phase was patented. A continuous flow reactor, loaded with a commercially available Ni catalyst, enabled 30% GVL yields and 7% AL yield from a feed composed of equimolar amounts of LA and FA at 275 ºC and atmospheric pressure[46].

2.2.1.7. Catalytic transfer hydrogenation (CTH)

The last reaction alternative for the production of GVL from LA reported is the *Meerwein–Ponndorf–Verley* (MPV) or *Catalytic Transfer Hydrogenation* (CTH) reaction. This reaction proceeds with an alcohol (preferably a secondary alcohol) as solvent and hydrogen donor over a metal oxide or supported metal catalyst. A communication using metal oxides as catalysts explored this reaction and concluded that ZrO_2 and 2-butanol were the most suitable catalyst and solvent/donor amongst the tested ones[47]. The reaction required 16 h at 150 ºC and 20 bar He (for the mixture to remain liquid) to attain 92% GVL yield from a 1 wt% LA solution in 2-butanol. Another article showed the activity of a Zr-β zeolite (Si/Zr = 100) for the MPV reaction using 2-pentanol as solvent in liquid phase[48]. After 10 h reaction time at 118 ºC, 96%

GVL yields were achieved. On the other hand, operating in gas phase at 250 ºC and ambient pressure, stable 99% GVL yields were achieved with 2-propanol as hydrogen donor for 87 h. Besides, the thermal stability of this catalyst allowed full activity recovery by calcination.

Using 2-propanol as solvent and hydrogen donor, three Zr based catalysts were reported to be active for GVL production: ethyl levulinate (EtLA) was converted to GVL with 97% yields at 200 ºC in 1 h reaction time over a Zr containing porous polymer (Zr-hydroxybenzene acid). The adjacent acid (Zr^{4+}) and basic (O^{2-}) sites provide the observed high activity and allow for stable 94% GVL yield at 150 ºC and 4 h reaction time for 5 consecutive runs[49]. A Zr-cyanuric acid coordination polymer was reported to reach over 90% GVL yields from LA and several levulinates at 130 ºC; and at 200 ºC it showed up to 98% GVL yield in 1 h reaction time[50]. Similarly, a Zr based metal organic framework allowed stable 90% GVL yields for 5 consecutive cycles at 200 ºC in 2 h reactions from EtLA[51].

Alcohols were also used as hydrogen donors over supported metal catalysts. Under 50 s microwave irradiation a commercial Pd(5%)/C catalyst effectively converted LA into GVL with up to 86% yields using ethanol or 2-propanol as hydrogen donor in the presence of 2 eq. of KOH[52]. When the base was not used, only trace amounts of GVL were obtained. In good agreement with this study, only 1% GVL yields were reported in 2-propanol using Pd/C; on the other hand, Raney Ni showed high activity for EtLA conversion to GVL using 2-propanol as hydrogen donor at temperatures as low as 25 ºC[43]. Since the CTH mechanism, the metal hydride route, requires the adjacent presence of acidic and metallic sites[53], the observed activity differences might be related to the more acidic nature of Raney Ni catalysts, due to the presence of unleached Al[54,55], compared to that of Pd/C.

The use of methanol as hydrogen donor was investigated over a Cu-Cr catalyst[56]. In this article, the hydrogen required for the conversion of MeLA into GVL was internally supplied by reforming of the methanol released during the reaction (MeLA + $H_2 \rightarrow$ GVL + MeOH). An initial load of methanol (0.29 methanol/MeLA mol) was necessary in order to start the reaction, which facilitated up to 90% GVL in 4 h at 250 ºC under N_2 atmosphere.

2.2.2. MTHF production from GVL

The GVL hydrogenation step is considered to be the most demanding in the MTHF production, owing to the high stability of the GVL[57,58]. This difficulty may be among the reasons why very few authors have reported research about this particular reaction.

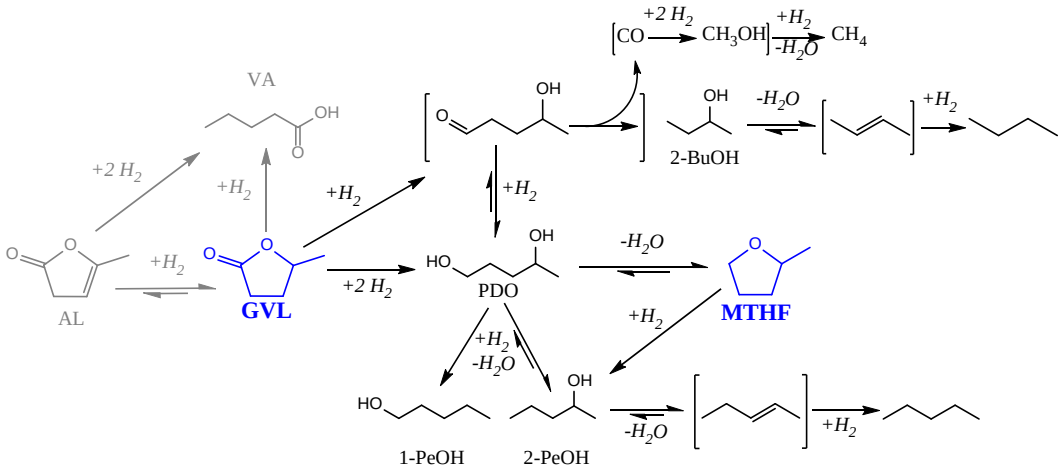

Figure 2.2. GVL to MTHF reaction mechanism and some possible side reactions.

A Pt(0.7%)/ZSM-5(25%)-SiO_2(75%) catalyst was reported to convert pure GVL to MTHF at 250 ºC under 45 bar H_2. The catalyst showed good selectivity, 60 to 85%, but GVL conversion remained at a modest 25%[19]. Another report on noble metal catalysts for gas phase GVL conversion to MTHF used Ru supported on graphene oxide[59]. Operating at 265 ºC under 25 bar H_2 and 0.512 h^{-1} WHSV full conversion of a 10 wt% GVL in 1,4-dioxane feed was achieved with up to 70% MTHF yield for more than 100 h on stream. Interestingly, for low H_2 pressures (< 10 bar), PDO was the main product with yields above 80% and MTHF became the main product only for high H_2 pressures. This is an anomalous result considering that the conversion of PDO to MTHF is an acid catalyzed dehydration and the mechanism should not involve hydrogen.

The use of non-noble metals was also reported for this reaction. A $CuCr_2O_3$ catalyst, which showed to be selective for the reaction of GVL to PDO with yields up to 83%, also favored the dehydration of PDO to MTHF at 270-290 ºC under 200 bar H_2[60]. The last catalyst studied for this reaction is Cu(30%)/ZrO_2, which facilitated the reaction of a 6 wt% GVL solution in ethanol at 200 to 240 ºC under 60 bar H_2. This catalyst was found to be especially interesting due to the fact that, depending on the reduction temperature, its selectivity could be tailored towards PDO (up to 96% yield

reducing at 700 ºC and reacting at 200 ºC) or to MTHF (up to 91% yield reducing at 400 ºC and reacting at 240 ºC)[61].

Despite the fact that the following articles selectively produce PDO instead of MTHF, they will be described in this section since they provide an interesting insight into the reaction and because PDO is the intermediate between GVL and MTHF. First, a series of *M*-MoOx/SiO_2 catalysts, where *M* was a noble metal (Pt, Rh, Ru, Pd, Ir), were tested in a continuous set-up for the conversion of a 10 wt% LA aqueous solution under 60 bar H_2 at 80 ºC[62]. The most active metal was Rh, and its activity was attributed to the special synergy existing between this noble metal and the oxophilic promoter (MoO_x). Further evidence supporting this statement was provided by carrying out experiments with a physical mixture of Rh/SiO_2 and MoO_x/SiO_2, which showed activity for GVL production from LA but not for its further conversion to MTHF.

A similar noble metal and oxophilic promoter screening was carried out testing several catalysts, prepared by impregnation of Pt over oxophilic supports, finding the best promoter to be MoO_x. Then, different noble metals impregnated over MoOx were tested and found that Pt was the most active one, reaching up to 73% PDO yield in 6 h[63]. The activity of the catalyst was improved when both the noble metal and the oxophilic promoter were impregnated over inorganic matrices. Different supports were tested and it was found that a hydroxyapatite (HAP) provided the highest activity, reaching 93% PDO yield in 5 h at 130 ºC under 50 bar H_2. Considering that the impregnated Pt/HAP was only active to produce GVL from an aqueous 4 wt% LA solutions, the presence of an oxophilic promoter, and its interaction with the noble metal, seems to be necessary in aqueous phase to activate the stable GVL to produce PDO.

Finally, PDO conversion to MTHF is an acid catalyzed dehydration and, hence, it can be accomplished by heating PDO in the presence of acids. When mineral acids were employed high temperatures (above 250 ºC) were required, however, the use of ion exchange resins (such as perflurinated *Nafion-H*) reported up to 90% MTHF yields at conditions as mild as 135 ºC[26,64]. This process is thermodynamically favored (ΔG [250 ºC] = -73 kJ/mol)[26], yet the reaction is reversible[65]. The equilibrium constant for a 1 mol/L PDO solution in liquid water at 300 ºC from a long term reaction process was determined to be:

$$Kc[300\ ºC] = \frac{[MTHF][H_2O]}{[PDO]} = 132 \pm 23$$

2.3. Direct production of MTHF from LA

The production of MTHF was first reported as a by-product of the hydrogenation of LA with a $CuCr_2O_3$ catalyst[60]. More recently, a procedure for the direct production of MTHF from LA by means of a Pd(5%)-Re(5%)/C catalyst at 221 to 242 ºC and 100 bar H_2 was patented[66]. The system allowed total LA conversion, fed as 60 vol% solution in 1,4-dioxane or pure LA, with up to 90% selectivity.

Another example of direct conversion was provided using Cu/SiO_2 catalysts in gas phase, at 265 ºC under 25 bar pressure with a feed made of a 10 wt% LA solution in 1,4-dioxane and a H_2-to-LA molar ratio of 80[67]. It was observed that the selectivity towards MTHF increased with the increase in the metal load (0.1% yield for 5 wt% Cu *vs.* 64% yield for 80 wt% Cu) of the catalyst, consistently with previous publications[68,69]. The process was further improved by promoting the catalyst with 8 wt% of Ni. This catalyst Cu(72%)-Ni(8%)/SiO_2 provided stable 89% MTHF yield for more than 300 h on stream.

The use of Ru over graphene oxide was reported to enable significant MTHF yields from a 10 wt% LA in 1,4-dioxane solution[59]. After a variable screening the best operation conditions produced a stable 48% MTHF yield for over 100 h on stream operating at 265 ºC under 25 bar H_2 pressure and 0.512 h^{-1} WHSV. Interestingly, in this reaction set-up MTHF yield strongly depended on the H_2 pressure. For pressures below 10 bar up to 90% GVL yields were obtained. Besides, for WHSV values above 10 h^{-1} GVL was produced with > 80% yields. These two facts corroborate the high hydrogen availability required for the hydrogenation of GVL and the fact that this step (GVL conversion) is the rate limiting step of the reaction.

The use of Pt-Mo supported on acidic supports was reported to be effective for the aqueous phase conversion of LA to MTHF. Pt(3.9%)-Mo(0.13%)/H-β was found to be the most active catalyst, achieving up to 86% MTHF yield from a 4 wt% LA aqueous solution at 130 ºC under 50 bar H_2 in 24 h[70]. The activity of the studied catalyst series was nicely related to the activity of the catalysts supports to promote the dehydration of

PDO to MTHF, which suggests that, under the applied reaction conditions, this last step of the reaction might became the limiting step. The authors suggest that the hydrophobic nature of the H-β zeolite surface allows for the equilibrium reaction to generate MTHF even in the presence of water. Considering this statement, it is also possible that water competes with the reactants for adsorption on the surface active sites.

Solvent free LA hydrogenation to MTHF was also carried out using a commercial Ru/C catalyst with up to 61% yield. The one-pot three-step reaction consisted on *i)* LA hydrogenation to GVL at 190 ºC under 12 bar H_2 for 45 minutes followed by *ii)* evaporation of the produced water and *iii)* GVL hydrogenation to MTHF at 190 ºC under 100 bar (loaded at room temperature) for 4 h[71]. Finally, the use of FA as the hydrogen source for the LA to MTHF reaction can also be found[72]. Under microwave irradiation a commercial Pd(5%)/C catalyst enabled up to 72% MTHF yields operating at 150 ºC from a 1:3 by volume LA solution in FA. When the reaction was set-up in a continuous flow reactor the yields notably decreased. Maximum 45 - 48% MTHF yields were achieved using Cu based catalysts, which underwent deactivation after 10 to 30 min reaction times.

As a summary, the next table shows the highlights of the reported MTHF production from either LA or GVL using heterogeneous catalysts.

Table 2.1. Literature overview of MTHF and PDO production from LA or GVL using heterogeneous catalysts.

Entry	Catalyst	Feed	T (°C)	P (bar)	Reactor type	Y (%)	Ref.
1	$CuCr_2O_3$	100% GVL	270-290	200	Batch	83 $_{PDO}$	[60]
2	Rh-MoO_x/SiO_2	10% LA in H_2O	80	60	FBR	70 $_{PDO}$	[62]
3	Pt-MoO_x/HAP	4% LA in H_2O	130	50	Batch	93 $_{PDO}$	[63]
4	Ru/GO	10% GVL in dioxane	265	25	FBR	70 $_{MTHF}$	[59]
5	Cu/ZrO_2	6% GVL in ethanol	240	60	Batch	91 $_{MTHF}$	[61]
6	Ru/GO	10% LA in dioxane	265	25	FBR	48 $_{MTHF}$	[59]
7	Pd-Re/C	60 % LA in dioxane	221-242	100	FBR	89 $_{MTHF}$	[66]
8	Cu-Ni/SiO_2	10 % LA in dioxane	265	25	FBR	89 $_{MTHF}$	[67]
9	Pd/C	24% LA in FA	150	Autogen.	MW	72 $_{MTHF}$	[72]
10	Cu/SiO_2	24% LA in FA	150	Autogen.	FBR	48 $_{MTHF}$	[72]
11	$Ru/C^{[c]}$	100% LA	190	100	Batch	61 $_{MTHF}$	[71]
12	Pt-MoO_x/H-β	4% LA in H_2O	130	50	Batch	86 $_{MTHF}$	[70]

FBR stands for Fixed Bed Reactor, *MW* stands for Microwave irradiation, *dioxane* stands for 1,4-dioxane [a] The reaction was carried out in two steps, removing water between them.

2.4. General conclusions

The presented State of the art section illustrates the high amount of research work devoted to the studied reaction. Besides, it also highlights the vast differences on the amount of publications regarding the different steps of the reaction: while GVL production using heterogeneous catalysts accounts for over 50 references in this document (although a higher number of references can be found in the literature), only the presented 12 references could be found in the literature dealing with MTHF or PDO production over heterogeneous catalysis from LA or GVL. Despite some high yield processes are reported for these last steps of the reaction, the low amount of reports on the MTHF production, along with the previously explained interesting properties of this chemical, where the motivating reasons for this thesis.

To briefly summarize the information in this chapter, the following remarks are provided:

- The first step of the reaction (LA hydrogenolysis to GVL) is a relatively easy reaction that can be carried out under conditions as mild as room temperature (25 ºC) under 12 bar H_2 or at 25 ºC in 2-propanol.
- When real biomass hydrolysis products were used for GVL production, the first step (LA production from biomass) was found to be the yield limiting step. In these cases solid filtration was required and, in many of them, acid neutralization, hence, stopping the acid solution recirculation and reuse.
- A number of catalysts effectively catalyze this reaction through different reaction mechanisms *i.e.* both noble and transition metal mediated hydrogenation with H_2; catalytic transfer hydrogenation (both the metal hydride route and *via* acid-base catalysts) using either alcohols or formic acid as the hydrogen source. In addition, acid functionalities seem to enhance the catalyst activity.
- Noble metal catalysts are predominant in this reaction, specially Ru, with many papers using commercial Ru(5%)/C catalyst.
- The second step of the reaction (GVL hydrogenation to PDO and MTHF) is a significantly more demanding and slower reaction, requiring harsher reaction conditions *i.e.* higher temperatures, pressures and longer reaction times.
- The most reported reaction mechanism is the metal (noble and transition) mediated hydrogenation using molecular H_2, using 1,4-dioxane in most cases. In addition, H_2 pressure appears to be a limiting factor which can switch the selectivity from 90% GVL to 48% MTHF on the same reaction set-up and catalyst.
- The use of noble metals is more abundant than transition metals use. Nevertheless, similar high MTHF yields were reported in 1,4-dioxane. On the other hand, aqueous media conversion of GVL is only reported over noble metal catalysts promoted with oxophilic metal oxides (Re, Mo).

2.5. References

[1] P. Kluson, L. Cerveny, *Appl. Catal. A Gen.* **1995**, *128*, 13–31.
[2] L. E. Manzer, *Reductive Intramolecular Cyclocondensation Process and Catalysts for the Manufacture of 5-Methylbutyrolactone from Levulinic Acid.*, **2002**.
[3] L. E. Manzer, *Production of 5- Methylbutyrolactone from Levulinic Acid*, **2003**.
[4] L. E. Manzer, *Appl. Catal. A Gen.* **2004**, *272*, 249–256.
[5] Z. Yan, L. Lin, S. Liu, *Energy & Fuels* **2009**, *23*, 3853.
[6] Y. Gong, L. Lin, Z. Yan, *BioResources* **2011**, *6*, 686–699.
[7] P. P. Upare, J.-M. Lee, D. W. Hwang, S. B. Halligudi, Y. K. Hwang, J.-S. Chang, *J. Ind. Eng. Chem.* **2011**, *17*, 287–292.
[8] M. G. Al-Shaal, W. R. H. Wright, R. Palkovits, *Green Chem.* **2012**, *14*, 1260–1263.
[9] J. Ftouni, A. Muñoz-Murillo, A. Goryachev, J. P. Hofmann, E. J. M. Hensen, L. Lu, C. J. Kiely, P. C. A. Bruijnincx, B. M. Weckhuysen, *ACS Catal.* **2016**, *6*, 5462–5472.
[10] C. Michel, J. Zaffran, A. M. Ruppert, J. Matras-Michalska, M. Jędrzejczyk, J. Grams, P. Sautet, *Chem. Commun.* **2014**, *50*, 12450–12453.
[11] C. Ortiz-Cervantes, J. J. García, *Inorganica Chim. Acta* **2013**, *397*, 124–128.
[12] J. C. Serrano-Ruiz, D. Wang, J. A. Dumesic, *Green Chem.* **2010**, *12*, 574–577.
[13] W. Luo, U. Deka, A. M. Beale, E. R. H. van Eck, P. C. A. Bruijnincx, B. M. Weckhuysen, *J. Catal.* **2013**, *301*, 175–186.
[14] X. X.-L. Du, Y. Y.-M. Liu, J. Wang, Y. Cao, K. K.-N. Fan, *Chinese J. Catal.* **2013**, *34*, 993–1001.
[15] M. Selva, M. Gottardo, A. Perosa, *ACS Sustain. Chem. Eng.* **2013**, 180–189.
[16] R. a Bourne, J. G. Stevens, J. Ke, M. Poliakoff, *Chem. Commun.* **2007**, *2*, 4632.
[17] J.-P. Lange, R. Price, P. M. Ayoub, J. Louis, L. Petrus, L. Clarke, H. Gosselink, *Angew. Chemie Int. Ed.* **2010**, *49*, 4479–4483.
[18] R. J. Haan, J.-P. Lange, *Process for Preparing a Hydroxyacid or Hydroxyester.*, **2011**, WO 2011015645 A2.
[19] P. M. Ayoub, J.-P. Lange, *Process for Converting Levulinic Acid into Pentanoic Acid*, **2008**, WO 2008/142127 A1.
[20] W. Luo, M. Sankar, A. M. Beale, Q. He, C. J. Kiely, P. C. A. Bruijnincx, B. M. Weckhuysen, *Nat. Commun.* **2015**, *6*, 6540.
[21] A. Villa, M. Schiavoni, C. E. Chan-Thaw, P. F. Fulvio, R. T. Mayes, S. Dai, K. L. More, G. M. Veith, L. Prati, *ChemSusChem* **2015**, *8*, 2520–2528.
[22] A. M. R. Galletti, C. Antonetti, V. De Luise, M. Martinelli, *Green Chem.* **2012**, *14*, 688.
[23] A. S. Piskun, J. E. de Haan, E. Wilbers, H. H. van de Bovenkamp, Z. Tang, H. J. Heeres, *ACS Sustain. Chem. Eng.* **2016**, *4*, 2939–2950.
[24] C. Moreno-Marrodan, P. Barbaro, *Green Chem.* **2014**, *16*, 3434.
[25] J. Tan, J. Cui, G. Ding, T. Deng, Y. Zhu, Y. Li, *Catal. Sci. Technol.* **2016**, *6*, 1469–1475.
[26] J. C. Serrano-Ruiz, A. Pineda, A. M. Balu, R. Luque, J. M. Campelo, A. A. Romero, J. M. Ramos-Fernández, *Catal. Biorefineries* **2012**, *195*, 162–168.
[27] J. C. Serrano-Ruiz, R. M. West, J. A. Dumesic, *Annu. Rev. Chem. Biomol. Eng.* **2010**, *1*, 79–100.
[28] D. M. Alonso, S. G. Wettstein, J. a. Dumesic, *Green Chem.* **2013**, *15*, 584.
[29] O. A. Abdelrahman, A. Heyden, J. Q. Bond, *ACS Catal.* **2014**, *4*, 2–9.
[30] K. Yan, J. Liao, X. Wu, X. Xie, *RSC Adv.* **2013**, *3*, 3853–3856.
[31] J. Zhang, J. Chen, Y. Guo, L. Chen, *ACS Sustain. Chem. Eng.* **2015**, *3*, 1708–1714.
[32] A. M. Hengne, C. V. Rode, *Green Chem.* **2012**, *14*, 1064–1072.
[33] J. Zhu, Y. Tang, K. Tang, *RSC Adv.* **2016**, *6*, 87294–87298.
[34] A. P. Dunlop, J. W. Madden, *Process for Preparing Gamma-Valerolactone*, **1957**, US 2786852 A.
[35] D. Di Mondo, D. Ashok, F. Waldie, N. Schrier, M. Morrison, M. Schlaf, *ACS Catal.* **2011**, *1*, 355.
[36] J. C. Serrano-Ruiz, D. J. Braden, R. M. West, J. A. Dumesic, *Appl. Catal. B Environ.* **2010**, *100*, 184–189.
[37] D. J. Braden, C. a. Henao, J. Heltzel, C. C. Maravelias, J. a. Dumesic, *Green Chem.* **2011**, *13*, 1755.
[38] L. Zhang, A. M. Karim, M. H. Engelhard, Z. Wei, D. L. King, Y. Wang, *J. Catal.* **2012**, *287*, 37–43.
[39] X.-L. L. Du, L. He, S. Zhao, Y.-M. M. Liu, Y. Cao, H.-Y. Y. He, K.-N. N. Fan, *Angew. Chemie Int. Ed.* **2011**, *50*, 7815–7819.

[40] D. Ding, J. Wang, J. Xi, X. Liu, G. Lu, Y. Wang, *Green Chem.* **2014**, *16*, 3846.
[41] X. Tang, Z. Li, X. Zeng, Y. Jiang, S. Liu, T. Lei, Y. Sun, L. Lin, *ChemSusChem* **2015**, *8*, 1601–1607.
[42] S. G. Wettstein, D. M. Alonso, Y. Chong, J. a. Dumesic, *Energy Environ. Sci.* **2012**, *5*, 8199.
[43] Z. Yang, Y.-B. Huang, Q.-X. Guo, Y. Fu, *Chem. Commun.* **2013**, *49*, 5328–5330.
[44] L. Deng, Y. Zhao, J. Li, Y. Fu, B. Liao, Q.-X. X. Guo, *ChemSusChem* **2010**, *3*, 1172–1175.
[45] R. R. Gowda, E. Y.-X. Chen, *ChemSusChem* **2016**, *9*, 181–185.
[46] R. J. Haan, J.-P. Lange, L. Petrus, C. J. Maria, *Hydrogenation Process for the Conversion of a Carboxylic Acid or an Ester Having a Carbonyl Group*, **2007**, US 2007208183 A1.
[47] M. Chia, J. a. Dumesic, *Chem. Commun.* **2011**, *47*, 12233–12235.
[48] J. Wang, S. Jaenicke, G.-K. Chuah, *RSC Adv.* **2014**, *4*, 13481–13489.
[49] J. Song, L. Wu, B. Zhou, H. Zhou, H. Fan, Y. Yang, Q. Meng, B. Han, *Green Chem.* **2015**, *17*, 1626–1632.
[50] Z. Xue, J. Jiang, G. Li, W. Zhao, J. Wang, T. Mu, *Catal. Sci. Technol.* **2016**, *6*, 5374–5379.
[51] A. H. Valekar, K.-H. Cho, S. K. Chitale, D.-Y. Hong, G.-Y. Cha, U.-H. Lee, D. W. Hwang, C. Serre, J.-S. Chang, Y. K. Hwang, *Green Chem.* **2016**, *18*, 4542–4552.
[52] A. S. Amarasekara, M. A. Hasan, *Catal. Commun.* **2015**, *60*, 5–7.
[53] M. J. Gilkey, B. Xu, *ACS Catal.* **2016**, *5*, 1420–1436.
[54] B. . Hoffer, E. Crezee, F. Devred, P. R. . Mooijman, W. . Sloof, P. . Kooyman, A. . van Langeveld, F. Kapteijn, J. . Moulijn, *Appl. Catal. A Gen.* **2003**, *253*, 437–452.
[55] A. Chojecki, M. Veprek-Heijman, T. E. Müller, P. Schärringer, S. Veprek, J. A. Lercher, *J. Catal.* **2007**, *245*, 237–248.
[56] Z. Li, X. Tang, Y. Jiang, Y. Wang, M. Zuo, W. Chen, X. Zeng, Y. Sun, L. Lin, *Chem. Commun.* **2015**, *51*, 16320–16323.
[57] M. Vasiliu, K. Guynn, D. A. Dixon, *J. Phys. Chem. C* **2011**, *115*, 15686–15702.
[58] I. T. Horváth, H. Mehdi, V. Fabos, L. Boda, L. T. Mika, *Green Chem.* **2008**, *10*, 238.
[59] P. P. Upare, M. Lee, S.-K. Lee, J. W. Yoon, J. Bae, D. W. Hwang, U.-H. Lee, J.-S. Chang, Y. K. Hwang, *Catal. Today* **2015**, *265*, 174–183.
[60] R. V. J. Christian, H. D. Brown, R. M. Hixon, *J. Am. Chem. Soc.* **1947**, *69*, 1961–1963.
[61] X.-L. Du, Q.-Y. Bi, Y.-M. Liu, Y. Cao, H.-Y. He, K.-N. Fan, *Green Chem.* **2012**, *14*, 935.
[62] M. Li, G. Li, N. Li, A. Wang, W. Dong, X. Wang, Y. Cong, *Chem. Commun.* **2014**, *50*, 1414–1416.
[63] T. Mizugaki, Y. Nagatsu, K. Togo, Z. Maeno, T. Mitsudome, K. Jitsukawa, K. Kaneda, *Green Chem.* **2015**, *17*, 5136–5139.
[64] G. A. Olah, A. P. Fung, R. Malhorta, *Synthesis (Stuttg).* **1981**, 474.
[65] A. Yamaguchi, N. Hiyoshi, O. Sato, K. K. Bando, Y. Masuda, M. Shirai, *J. Chem. Eng. Data* **2009**, *54*, 2666–2668.
[66] D. C. Elliott, J. G. Frye, *Hydrogenated 5C Compound and Method of Making*, **1999**, US 5883266.
[67] P. P. Upare, J.-M. Lee, Y. K. Hwang, D. W. Hwang, J.-H. Lee, S. B. Halligudi, J.-S. Hwang, J.-S. Chang, *ChemSusChem* **2011**, *4*, 1749–1752.
[68] C.-H. Zhou, X. Xia, C.-X. Lin, D.-S. Tong, J. Beltramini, *Chem. Soc. Rev.* **2011**, *40*, 5588.
[69] R. Palkovits, *Angew. Chemie Int. Ed.* **2010**, *49*, 4336–4338.
[70] T. Mizugaki, K. Togo, Z. Maeno, T. Mitsudome, K. Jitsukawa, K. Kaneda, *ACS Sustain. Chem. Eng.* **2016**, *4*, 682–685.
[71] M. G. Al-Shaal, A. Dzierbinski, R. Palkovits, *Green Chem.* **2014**, *16*, 1358–1364.
[72] J. M. Bermudez, J. A. Menendez, A. A. Romero, E. Serrano, J. Garcia-Martinez, R. Luque, *Green Chem.* **2013**, *15*, 2786–2792.

Chapter 3

Objective and scope of the thesis

In the first chapter of this Ph.D. thesis the nowadays energy system has been briefly described as well as the forecasted switch towards renewable energy sources and vectors. The advantages and drawbacks of this new energy system have been described in order to provide an energetic context overview. As part of this new energy system, the transformation of LA into the drop-in biofuel MTHF has been presented. In Chapter 2 the interest of this particular reaction has also been highlighted thrugh a critical literature review of the reported processes producing the intermediate GVL and MTHF.

Against this background, the objective of this thesis is the **study of MTHF production from LA using non-noble metals and green solvents.** This research is motivated not only by an academic interest, improving the basic knowledge of this biorefinery reaction, but also others related to it, such as a contributions to the green chemistry and sustainable process engineering fields.

For this purpose, **Ni-Cu-Al based catalysts** were selected since they are well known hydrogenolysis catalysts and a more sustainable and cheaper alternative to noble metal based catalysts. **Green solvents,** such as water or biogenic alcohols, are the only viable choice for the biorefinery processes in order to fulfill the sustainability criterion.

In order to achieve the primary objective of the thesis, a series of milestones need to be fulfilled:

- Selection of the most suitable solvent for the reaction. The literature review showed that many different solvents have been used for this reaction; hence, the first objective should be the selection of the best ones for our reaction conditions. Besides, understanding the role of the solvent in the reaction is regarded as an important issue from both the mechanistic and the process point of views.
- Optimization of the catalyst formulation and preparation method. Again, a number of different catalysts prepared by a variety of methods have been reported. The goal of this research is to find a Ni-Cu-Al based catalyst which shows high activity and selectivity for the conversion of LA to MTHF. Therefore, an appropriated tune of the metal phases and the acidity of the support is considered fundamental.
- A thorough characterization of the fresh and used catalysts is essential in order to correlate the observed activity results with the properties of the different catalysts and its further improvement.
- Catalyst stability assessment is a must for any catalytic process and understanding of the deactivation causes the first step for catalyst deactivation prevention or regeneration.

Despite the academic focus of the presented research, the generated knowledge could help to develop future biorefinery processes. It should be noted that biomass conversion into LA processes are currently working at semi industrial scale. The profitability of those processes will depend on the marketability of the products and, thus, on the development of LA valorization routes and processes. In this regard, a drop-in biofuel production presents an overwhelming market potential compared to any other product, provided that competitive prices can be achieved.

Chapter 4

Experimental

Table of contents

4.1. Abstract 71

4.2. Catalyst preparation 71

4.2.1. Impregnation 71

4.2.2. Co-precipitation 71

4.2.3. Sol-gel 72

4.2.4. Calcination and reduction 72

4.3. Experimental set-ups 72

4.4. Analytical techniques 74

4.4.1. Liquid sample analysis 74

4.4.2. Gas sample analysis 74

4.4.3. CG-MS 74

4.5. Characterization techniques 75

4.5.1. Elemental analysis, catalyst composition 75

4.5.2. CO Chemisorption 75

4.5.1. NH_3 Temperature programmed desorption (NH_3-TPD) 75

4.5.2. Surface area 75

4.5.3. Temperature programmed reduction (TPR) 76

4.5.4. Thermogravimetric analysis (TGA) 76

4.5.5. X-ray diffraction analysis (XRD) 76

4.5.6. Transmission microscopy analysis (TEM) 76

4.5.7. X-ray photoelectron spectroscopy (XPS) 77

4.6. Equations 77

4.1. Abstract

This chapter will summarize the main experimental procedures used during this thesis. This way, all the technical details will be easy to find and it will help the fluency of the following chapters dealing with the experimental results, discussion and conclusions.

4.2. Catalyst preparation

4.2.1. Impregnation

Impregnated catalysts were prepared according to the following procedure. The desired amounts of γ-Al_2O_3 (Alfa-Aesar) were mixed with deionized water in a 1:9 weight ratio and the proper amounts of metal precursor salts ($Ni(NO_3)_2 \cdot 6H_2O$, Sigma-Aldrich and $Cu(NO_3)_2 \cdot 5/2H_2O$, Alfa-Aesar) were added and stirred overnight at 90 rpm. Water was removed by heating the solution to 60 ºC in a rotatory vacuum evaporator.

Sequential impregnation catalysts were prepared following the same procedure but only one of the metal precursor salts was added to the solution. Water was removed under vacuum and the powder was crushed and calcined. The so obtained powder was, then, impregnated with the other metal precursor salt following the same procedure.

4.2.2. Co-precipitation

Co-precipitated catalysts were prepared according to the following procedure. 0.5 mol/L concentration metal precursor salt ($Al(NO_3)_3 \cdot 18H_2O$, Alfa Aesar, $Ni(NO_3)_2 \cdot 6H_2O$, Sigma-Aldrich and $Cu(NO_3)_2 \cdot 5/2H_2O$, Alfa-Aesar) solutions were prepared with deionized water and mixed. The resulting solution was then added drop-wise to 200 mL of deionized water under 500 rpm stirring while keeping the pH of the solution fixed at 7.0 by addition of concentrated NH_4OH. The formed slurry was then aged overnight at 60 ºC and vacuum filtered.

4.2.3. Sol-gel

The sol-gel catalysts were prepared according to the following method. Calculated amounts of aluminum isopropoxyde (AIP, Sigma-Aldrich) were dissolved in deionized water (AIP:H_2O 9:1 weight ratio) at 40 ºC under vigorous stirring. Ni and Cu precursor salts were dissolved in ethanol and added drop wise to the AIP solution. The pH was kept between 3.8 and 4.2 by addition of 1 mol/L HNO_3 solution during the whole process. The resulting solution was then aged for 30 min, sonicated for another 30 min and, then, evaporated at 50 ºC for 48 h.

4.2.4. Calcination and reduction

Regardless of the preparation method, the catalysts were dried overnight at 110 ºC, crushed to < 425 μm and calcined at 300 ºC (or other temperature where specified) for 2 h (2 ºC/min ramp). Prior to activity tests, the catalysts were reduced at 450 or 600 ºC (10 ºC/min heating ramp) for 1 h under H_2 flow and cooled down under N_2 flow.

4.3. Experimental set-ups

The catalyst activity tests of Chapters 4 and 5 were carried out in an Autoclave Engineers bench scale plant with a 300 mL 316SS reactor (see Figure 4.1). Once the reactant (35 g of 5 wt% LA, GVL, or MTHF in the selected solvent) and the freshly activated (pre-reduced) catalyst were fed to the reactor, the system was sealed, purged three times with H_2, loaded with H_2, and heated to the reaction temperature. The initial H_2 load was controlled so that at the beginning of the reaction the pressure in the reactor was 70 bar. After the desired temperature was reached, the stirring (600 rpm) was started. At the end of the reaction the stirring was stopped and the reactor was left to cool to room temperature. The used catalysts were separated from the liquid products by centrifugation and gas and liquid samples were taken for GC analysis.

Figure 4.1. Bench scale plant (left), detail of the top of the reactor (center) and the 300 mL reactor and heating jacket (right).

A second reaction set-up was used for the activity tests of Chapters 6 and 7. It consisted on 50 mL Hastelloy autoclaves with a magnetic stirrer and a glass liner (see Figure 4.2). The typical reaction mixtures consisted of 5.3 g of a 5 wt% substrate in solvent solution with a substrate/catalyst weight ratio of 10. The autoclaves were fed with the reduced catalysts and the reaction mixture, sealed, flushed three times with the appropriate gas, loaded with 40 bar H_2 or N_2, placed in preheated heating plates, and stirred at 500 rpm, typically for 5 h. At the end of the reaction, the stirring was stopped, the autoclaves were cooled down, and the pressure in the autoclaves was slowly released. The sampling procedure was analogous to the previously described one.

Figure 4.2. 50 mL batch reactors and heating plates.

4.4. Analytical techniques

4.4.1. Liquid sample analysis

Liquid samples were analyzed using a 6890N gas chromatograph (GC, Agilent Technologies) equipped with a flame ionization detector (FID) and a thermal conductivity detector (TCD). The GC was equipped with a DB-1 column (60 m × 530 μm × 5 μm, Agilent Technologies), He as carrier gas and 2-hexanol was used as external standard. The used temperature program consisted on 5 min isotherm at 40 ºC followed by a 10 ºC/min heating ramp up to 250 ºC and 10 min isotherm at the final temperature.

The analyses in Chapter 7 were carried out in an Agilent HP6890 series GC device equipped with a CP-WAX-52-CB column (60 m x 0.25 mm x 0.25 μm) and a FID detector with N_2 as carrier gas and 1-hexanol as external standard. The temperature program in this case was analogous to that used in the other GC device.

4.4.2. Gas sample analysis

Gas samples were collected in plastic gas sample bags and analyzed using an Agilent 7890 GC equipped with a HP-Molesieve (30 m × 535 μm × 25 μm) and a HP-PLOT/Q (30 m × 320 μm × 20 μm) column, FID and TCD detectors, and He as carrier gas. The calibration of the device was carried out using different injection splits of a standard gas bottle containing H_2, N_2, CO, CO_2, and C1 to C4 alkanes and alkenes (Air Liquide).

4.4.3. CG-MS

Unidentified reaction products were identified by a 5973 GC (Agilent technologies) apparatus equipped with a quadrupole mass-spectrometer detector and an Agilent 123-3262 (60 m × 320 μm × 0.25 μm) column and He as carrier gas. The experimental mass spectra were compared by the devices software with spectra in the library and logical matches with above 80% similarity were typically accepted.

4.5. Characterization techniques

4.5.1. Elemental analysis, catalyst composition

The metal content of the catalysts was measured by inductively coupled plasma–optical emission spectroscopy (ICP-OES) on a Perkin Elmer Optima 2000 OV device. Prior to the analysis samples were digested in a mixture of HCl, HNO_3, and HF using an ETHOS 1 Advanced Microwave Digestion System.

4.5.2. CO Chemisorption

CO chemisorption was carried out in an AutoChem II (Micromeritics) device equipped with a calibrated TCD detector. The weighted samples were placed in a U shaped quartz cell, reduced (except for Ru/C which was supplied at reduced state) with the same temperature program used for the activation of the catalyst (*i.e.* 10 ºC/min ramp under H_2 up to 450 or 600 ºC and one hour isotherm followed by cooing under He in this case), flushed with He and cooled down to 35 ºC. At this temperature CO pulses, 0.01778 cm^3 of a 5 vol% CO in He mixture, were injected to the sample until saturation was observed. As this technique allows no differentiation between the CO chemisorbed on Ni and Cu, only the total CO uptake (mmol CO/g catalyst) will be considered.

4.5.1. NH_3 Temperature programmed desorption (NH_3-TPD)

Ammonia temperature programmed desorption was carried out in an AutoChem II (Micromeritics) device. The weighted samples were placed in a U shaped quartz cell, reduced (except for Ru/C, which was supplied at reduced state) with the temperature program used prior to the activity tests, saturated with 50 mL/min of a 10 vol % NH_3 in He gas flow for 30 min at 100 ºC and then flushed with He at 150 ºC for 60 min to remove the physically adsorbed NH_3. The samples were then heated to 900 ºC by a 10 ºC/min ramp while monitoring NH_3 release by means of a calibrated TCD detector.

4.5.2. Surface area

Surface area, pore volume, and pore size distribution were determined by N_2 physisorption at –196 ºC on an Autosorb 1C-TCD (Quantachrome). Prior to analysis, all samples were degassed at 250 ºC and 10 Pa for 3 h. The surface area was calculated

using the Brunauer - Emmett - Teller (BET) method, and pore size distribution was calculated using the Barrett-Joyner- Halenda (BJH) method on the N_2 desorption curve.

4.5.3. Temperature programmed reduction (TPR)

The weighted, non-activated, catalyst samples were placed in a U shaped quartz cell and subjected to temperature programmed reduction (TPR) in the cited AutoChem II instrument (Micromeritics) equipped with a TCD detector. The measurements were carried out at a 10 ºC/min heating rate up to 1100 ºC with 50 mL/min gas flow of a 5 vol% H_2 mixture in Ar while monitoring H_2 consumption.

4.5.4. Thermogravimetric analysis (TGA)

Thermogravimetric analyses (TGA) of the catalysts were performed on a Mettler Toledo TGA/SDTA851 using pure oxygen as an oxidizing agent. The catalysts were heated at 800 ºC at a heating rate of 5 ºC/min while continuously recording the mass of the sample.

4.5.5. X-ray diffraction analysis (XRD)

Pre-reduced catalyst samples were analyzed by XRD in an Xpert PRO device equipped with a Bragg-Brentano goniometer and a Cu cathode working at 40 kV and 40 mA. The spectra were recorded in the 10º to 80º 2θ range with a 0.026 step size.

High resolution XRD data were collected on a Bruker D8 Advance diffractometer equipped with a Cu tube, Ge(111) incident beam monochromator (λ = 1.5406 Å) and a Sol-X energy dispersive detector. The sample was mounted on a zero background silicon wafer embedded in a generic sample holder. Data were collected from 40º to 50º 2θ (step size 0.01 and time per step = 517 s) at room temperature. A fixed divergence and antiscattering slit 1º giving a constant volume of sample illumination were used.

The obtained XRD patterns were compared with the *Powder Diffraction Files* (PDF) by Xpert-Pro Score tool.

4.5.6. Transmission microscopy analysis (TEM)

TEM/Scanning TEM images were obtained on a TECNAI G2 20 TWIN operated at 200 kV and equipped with LaB_6 filament, EDAX energy dispersive electron

spectroscopy (EDS) microanalysis system and high angle annular dark-field-scanning transmission electron microscopy (HAADF-STEM).Samples used for TEM analysis were prepared via dispersion into octane solvent and keeping the suspension in an ultrasonic bath for 15 min, after which a drop of suspension was spread onto a TEM molybdenum grid (300 Mesh) covered by a *holey* carbon film followed by drying under vacuum.

4.5.7. X-ray photoelectron spectroscopy (XPS)

XPS spectra of the reduced catalysts were obtained on a VG Escalab 200R spectrometer equipped with a hemispherical electron analyzer and a Mg Kα (hν = 1253.6 eV) X-ray source. Binding Energy (BE) values were referred to C1s peak at 284.6 eV.

4.6. Equations

Reaction yield (Y), conversion (X), selectivity (S) and carbon balance (CB) were calculated according to the following equations:

$$X = 100\left(1 - \frac{n^{t}_{React} \times \vartheta^{C}_{React}}{n^{t=0}_{React} \times \vartheta^{C}_{React}}\right) = 100\left(1 - \frac{n^{t}_{React}}{n^{t=0}_{React}}\right) \quad [\%]$$

$$Y_i = 100\frac{n^{t}_{i} \times \vartheta^{C}_{i}}{n^{t=0}_{React} \times \vartheta^{C}_{React}} \quad [\%] \qquad\qquad S_i = 100\,{}^{Y_i}/_{X} \quad [\%]$$

$$CB = 100\frac{\sum_{\forall i}(n^{t}_{i} \times \vartheta^{C}_{i})}{n^{t=0}_{React} \times \vartheta^{C}_{React}} = 100 - X + \sum_{\substack{\forall i \\ i \neq React}} Y_i \quad [\%]$$

$$SiteTimeYield\ (STY) = \frac{n^{\Delta t}_{MTHF}}{m_{Cat.} \times \frac{mmol_{CO}}{g_{Cat.}} \times \Delta t} \quad [h^{-1}]$$

Where n^{t}_{i} is the moles of the product "i" at reaction time "t", ϑ^{C}_{i} is the carbon atoms in the molecule "i", "React" stands for reactant and "t = 0" means

at the beginning of the reaction. $n_{MTHF}^{\Delta t}$ Stands for the amount of MTHF mol produced in the Δt reaction time. $m_{Cat.}$ is the used catalyst mass, $mmol_{CO}/g_{Cat.}$ stands for the adsorbed CO amount per gram of catalysts, determined by CO chemisorption.

The *Site Time Yield* (STY) is calculated as a pseudo turnover frequency and expresses the produced MTHF mol per metal active site mol (determined by CO chemisorption) and time.

Chapter 5

Levulinic acid hydrogenolysis on Al_2O_3 supported Ni-Cu bimetallic catalysts

The work contained in this chapter was published under the title “Levulinic acid hydrogenolysis on Al_2O_3-based Ni-Cu bimetallic catalysts” in the *Chinese Journal of Catalysis* **2014**, 35, 656-662.

Table of contents

5.1. Introduction 83

5.2. Catalyst characterization 84

5.3. Catalyst activity 87

5.4. Conclusions 93

5.5. References 94

5.1. Introduction

In this Chapter an initial study on the aqueous phase LA hydrogenolysis is presented. This research served the purpose of setting up all the experimental, analytical and characterization devices at the beginning of this thesis. It also provided a first contact with the studied reaction and some helpful conclusions for the future work were extracted from it.

As previously described in the introduction chapter, LA can be obtained in aqueous solution from the hydrolysis of lignocellulosic biomass. For this reason, and considering that water is produced during LA hydrogenolysis, it arose as the first solvent choice for the reaction. Additional benefits of water are its low cost and environmentally friendly characteristics.

In the literature MTHF production in aqueous media is reported using noble metal (Pt, Pd) catalysts promoted with oxophilic metals/oxides (Mo, Re)[1,2]. The use of milder reaction conditions[3] or catalysts with lower acidity[4] led to the formation of PDO instead of MTHF, whereas the absence of the oxophilic promoter on the catalyst dramatically reduced the activity for GVL conversion to either PDO or MTHF[2–4].

In this chapter, LA hydrogenolysis in an aqueous medium was studied using Ni-Cu based catalysts searching for a more economical alternative to noble metal catalysts. Three catalysts were prepared by a wet impregnation process over a commercial γ-Al_2O_3: Ni monometallic (denoted as NiWI), Cu monometallic (CuWI) and Ni-Cu (2:1 weight ratio) bimetallic (Ni-CuWI). The assessment of their catalytic activity was carried out in order to determine the most active metal phase and check for possible bimetallic promotion effects. After finding the interesting activity of the bimetallic catalyst, two more catalysts prepared *via* sol-gel procedure and calcined at different temperatures (denoted as SG300 and SG450 respectively) were also tested.

Catalyst characterization was conducted on fresh and used catalysts samples in order to gain a deeper understanding on the reaction and the required catalyst properties.

5.2. Catalyst characterization

Table 5.1 presents the textural properties and the experimentally determined metal contents of the calcined catalysts.

Table 5.1. Elemental and textural characterization of the calcined catalysts

Catalyst	Ni (wt%)	Cu (wt%)	Ni + Cu	Ni/Cu	BET Area (m^2/g)	Pore volume (cm^3/g)	Pore radius (nm)
γ-Al_2O_3	0	0	0	-	227.2	0.81	6.8
NiWI	36.1	0	36.1	∞	146.9	0.35	4.6
CuWI	0	30.0	30.0	0	152.9	0.58	7.6
Ni-CuWI	19.6	12.9	32.5	1.5	151.0	0.36	4.8
SG300	13.3	8.9	22.2	1.5	186.1	0.20	2.1
SG450	8.6	5.5	14.1	1.6	132.4	0.16	4.9

The experimentally determined metal contents of the WI catalysts were comparable with the theoretical metal contents. Ni contents were either higher or lower than the theoretical values, whereas Cu contents were consistently lower than the expected compositions. The SG catalysts featured a comparable Ni-Cu ratio with that of the Ni-CuWI catalyst despite the lower metal contents of the SG catalysts.

The three WI catalysts featured lower surface areas (~ 150 m^2/g) than that of the bare commercial γ-Al_2O_3 support (~ 230 m^2/g). Pore volume was also lower, but the decrease was more significant for the Ni-containing catalysts by a factor of two. The addition of Cu only resulted in a pore volume loss of 25 %, suggesting that *i)* Ni preferentially deposited onto the pores of the Al_2O_3, whereas Cu deposited on the outer surface of the Al_2O_3 support or *ii)* Cu obstructed smaller pores, whereas Ni deposited on larger pores. Considering the differences in the average pore radius between the WI catalysts and the Al_2O_3 support, the first option is more likely because incorporation of Ni decreased the pore radius, whereas Cu addition enlarged the average pore size. Nevertheless, the effects associated with Ni deposition seem to prevail over the changes induced by Cu deposition.

Using the SG method, a higher surface area was achieved at a calcination temperature of 300 ºC. However, a reduced surface area was obtained at the highest calcination temperature (450 ºC) despite the lower metal loading of the corresponding catalyst. Calcination had a minimal effect on the pore volume of the final catalysts; however, the pore volume of the SG450 catalyst was approximately three times lower

than that of the Ni-CuWI catalyst. Also, a higher calcination temperature enlarged the average pore size.

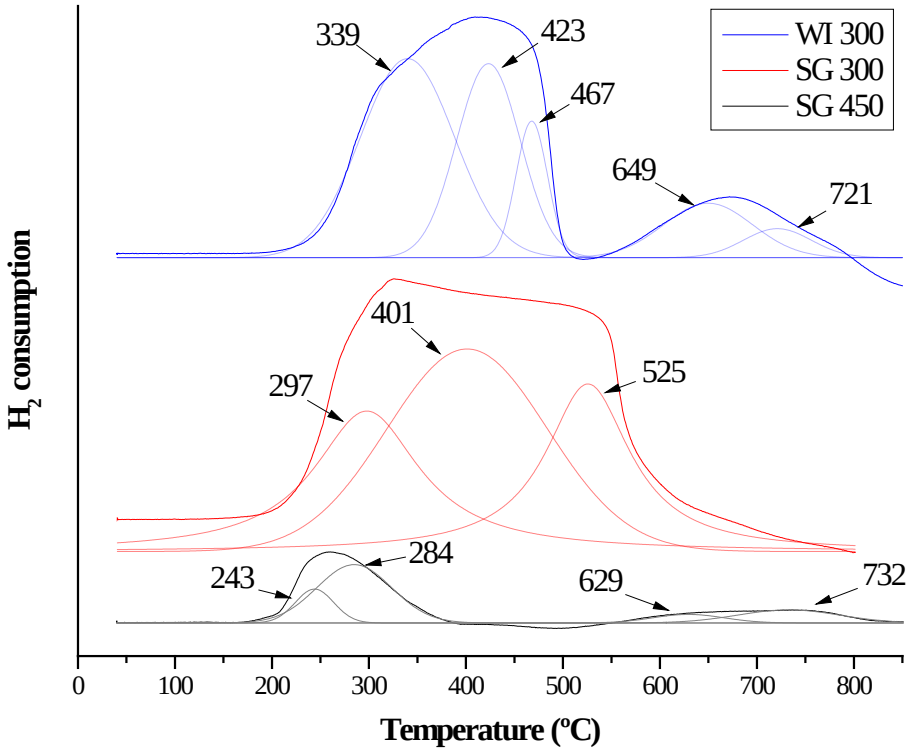

Figure 5.1. TPR analysis of the bimetallic catalysts (Ni-CuWi, SG300 and SG450).

Figure 5.1 show the results of the TPR analysis of the three bimetallic catalysts where important differences regarding the composition and reducibility of the metallic species became evident. The strong Ni-alumina interactions, corresponding to peaks observed above 600 ºC in the SG450 catalyst, forming nickel aluminates were absent in the SG300 catalyst. This fact indicates that these interactions are strongly dependent on the calcination temperature[5]. However, the Ni-CuWI catalyst, which was calcined at 300 ºC, also showed Ni aluminate species[6] with reduction peaks (above 600 ºC). This discrepancy may be attributed to the higher nickel content in the WI catalyst (compared to that in the SG catalyst) and the different Al_2O_3 supports; the sol-gel-derived alumina calcined at 300 ºC is not expected to be fully converted to γ-Al_2O_3[7]. Thus, the differences between the supports can instigate the formation of different species[5].

Copper species were reduced at temperatures ranging from 245 to 340 ºC and the reduction peaks maximum switched to higher temperatures in direct relation to the Cu loading of the catalyst. Higher metal loadings promote agglomeration and formation of larger crystals that required higher temperatures and longer times for reduction[8].

Additionally, Cu addition induced a shift to lower temperatures in the reduction peaks ascribed to weakly interacting Ni, most probably *via* hydrogen spillover mechanism[8] that facilitate the reduction reaction of Ni oxydes and nucleate the formation of metallic Ni particles. This reduction took place at lower temperatures in the SG300 catalyst (compared to SG450), as indicated by the overlapping peaks and the fewer nickel aluminates formed.

After the metallic phase characterization, the acidic properties of the Al_2O_3 support and the catalysts prepared by impregnation, and its dependence on the composition were characterized by NH_3-TPD. The profiles are presented in Figure 5.2.

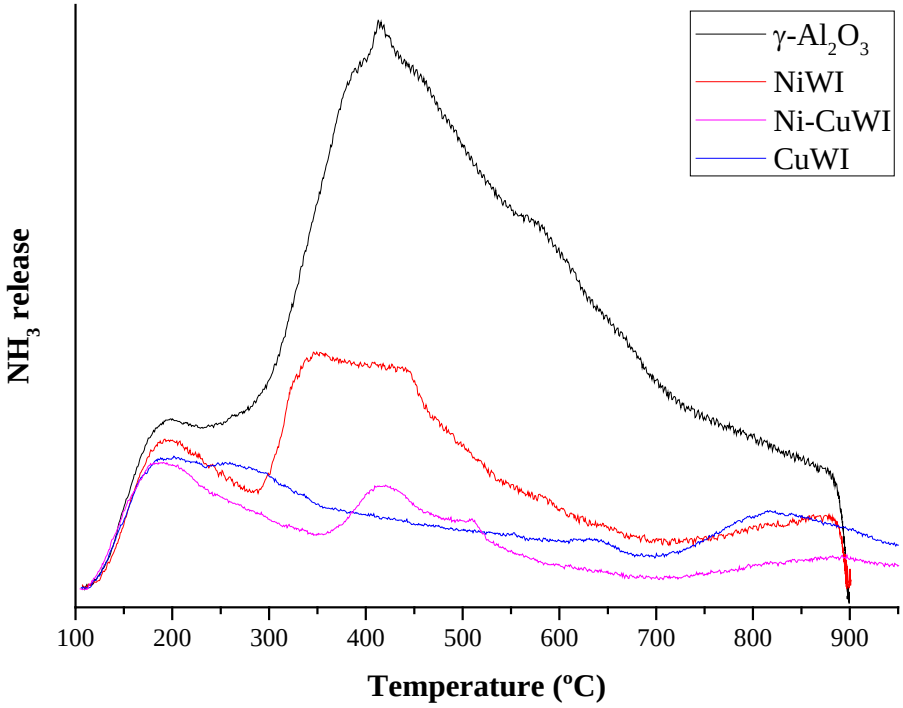

Figure 5.2. NH_3-TPD profiles of γ-Al_2O_3, NiWI, CuWI and Ni-CuWI catalysts.

As observed in Figure 5.2, the bare γ-Al_2O_3 support exhibited the highest acidity, displaying a small peak centered at 200 ºC and a broad peak between 300 and 700 ºC with its maximum at 410 ºC. The incorporation of Ni resulted in a minor acidity loss in the low-temperature region (< 250 ºC) while a considerable reduction in acidity was observed in the high-temperature region. However, significant desorption peaks centered at 400 ºC were also observed. Acidity loss by metal incorporation may occur by the metal anchoring on the supports acid sites[9] or by site blocking by larger metal particles. Cu addition, on the other hand, evenly decreased the acidity across the studied temperature range. The Ni-CuWI catalyst featured an intermediate acidity profile, but

with a higher acidity loss in the low-temperature region when compared with that of the other catalysts. In the high-temperature region, Ni-CuWI showed two small peaks with an appreciable shift to higher temperatures when compared with the peaks of NiWI. These observations were attributed to the co-existence of the Cu and Ni species.

5.3. Catalyst activity

The hydrogenolysis activities of the five catalysts were measured for the conversion of LA into α-angelica lactone (AL), GVL, and MTHF in aqueous solutions at 250 ºC under 65 bar H_2. First, a series of experiments was carried out using the WI catalysts to determine the most active metal phase for this reaction and evaluate the effect of the co-existence of Cu and Ni phases in the bimetallic catalyst. The results are summarized in Figure 5.3.

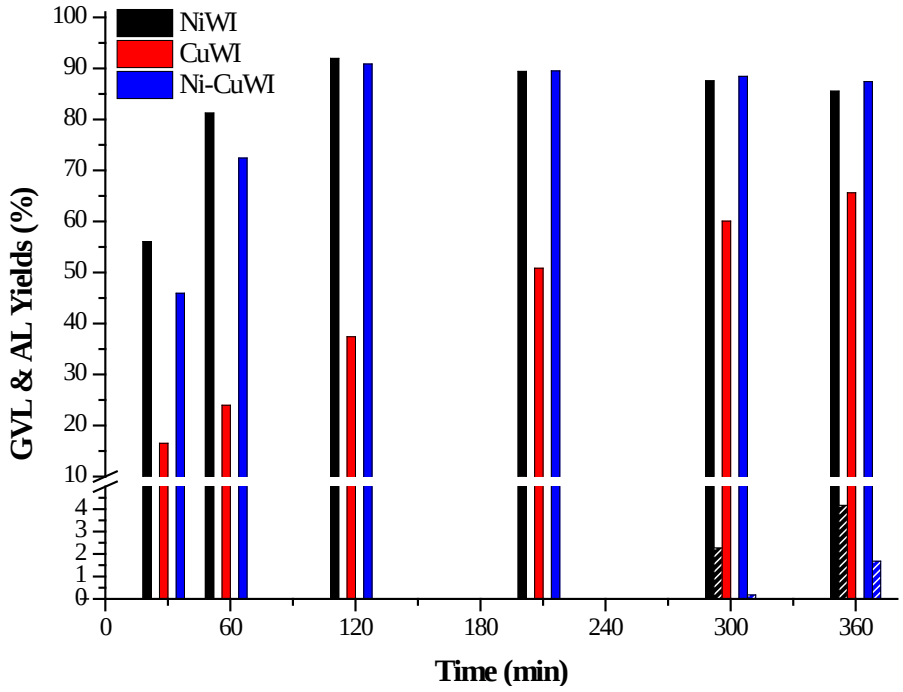

Figure 5.3. GVL (solid) and AL (stripped) yields *vs.* reaction time for the WI catalysts. Reaction conditions: 250 ºC, 65 bar H_2, LA/Cat = 10 g/g, stirring 600 rpm.

In Figure 5.3 it is showed that the NiWI and Ni-CuWI catalysts were the most active and produced maximum 92% GVL yields after 2 h of reaction, with total LA conversion. Nevertheless, only trace amounts of MTHF were detected in the reaction mixture, showing this reaction system to be inadequate for its production. On the other hand, the CuWI catalyst exhibited a significantly lower activity, achieving a non-

asymptotic maximum 66% GVL yield after 6 h of reaction, with 75% LA conversion. Despite the lower activity of Cu, its presence seems to inhibit AL production, as shown by the ~ 0 %, 1.6 %, and 4.1 % AL yields obtained with the CuWI, Ni-CuWI, and NiWI catalysts respectively. This is an important finding since AL is a well-known coke precursor over acidic surfaces[10–12]. AL concentrations became significant at reaction times greater than 3 h, well after complete LA conversion was achieved (< 2 h). Thus, the detected AL is believed to be produced out of the previously formed GVL or by AL desorption from the catalyst surface. The first option is considered to be the real cause considering that GVL dehydrogenation in aqueous solutions under H_2 atmospheres was previously reported in the presence of homogeneous catalysts[13].

In order to further prove the above mentioned hypothesis GVL was used as substrate in the presence of the most active catalyst, NiWI, and under the same reaction conditions. This experiment also served to check if the fact that only trace amounts of MTHF were observed in the reaction mixture was due to insufficient activity on the original catalyst or a consequence of catalyst deactivation. In the following figure the results of the test are displayed.

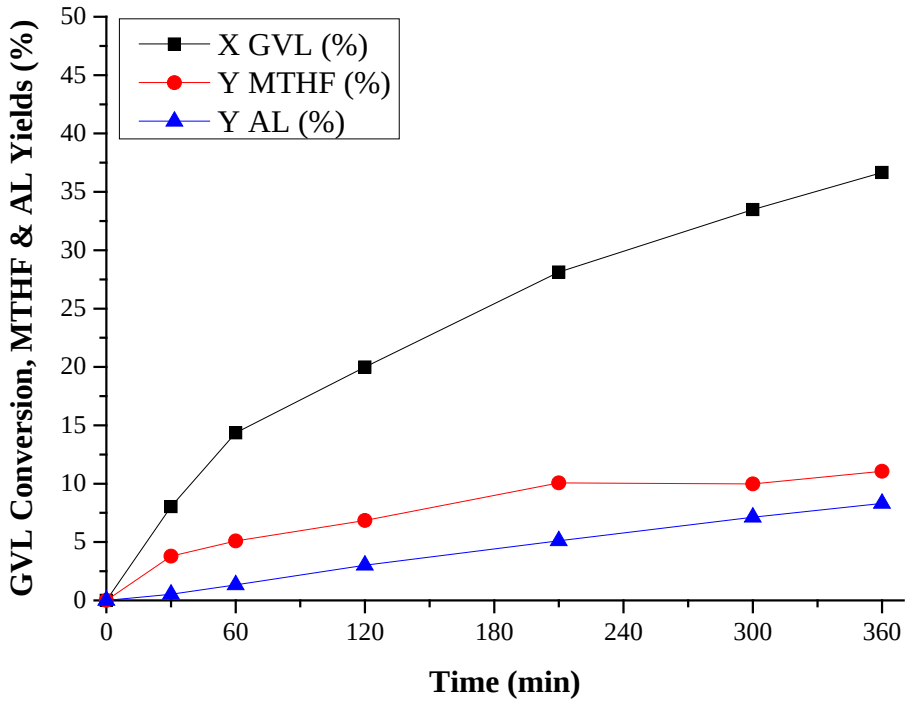

Figure 5.4. Time evolution profile of GVL hydrogenation in aqueous solution over NiWI catalyst.

The conversion profile shows a slow GVL reaction rate compared to that of LA, which reached complete conversion in less than 2 h. Besides, increasing AL yields were

detected along with up to 10% MTHF yields. It is noteworthy the difference between GVL conversion and products yields, which may be indicative of mass loss *via* carbon deposition on the catalysts. This experiment confirmed that GVL can be simultaneously, and with similar reaction rates, hydrogenated and dehydrogenated over the same catalyst. As already discussed, this is an undesired reaction both for the objective of MTHF production and for the catalyst stability considering that AL is a coke precursor.

Once the benefits of the bimetallic catalysts were stated, the influence of the preparation method on the activity of bimetallic catalysts was investigated. The activity of the two bimetallic catalysts prepared by the SG method and calcined at two different temperatures (300 and 450 ºC) was examined and the results are shown in Figure 5.5.

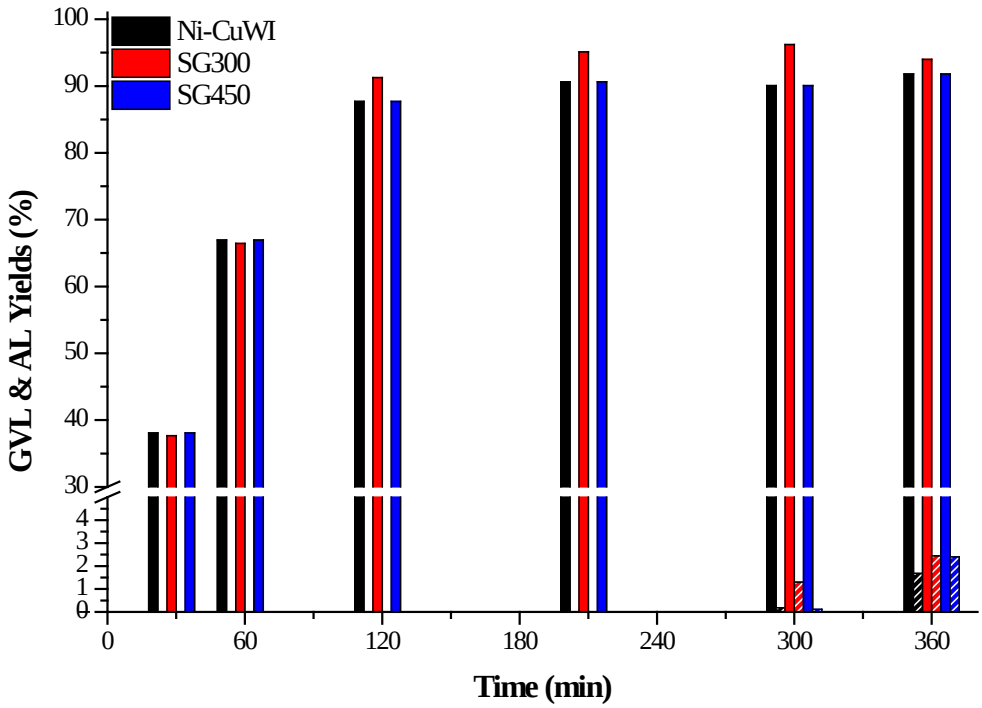

Figure 5.5. GVL (solid) and AL (stripped) yields *vs.* reaction time for Ni-CuWI, SG300 and SG450 catalysts.

As observed in Figure 5.5 all studied catalysts achieved comparable GVL yields (~ 90%) in less than 2 h reaction time with complete LA conversion. Similarly to the previous LA hydrogenation experiments, only trace amounts of MTHF were detected in the presence of these catalysts. Regarding GVL production, both SG catalysts exhibited similar initial activities and GVL yields to that of Ni-CuWI. Moreover, the SG catalysts achieved slightly higher AL yields (2.4%) when compared to Ni-CuWI catalyst (1.6%); in any case, these AL yields were considerably lower than that obtained for the NiWI

catalyst. Considering the large differences in the total metal loading between these three catalysts, the different yields obtained could be attributed to the higher dispersion obtained by the SG method when compared with the WI method[14]. The higher dispersion would produce a higher metal active sites concentration even when lower total metal loadings were added. Carbon deposition was further investigated by thermogravimetric analysis (TGA) of calcined and used catalysts. The results are presented in Figure 5.6.

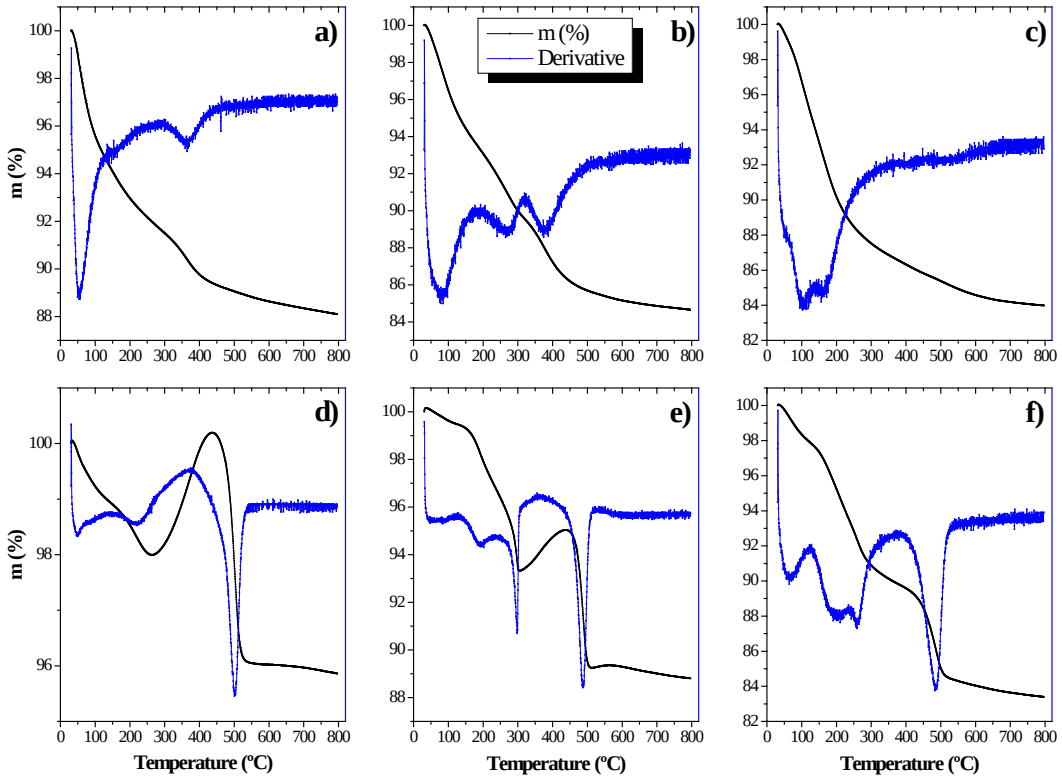

Figure 5.6. TGA results of CuWI (a, d), NiWI (b, e) and SG300 (c, f) catalysts. Upper row for the freshly calcined and the lower row for the used catalysts.

The calcined catalysts, Figure 5.6 (a-c), showed a water desorption peak between 50 and 100 ºC and additional peaks at higher temperatures depending on the catalyst. The additional peaks can be associated with the decomposition of the metal precursor salts. It is worth noting that these peaks are shifted to lower temperatures for the SG catalyst, which may indicate a greater dispersion and/or exposure of the metal particles.

The profiles of the used catalysts differ significantly among themselves and from those of the calcined catalysts. The graph of the used CuWI catalyst, Figure 5.6 d), featured a water desorption peak at 50 ºC, a reaction product (most probably GVL) desorption peak at 220 ºC, and a large weight gain peak at ~ 450 ºC caused by oxidation of metallic Cu to CuO. At higher temperatures (500 ºC), a sharp weight loss peak

attributed to the combustion of carbon deposited on the surface of the catalyst[14,15] was observed. The profile of the NiWI catalyst, Figure 5.6 e), is comparable with the graph of the CuWI catalyst, except for the sharp weight loss at 300 ºC that can be attributed to desorption of heavier reaction by-products. Also, the NiWI catalyst showed a lower weight increase at 450 ºC. This fact is a consequence of the previously explained Ni aluminate formation, which are not reduced during the activation process and lead to lower reduced metal contents on the catalysts.

The profile of the SG300 catalyst, Figure 5.6 f), exhibited the same desorption peaks; however, the profile differs from those of the WI catalysts. There is no net weight increase in the metal oxidation temperature range (250 to 500 ºC) as it was on the WI catalysts, but the weight loss rate is slower. This effect may be a consequence of simultaneous metal oxidation and carbon combustion or partial oxidation of the catalyst sample before the TGA analysis, as the used catalysts samples were stored under air. For the purpose of estimating/quantifying the carbon content on the catalysts two assumptions were proposed because of the interfering of metal oxidation peaks. The first estimation was based on the area of the peak associated with carbon combustion, whereas the second estimation was based on the weight difference between the pre- and post-combustion states where the metal oxidation peak is unaccounted for. The results, presented in Table 5.2 are consistent with the previously discussed hypothesis that correlated the deposited carbon amount with the AL yields observed in the WI catalysts.

Table 5.2. Carbon content estimation on the used catalysts.

	NiWI	CuWI	Ni-CuWI	SG 300	SG 450
Carbon %[a]	5.7	4.1	5.1	4.8	3.6
Carbon %[b]	4.5	2.0	3.7	4.7	4.0

[a] Carbon content estimated by the area of the combustion peak. [b] Carbon content estimated by the difference between the pre- and post-combustion sample weights.

The measured carbon contents are in good agreement with the previously discussed catalyst acidity profiles. The deposited carbon amount is clearly related to the high-temperature acidity shown in Figure 5.2; the NiWI catalyst showed the highest amount of strong acid sites, whereas CuWI catalyst showed negligible amounts of these type of acid sites and the Ni-CuWI catalyst featured an intermediate acidity. In good agreement with the activity results, the SG catalysts showed a similar carbon content to that of Ni-CuWI. TGA results also provide further proof of the significant role of Cu for

AL production inhibition and, accordingly, mitigation of carbon deposition on the catalyst.

To further compare the activities of the five prepared catalysts, the initial reaction rate (LA conversion per mole of metal) was calculated. This parameter was estimated using the LA conversion obtained at the first sampling time (30 min) and the total metal content of each catalyst, as measured by ICP-OES (Table 5.1). The results are displayed in Figure 5.7.

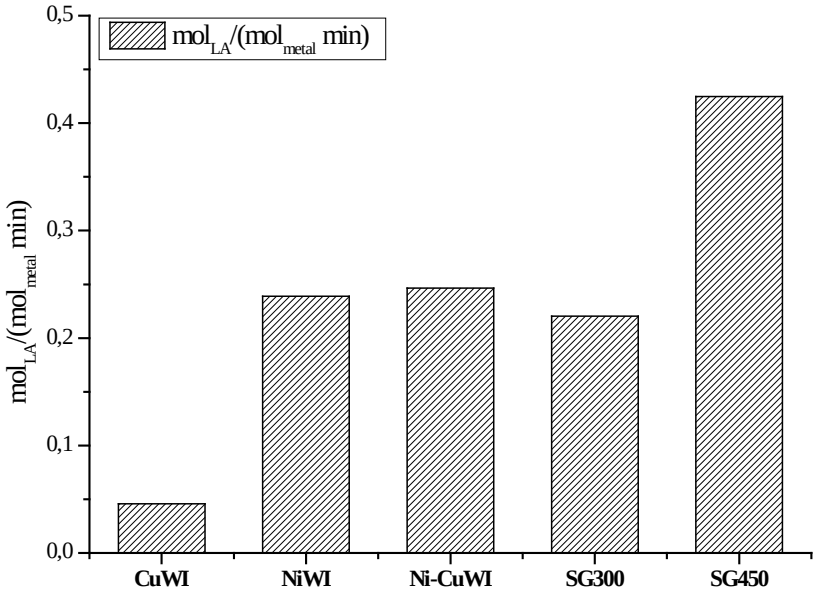

Figure 5.7. Metal-normalized initial reaction rates of the catalysts.

The metal-normalized initial reaction rates of the different catalysts differ significantly. First, the CuWI catalyst was the least active, displaying < 0.05 mol_{LA} mol_{metal}^{-1} min^{-1}, whereas the NiWI and the Ni-CuWI were five times more active. Regarding the SG catalysts, the calcination temperature plays an important role. The SG300 catalyst achieved a lower activity than that of the Ni-CuWI catalyst, while the SG450 catalyst showed the highest activity, achieving up to 0.42 mol_{LA} mol_{metal}^{-1} min^{-1}. These activity differences evidence the important effect of the catalyst preparation method, its thermal treatment and the metal load on the activity. The appropriate tuning of these variables is then expected to enable the production of catalysts with enhanced activities and selectivities.

5.4. Conclusions

Aqueous phase LA hydrogenation to GVL was carried out to achieving up to 96% yield, but with only trace amounts of MTHF. Interestingly, GVL was found to be simultaneously hydrogenated (to MTHF) and dehydrogenated (to AL) over the same catalysts under 65 bar H_2. Water, despite its interesting properties and ubiquity in biomass processing, was found not to be a good solvent for LA conversion to MTHF, since, to the best of our knowledge, the reversibility of the AL ⇔ GVL reaction under H_2 atmosphere was only reported to occur in aqueous phase. This dehydrogenation reaction is the opposite to the desired reaction path.

Among the tested metal phases, Ni was found to be the most active metal for LA hydrogenation but also led to higher AL yields. Cu, on the other hand, was significantly less active but it inhibited AL formation. The simultaneous presence of both metals produced a catalyst with similar activity to Ni but with lower selectivity towards AL, whose concentration in the reaction mixture was correlated with the carbon content on the used catalysts. Therefore, Cu incorporation did not reduce the catalyst activity and, at the same time, improved its selectivity and most probably catalyst stability against carbon deposition.

The activity of the catalyst formulation was found to be dependent on the preparation method as well as on the calcination temperature, achieving a 1.7 times higher initial reaction rate per metal mol with a sol-gel prepared catalysts *vs.* the impregnation counterpart.

5.5. References

[1] D. C. Elliott, J. G. Frye, *Hydrogenated 5-Carbon Compound and Method of Making.*, **1999**, 5883266.

[2] T. Mizugaki, K. Togo, Z. Maeno, T. Mitsudome, K. Jitsukawa, K. Kaneda, *ACS Sustain. Chem. Eng.* **2016**, *4*, 682–685.

[3] M. Li, G. Li, N. Li, A. Wang, W. Dong, X. Wang, Y. Cong, *Chem. Commun.* **2014**, *50*, 1414–1416.

[4] T. Mizugaki, Y. Nagatsu, K. Togo, Z. Maeno, T. Mitsudome, K. Jitsukawa, K. Kaneda, *Green Chem.* **2015**, *17*, 5136–5139.

[5] P. Salagre, J. L. G. Fierro, F. Medina, J. E. Sueiras, *J. Mol. Catal. A Chem.* **1996**, *106*, 125–134.

[6] I. Gandarias, J. Requies, P. L. Arias, U. Armbruster, A. Martin, *J. Catal.* **2012**, *290*, 79–89.

[7] G. K. Priya, P. Padmaja, K. G. K. Warrier, A. D. Damodaran, G. Aruldhas, *J. Mater. Sci. Lett.* **1997**, *16*, 1584–1587.

[8] J. Ashok, M. Subrahmanyam, A. Venugopal, *Int. J. Hydrogen Energy* **2008**, *33*, 2704–2713.

[9] J. R. H. Ross, *Heterogeneous Catalysis*, Elsevier, Amsterdam, **2012**.

[10] J. C. Serrano-Ruiz, R. M. West, J. A. Dumesic, *Annu. Rev. Chem. Biomol. Eng.* **2010**, *1*, 79–100.

[11] J. C. Serrano-Ruiz, A. Pineda, A. M. Balu, R. Luque, J. M. Campelo, A. A. Romero, J. M. Ramos-Fernández, *Catal. Biorefineries* **2012**, *195*, 162–168.

[12] D. M. Alonso, S. G. Wettstein, J. a. Dumesic, *Green Chem.* **2013**, *15*, 584.

[13] J. Deng, Y. Wang, T. Pan, Q. Xu, Q.-X. Guo, Y. Fu, *ChemSusChem* **2013**, *6*, 1163–1167.

[14] M. El Doukkali, A. Iriondo, P. L. Arias, J. F. Cambra, I. Gandarias, V. L. Barrio, *Int. J. Hydrogen Energy* **2012**, *37*, 8298–8309.

[15] A. Shamsi, J. P. Baltrus, J. J. Spivey, *Appl. Catal. A Gen.* **2005**, *293*, 145–152.

Chapter 6

One pot 2-methyltetrahydrofu-ran production from levulinic acid in green solvents over Ni-Cu/Al_2O_3 catalysts

The work contained in this chapter was published under the title “One-Pot 2-Methyltetrahydrofuran Production from Levulinic Acid in Green Solvents Using Ni-Cu/Al_2O_3 Catalysts” in *ChemSusChem* **2015**, 8, 3483-3488.

Table of contents

6.1. Introduction 99

6.2. Results and discussion 101

6.3. Conclusions 109

6.4. References 110

6.5. Appendix 111

6.1. Introduction

In this chapter the results reported in the previous chapter were taken one step further achieving significant MTHF yields from LA in a single reaction step. This improvement over previously presented results was accomplished by switching the reaction solvent from water to alcohols, which can be derived from biological processes. Besides, the catalyst formulation was screened for the Ni-Cu/Al_2O_3 catalysts and an optimum Ni:Cu ratio was found. This optimal formulation allowed high GVL conversion rates combined with low activity for MTHF degradation.

For the large-scale production of MTHF to be technically and economically viable it should be carried out through a low energy demanding process and using highly available, low cost materials. In this regard, one-pot reaction systems are normally preferred because intermediate separation-purification steps are avoided. Concerning the catalyst, non-noble metals are more widely available, generate lower environmental impacts and their prices are considerably lower than those of noble metals[1,2].

As already explained, the biorefinery concept was proposed as an integrated industrial complex where biomass-derived feedstocks are converted into fuels and value-added chemicals[3]. While in petrochemical industries oxygen addition to unfunctionalized feedstocks is carried out typically in gas phase[4], most biorefinery processes deal with oxygen removal from overly functionalized raw materials in liquid mediums[5,6]. The need for liquid phase reactions in these processes is a consequence of limited thermal stability of biomass-derived building block molecules and process economics.

The use of solvents for biorefinery reactions is common[7] and may serve different objectives such as enhancing catalytic activity[8], switching the selectivity[9], improving heat and mass transfer, and facilitating product separation[9]. The use of solvents for this particular system appears to be interesting since LA is solid at room temperature, which makes its handling complicated, and the stability of the heterogeneous catalysts in highly acidic media is an issue to be considered[10,11]. Water arose as a very convenient solvent for this process, since LA is industrially produced in aqueous solutions[12] and,

hence, no separation steps would be required. Moreover, water is obtained as a by-product when MTHF is produced from LA (see Figure 6.1).

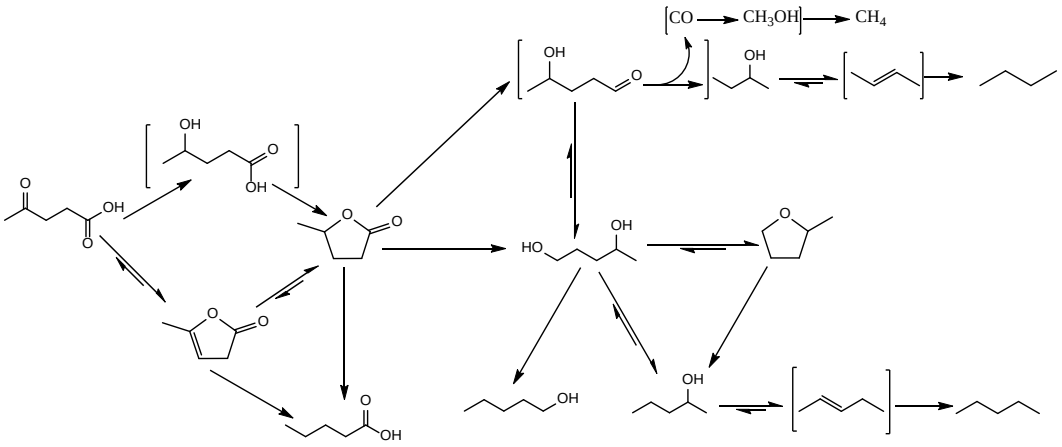

Figure 6.1. LA to MTHF reaction mechanism adapted from[13].

Based on these criteria water was tested as solvent, feeding LA and using a 35% Ni/Al_2O_3 catalyst. As it can be observed in Table 6.1, under the used operating conditions, high yields of GVL were obtained, but insignificant amounts of MTHF were detected after 5 h reaction time. LA aqueous solutions are known to be corrosive[14] so it was speculated that the catalyst could be rapidly deactivated and, hence, lack the required activity for the activation of the highly stable GVL[11]. To prove this hypothesis an activity test was carried out under the same operation conditions but feeding a 5 wt% GVL aqueous solution. After 5 h reaction time, 37% of the initial GVL was converted into MTHF (11% yield), AL (8% yield) and heavy carbonaceous by-products. Consistently, GVL dehydrogenation to LA under 10 bar H_2 was previously reported in the presence of homogeneous Ir based catalysts[15]. This is an undesired reaction since AL is known to easily polymerize in the presence of acids, which results in selectivity losses in addition to catalyst deactivation by carbon deposition[16,17]. These results revealed the unsuitability of water as solvent for MTHF production, as previously reported in the literature[13,18].

Several solvents were reported to be suitable for the La to MTHF reaction. For instance, high yields of MTHF were achieved in 1,4-dioxane, which is considered amongst the most undesirable solvents[19], using both noble (Pd-Re)[20] and non-noble metal (Cu-Ni)[21] based catalysts. FA, which is produced in equimolar amounts with LA, was found to be an appropriated solvent under microwave irradiation but the system rapidly lost activity when set-up in a fixed bed reactor configuration[10]. Besides, GVL

conversion into MTHF was reported to efficiently occur in ethanol over a Cu/ZrO_2 catalyst[22]. Also, neat LA conversion to MTHF was reported over a Ru/C catalyst; nevertheless, the water produced in the LA to GVL step must be eliminated for the GVL to MTHF reaction to proceed[13]. Against this background, the present study aimed at approaching scalable reaction conditions by studying the direct reaction from LA to MTHF in a single reaction step using non-noble metal based catalysts and green solvents.

6.2. Results and discussion

In the search for suitable solvents for the production of MTHF from LA biomass derived alcohols, such as ethanol, 1-butanol (1-BuOH) and 2-propanol (2-PrOH), present some common and very interesting features[23]: *i)* they can be easily obtained from biomass derived feedstock, *ii)* they are currently used as fuel additives, and despite lower energy densities *iii)* they have octane numbers on the range of gasoline. Moreover, 1-BuOH is also hydrophobic[23] which makes it more compatible with gasoline.

These properties are highly beneficial from a process engineering point of view, as high separation grades between the product and the solvent would not be required because the solvent itself is a useful fuel additive.

Table 6.1. Solvent and catalyst screening results.

Entry	Catalyst ($/Al_2O_3$)	Solvent	LA Conv. (%)	Yield (%)				CB (%)
				MTHF	GVL	Other[c]	Gas[d]	
1	35Ni	H_2O	100.0	1.4	87.7	0	-	89.1
2	35Ni	EtOH	100.0	0.5	79.8	0	9.8	90.1
3	35Ni	1-BuOH	92.7	9.8	70.9	12.3	-	100.3
4	35Ni	2-PrOH	100.0	45.9	3.6	24.1	10.4	84.0
5	30Ni-5Cu	2-PrOH	100.0	43.2	23.6	12.4	4.3	83.5
6	23Ni-12Cu	2-PrOH	100.0	56.0	13.3	13.1	4.4	86.8
7	17Ni-17Cu	2-PrOH	100.0	36.8	36.7	12.3	0.8	86.6
8	12Ni-23Cu	2-PrOH	100.0	34.4	40.1	8.2	2.7	85.4
9	35Cu	2-PrOH	100.0	22.7	64.5	3.8	1.1	92.1
10[a]	35Cu	2-PrOH	100.0	75.0	8.0	11.7	1.3	96.0
11[b]	35Ni	2-PrOH	100.0	29.9	42.4	9.6	-	81.9
12[b]	23Ni-12Cu	2-PrOH	100.0	44.5	34.4	6.6	1.2	86.7

Reaction conditions: 5 wt% LA in solvent, LA/Cat. ratio 10 g/g, 250 ºC reaction T, 70 bar H_2, 5 h reaction time. [a] 250 ºC and 24 h reaction time. [b] 230 ºC and 5 h reaction time. [c] main products: 2-butanol, 1- and 2-pentanol and valeric acid, [d] main products: methane, butane and pentane.

The results from the activity tests using the same 35Ni/Al_2O_3 catalyst with these different solvents are summarized in Table 6.1 (entries 2-4). Using ethanol the yields of MTHF were negligible and similar to those obtained with water. 1-BuOH was found to be a more suitable solvent allowing almost 10% MTHF and 70% GVL yields. Nonetheless, the biggest improvement could be observed when 2-PrOH was used as the solvent, as a significant 45.9% MTHF yield was achieved. These results show that 2-PrOH is an excellent reaction medium to convert the highly stable GVL intermediate, presumably due to its high hydrogen donning capacity[24]. It is well known that the hydrogenolysis reaction of GVL into PDO requires very high hydrogen pressures[13,25], therefore hydrogen availability arises as a key parameter in this reaction.

The reversible *2-PrOH* ↔ *acetone* + H_2 reaction can continuously produce hydrogen on the active sites of the catalyst, dramatically increasing the hydrogen availability and, hence, the GVL ring opening reaction rate. Despite the activity tests were carried out at high H_2 pressure, 2-PrOH dehydrogenation was confirmed by the significant amounts of acetone detected in the reaction products (up to 1.5 mol/L). However, when the experiment was carried out with LA in 2-PrOH without any catalyst only trace amounts of acetone were detected, pointing to the need of a catalyst for the 2-PrOH dehydrogenation to occur.

Moreover, the formation of AL from GVL seems to be negligible at these reaction conditions as no AL was detected in the reaction medium. It can be speculated that this higher hydrogen availability minimizes dehydrogenation reactions. Besides, AL was reported to react with alcohols to produce LA esters over acidic surfaces[26], which would also reduce the AL concentration, if any is formed. On the other hand, significant yields of side products were obtained (14.2% of 2-butanol, 2-BuOH, 9.3% of CH_4 and 4.1% of 2-pentanol, 2-PeOH). According to Figure 6.1 and the observed reaction products, the reaction seems to proceed by the hydrogenation of GVL to PDO and this compound undergoes *i)* dehydration-cyclation to produce MTHF, *ii)* dehydrogenation and decarbonylation to give 2-BuOH and CO or CH_4, and *iii)* hydrogenolysis of the terminal –OH group to end in 2-PeOH. In addition to this, MTHF can further react to yield 2-PeOH. Ni is well known for his high C-C cleavage activity[24], which seems to be the reason for the high yield of 2-BuOH. Looking for catalysts with at least similar activity and enhanced selectivities towards MTHF a series of Ni-Cu/Al_2O_3 catalysts was prepared and tested.

Table 6.1 (entries 4-9) shows MTHF and GVL yields and the carbon balance (CB) for the six pre-reduced Ni-Cu/Al_2O_3 catalysts (with different Ni:Cu atomic ratio) and using 2-PrOH as the reaction solvent. In the results from the tests carried out at 250 ºC there is a nice trend showing that when the Ni:Cu ratio increased from 0:35 to 23:12 the yield of GVL decreased from 64.5% to 13.3%. A decrease in the GVL conversion activity was noticed when increasing the Ni:Cu ratio from 23:12 to 30:5, however, the monometallic Ni/Al_2O_3 catalyst converted almost all the GVL (only a 3.6% GVL yield was detected). These results clearly indicated that Ni is more active than Cu to convert the stable GVL.

The MTHF yield profile, on the other hand, showed a typical "volcano" shape. MTHF yield slowly increased with the Ni:Cu ratio, for ratios lower than 17:17 (average MTHF yields around 33% for these three catalysts). For the 23:12 ratio the maximum 56% MTHF yield was achieved and higher Ni contents resulted in lower yields with a plateau around 44%. Interestingly, the yields of other products (2-BuOH, 1- and 2-PeOH, and valeric acid, VA) also increased with the Ni:Cu ratio. Therefore, high Cu proportions seem to prevent the side reactions leading to these products (see Figure 6.1). To prove that the presence of Cu is beneficial to improve the selectivity towards MTHF, a 24 h test was carried out at 250 ºC with the Cu/Al_2O_3 catalyst. The results (Table 6.1, entry 10), showed a 75% MTHF yield with most of the GVL converted (8% yield). In this case, however, a 9.6% valeric acid yield was detected as the main side product.

These results suggest a synergetic effect between Ni and Cu, Ni providing high activity to convert the intermediate GLV and Cu improving the selectivity towards MTHF. The superior performance of the bimetallic 23Ni-12Cu catalyst compared to the Ni monometallic one was confirmed by the results at lower reaction temperatures (Table 6.1, entries 11 and 12). At 230 ºC the 23Ni-12Cu catalyst allowed 44.5% MTHF yield while with the Ni/Al_2O_3 catalyst the yield of MTHF was only 29.9%.

As pointed out before, MTHF can further react to give side products; hence, the stability of the produced MTHF in the reaction medium is a point of paramount importance to determine the suitability of the catalyst. To test this point, MTHF stability tests were carried out under the same reaction conditions feeding 5 wt% MTHF in 2-PrOH solutions with the reduced catalyst. The results are shown in Table 6.2.

Table 6.2. Results from MTHF stability tests.

Catalyst	Temp. (ºC)	MTHF Conv. (%)	Yield (%)			CB (%)
			2-BuOH	2-PeOH	1-PeOH	
35Ni	250	55.3	5.0	23.0	0.0	104.4
35Cu	250	12.1	0.0	0.0	8.1	96.0
23Ni-12Cu	250	20.7	0.7	5.1	15.2	100.3
23Ni-12Cu	230	12.0	0.7	2.3	3.8	94.8

Reaction conditions: Reaction temperature 250 ºC, 5 wt% MTHF in 2-PrOH, MTHF/Cat. ratio 10 g/g, 70 bar H_2, 5 h reaction time.

These tests confirmed that the monometallic Ni catalyst was also the most active for the MTHF degradation and the monometallic Cu one the least. The 23Ni-12Cu catalyst, which was nearly as active to convert GVL, showed less than two times lower MTHF conversion than the monometallic Ni one. Based on these results it can be concluded that the highest MTHF yield obtained using the 23Ni-12Cu catalyst (see Table 6.1 entry 4) seems to be the result of an optimal combination of the high activity of Ni for GVL conversion and the high selectivity of Cu towards MTHF.

A very interesting finding concerns the product distribution related to the metal active sites; The Cu/Al_2O_3 catalyst selectively opened the MTHF cycle by the substituted side while Ni/Al_2O_3 preferably opened the cycle from the less impeded side, in good agreement with previous works on this mechanism[27]. These data help to clarify the mechanism of the side reactions discussed before. They suggest that the main route for the production of 2-PeOH is MTHF degradation while 2-BuOH is mainly obtained from GVL and/or PDO. The 23Ni-12Cu bimetallic catalyst, which exhibited intermediate activity for the conversion of MTHF, showed an intermediate product distribution too, but closer to that of Cu. The activity for MTHF conversion of this catalyst was two times lower when operating at 230 ºC (Table 6.2), matching the conversion showed by the Cu catalyst at 250 ºC but similarly favoring both ring opening options.

In order to get a better understanding of the observed synergetic effect between Ni and Cu, the complete $Ni\text{-}Cu/Al_2O_3$ catalyst series was characterized. Temperature programmed reduction (TPR) results of monometallic Ni catalyst showed three reduction peaks; the one at the lowest temperature can be related to bulk nickel oxide and the two at higher temperatures correspond to the reduction of nickel aluminates with increasing interaction with the alumina support. The addition of Cu (and therefore the decrease of the Ni:Cu ratio) decreased the reduction temperature of the nickel

aluminate species. For the monometallic Cu catalyst, a peak related to the reduction of copper oxides was detected. For the bimetallic catalysts a reduction peak located around 320 ºC (red peaks in Figure 6.1) which was not present in the monometallic catalysts was observed. This peak might be related to the reduction of a mixed Ni-Cu species (see XRD results). The proportion of this species in the catalyst can be related to the catalytic activity, being higher for more active catalysts and presenting its maximum for the most active catalyst, the 23Ni-12Cu.

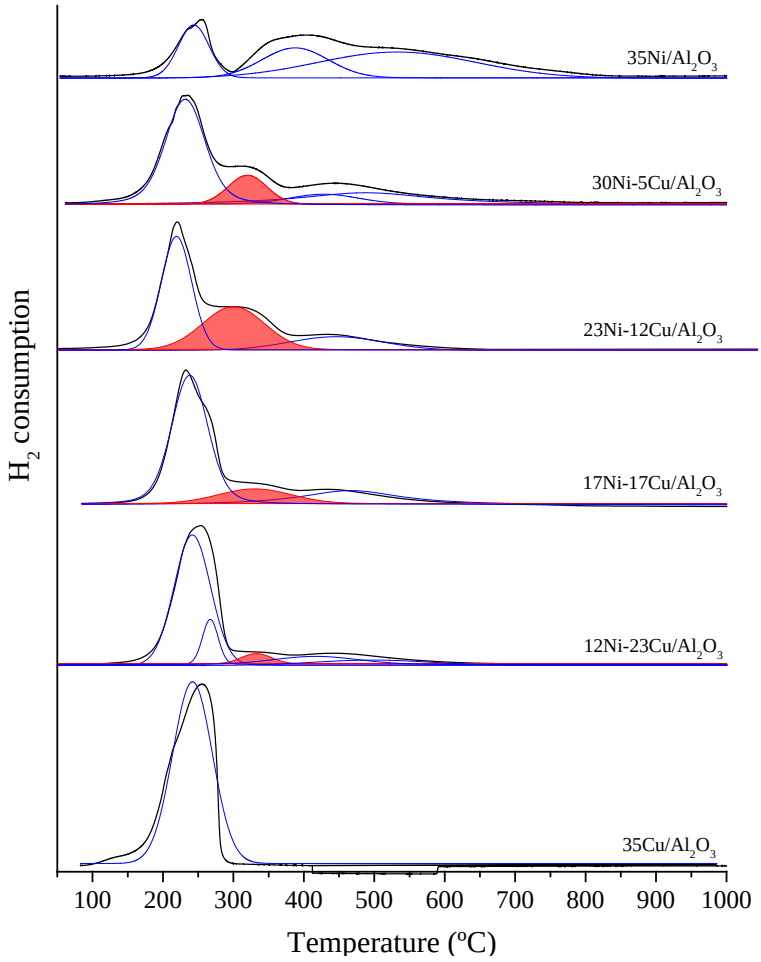

Figure 6.2. TPR profiles of the catalysts and peak fitting.

The presence of this Ni-Cu mixed species was confirmed by XRD analysis of freshly reduced catalysts. As observed in Figure 6.3, the diffraction peaks related to metallic Cu (43.4 º and 50.6 º, JCPDS 01-085-1326) did not change in position, which indicates that no significant amounts of Ni were incorporated into the Cu crystal network. On the other hand, the continuous displacement to lower 2θ values of the diffraction peak related to metallic Ni (44.7 º and 51.9 º, JCPDS 00-001-1260) indicated Cu incorporation into the Ni crystal structure (see Figure 6.3). Moreover, no peaks

related to Cu can be observed in the samples with more than 17% of Ni content, which indicates that Cu incorporation into the Ni crystals building the mixed phase is extensive enough to prevent the formation of large Cu particles.

The sharper diffraction peaks observed for Cu in the monometallic Cu catalyst compared to the Ni diffraction peaks in the monometallic Ni catalyst indicate that Cu particles were significantly bigger. This fact can be explained by the differences in the sintering temperatures of the two metals, 100 ºC lower for copper[28], and the fact that Ni strongly interacts with alumina producing highly stable nickel aluminates[29] which would hinder particle mobility. These nickel aluminates can be observed in the reduction peaks at temperatures higher than 600 ºC[29] in Figure 6.2. This size difference can explain why Cu crystals were not modified by Ni in the bimetallic catalysts, but Ni crystals were modified by Cu, as smaller Ni particles having higher surface areas are more reactive. Therefore Cu rich bimetallic catalysts, 12Ni-23Cu and 17Ni-17Cu, presented a bimodal particle size distribution, with big Cu particles and incipient small Ni and Ni-Cu bimetallic particles. On the other hand Ni rich bimetallic catalysts, 23Ni-12Cu and 30Ni-5Cu, presented small Cu and Ni particles and bigger Ni-Cu particles. Noteworthy, the catalyst showing the best performance, 23Ni-12Cu, was the one presenting the biggest displacement of the metallic Ni phase and no monometallic Cu particles.

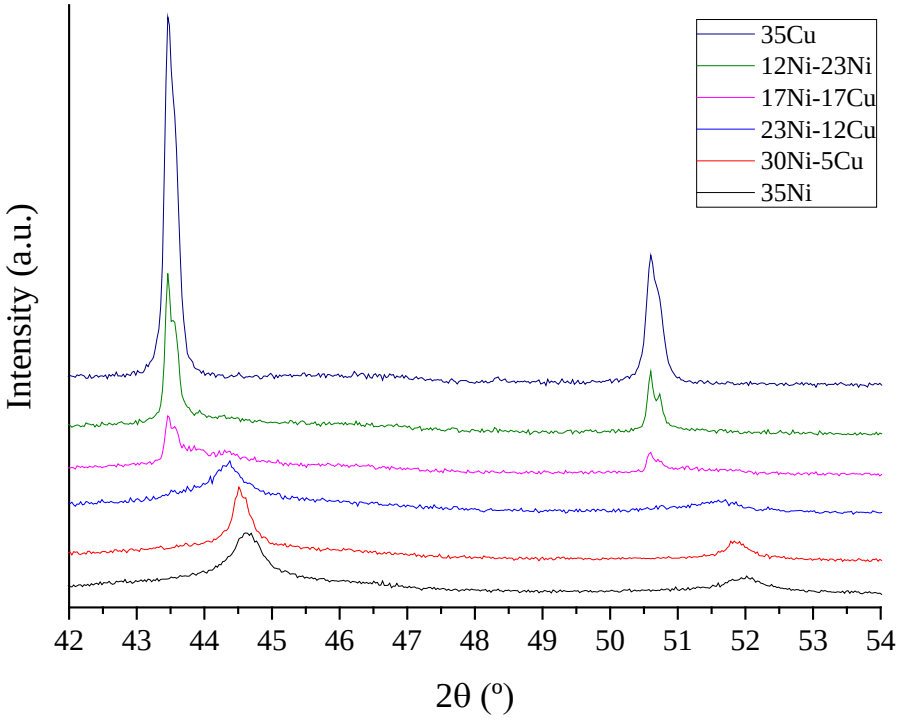

Figure 6.3. XRD graph of the reduced catalysts.

Electronic microscopy images of the 23Ni-12Cu catalyst showed well dispersed metal particles over the Al_2O_3 support (see Figure 6.4). Chemical composition mapping showed even metal distribution on the surface of the catalyst and metallic particles containing Ni and Cu simultaneously, in good agreement with XRD results. The presence of a mixed Ni-Cu phase, which was confirmed by TPR, XRD and STEM, is considered to be necessary to promote the conversion of the stable GVL intermediate and, at the same time, to promote the selectivity towards MTHF.

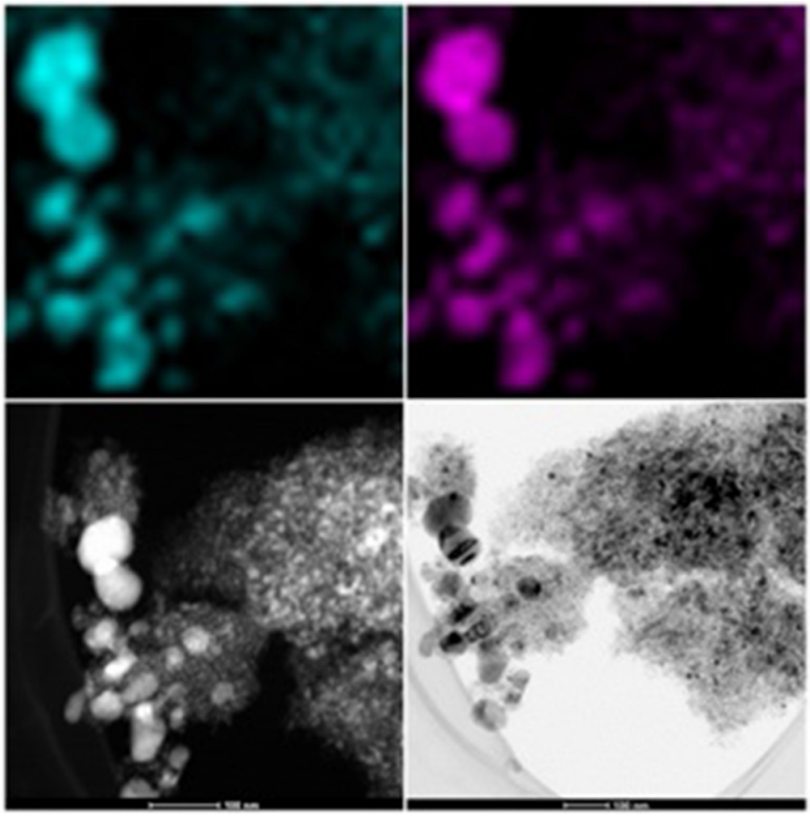

Figure 6.4. STEM images of the 23Ni-12Cu/Al_2O_3. Cu (upper left) and Ni (upper right) element scanning images. Drift spectrum (lower left) and bright field. TEM (lower right) images

Besides activity and selectivity, the stability of the active metallic particles in the reaction media is also a point of paramount importance when using heterogeneous catalysts. To prove this point, the amount of Ni and Cu that leached out into the reaction mixture was determined for the optimum 23Ni-12Cu catalyst. The harshest reaction conditions *i.e.* 250 ºC for 5 h were chosen. The results with 2-PrOH as the reaction solvent were compared to those obtained with water as solvent. The results showed around 2% Ni leaching in water (see Table A6.2 in the Appendix) and insignificant amounts of leached metals in the experiment using 2-PrOH. These results indicate that besides promoting the yield of MTHF, the use of 2-PrOH as solvent is also beneficial for the stability of the bimetallic 23Ni-12Cu/Al_2O_3 catalyst.

In order to obtain the product evolution with reaction time, a 24 h experiment was carried out with intermediate sampling and using the most promising catalyst: 23Ni-12Cu/Al_2O_3. The reaction temperature was set to 230 ºC. In Figure 6.5 the very high LA to GVL reaction rate is evidenced by the 90% GVL yield and total LA conversion reached after the first 30 min of the reaction.

After the first hour GVL yield started to decrease with a pseudo exponential trend until 17.3% yield was reached at 24 h reaction time. MTHF yield increased from 3.2% at 30 min of reaction time up to 62.0% after 24 h. The major byproducts were VA and 2-BuOH, which reached 5.4% and 8.3% yields at 24 h respectively.

The fact that no LA was detected in the first sample (30 min of reaction) did not allow further insight on its reaction kinetics and so, the data was fit considering GVL as the starting material. The kinetic analysis of the data showed pseudo-first order kinetics for MTHF, 2-BuOH and VA formation from GVL. According to the reaction network presented on Figure 6.1, the production of MTHF and 2-BuOH proceeds through intermediate chemicals which were not detected in the reaction products. This fact indicates the instability of the aforementioned intermediates in the reaction conditions and, hence, their high conversion rates.

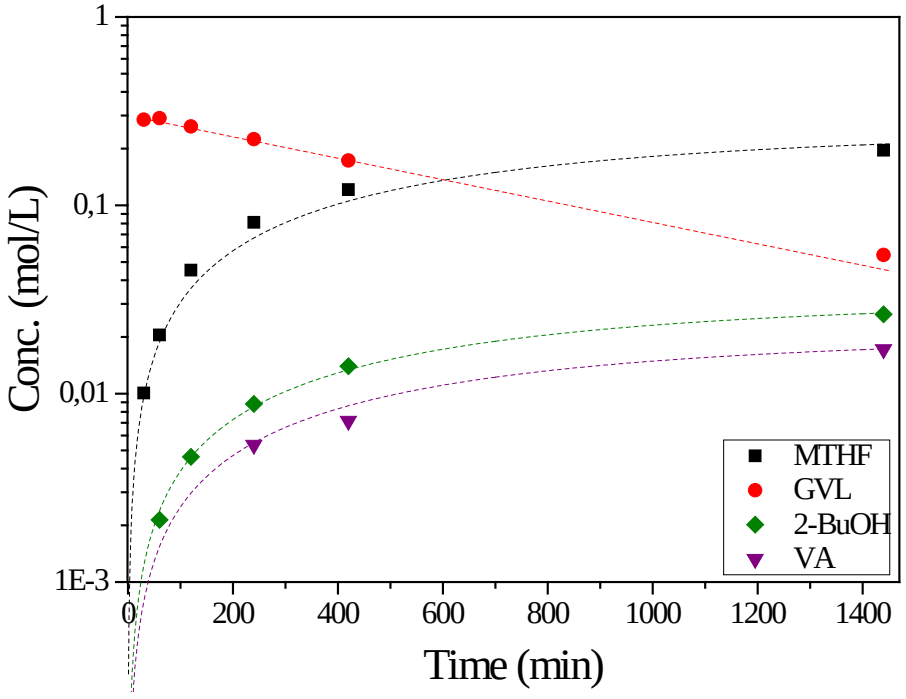

Figure 6.5. Concentration of the reaction products as function of the reaction time (dots) for 23Ni-12Cu catalyst and data fitting (lines). Reaction conditions: 5 wt% LA in 2-PrOH, LA/Cat. ratio 10 g/g, 230 ºC reaction T, 70 bar H_2.

This point was confirmed carrying out an experiment with PDO as substrate at 230 ºC for 5 h in the presence of the 23Ni-12Cu catalyst. Total PDO conversion with quantitative MTHF yields were achieved with trace concentrations of 2-BuOH, 1-PeOH and 2-PeOH. This experiment indicated that the main route for 2-BuOH formation starts from GVL. Side product formation kinetic constants are lower than that of MTHF production by an order of magnitude which shows the high selectivity of this catalytic system to the desired product.

6.3. Conclusions

In this chapter the feasibility of using non-noble metal catalysts and green solvents (such as 1-BuOH or 2-PrOH) for the hydrogenation of LA to MTHF was proved as an alternative for the most reported catalytic systems based on Au, Pd or Ru.

The activity of the Ni based catalytic system was found to be very dependent on the solvent. Water allowed high GVL yields but severely inhibited MTHF formation. Moreover, in the reaction of GVL in aqueous solution significant amounts of AL where achieved, proving the reversibility of a reaction. The hydrogen donning capacity of 2-PrOH is considered vital to provide a sufficient hydrogen availability on the catalyst, which can facilitate the reaction of the highly stable GVL intermediate. The Ni-Cu/Al_2O_3 bimetallic catalysts showed interesting synergetic effects allowing higher activity and improved selectivity towards the desired product compared to the monometallic catalysts. These features can be related to characterization data showing mixed Ni-Cu particles, which are considered responsible for the improved catalytic activity. The effect of this mixed phase was also highlighted by the different mechanisms for MTHF degradation showed by the different metal phases.

6.4. References

[1] A. M. Hengne, C. V. Rode, *Green Chem.* **2012**, *14*, 1064–1072.
[2] K. Yan, J. Liao, X. Wu, X. Xie, *RSC Adv.* **2013**, *3*, 3853–3856.
[3] D. J. Hayes, *Catal. Today* **2009**, *145*, 138–151.
[4] J. C. Serrano-Ruiz, R. M. West, J. A. Dumesic, *Annu. Rev. Chem. Biomol. Eng.* **2010**, *1*, 79–100.
[5] L. Petrus, M. a. Noordermeer, *Green Chem.* **2006**, *8*, 861.
[6] G. W. Huber, S. Iborra, A. Corma, *Chem. Rev.* **2006**, *106*, 4044–4098.
[7] A. Corma, S. Iborra, A. Velty, *Chem. Rev.* **2007**, *107*, 2411–2502.
[8] C. Michel, J. Zaffran, A. M. Ruppert, J. Matras-Michalska, M. Jędrzejczyk, J. Grams, P. Sautet, *Chem. Commun.* **2014**, *50*, 12450–12453.
[9] M. J. Climent, A. Corma, S. Iborra, *Green Chem.* **2014**, *16*, 516–547.
[10] J. M. Bermudez, J. A. Menendez, A. A. Romero, E. Serrano, J. Garcia-Martinez, R. Luque, *Green Chem.* **2013**, *15*, 2786–2792.
[11] O. A. Abdelrahman, A. Heyden, J. Q. Bond, *ACS Catal.* **2014**, *4*, 2–9.
[12] D. J. Hayes, S. W. Fitzpatrick, M. H. B. Hayes, J. R. H. Ross, in *Biorefineries-Industrial Process. Prod.* (Eds.: B. Kamm, P.R. Gruber), Wiley-VCH Verlag GmbH, **2006**, pp. 139–164.
[13] M. G. Al-Shaal, A. Dzierbinski, R. Palkovits, *Green Chem.* **2014**, *16*, 1358–1364.
[14] W. Luo, U. Deka, A. M. Beale, E. R. H. van Eck, P. C. A. Bruijnincx, B. M. Weckhuysen, *J. Catal.* **2013**, *301*, 175–186.
[15] J. Deng, Y. Wang, T. Pan, Q. Xu, Q.-X. Guo, Y. Fu, *ChemSusChem* **2013**, *6*, 1163–1167.
[16] P. M. Ayoub, J.-P. Lange, *Process for Converting Levulinic Acid into Pentanoic Acid*, **2008**, WO 2008/142127 A1.
[17] J. C. Serrano-Ruiz, D. Wang, J. A. Dumesic, *Green Chem.* **2010**, *12*, 574–577.
[18] X. Tang, Z. Li, X. Zeng, Y. Jiang, S. Liu, T. Lei, Y. Sun, L. Lin, *ChemSusChem* **2015**, *8*, 1601–1607.
[19] P. G. Jessop, *Green Chem.* **2011**, *13*, 1391.
[20] D. C. Elliott, J. G. Frye, *Hydrogenated 5C Compound and Method of Making*, **1999**, US 5883266.
[21] P. P. Upare, M. Jeong, Y. Kyu, D. Han, Y. Dok, D. Won, U. Lee, J. Chang, *Appl. Catal. A Gen.* **2015**, *491*, 127–135.
[22] X.-L. L. Du, L. He, S. Zhao, Y.-M. M. Liu, Y. Cao, H.-Y. Y. He, K.-N. N. Fan, *Angew. Chemie Int. Ed.* **2011**, *50*, 7815–7819.
[23] P. P. Peralta-Yahya, J. D. Keasling, *Biotechnol. J.* **2010**, *5*, 147–162.
[24] I. Gandarias, J. Requies, P. L. Arias, U. Armbruster, A. Martin, *J. Catal.* **2012**, *290*, 79–89.
[25] D. C. Elliott, J. G. Frye, *Hydrogenated 5-Carbon Compound and Method of Making.*, **1999**, 5883266.
[26] M. G. Al-Shaal, W. Ciptonugroho, F. J. Holzhäuser, J. B. Mensah, P. J. C. Hausoul, R. Palkovits, *Catal. Sci. Technol.* **2015**, *5*, 5422–5428.
[27] A. Cho, H. Kim, A. Iino, A. Takagaki, S. Ted Oyama, *J. Catal.* **2014**, *318*, 151–161.
[28] J. . Moulijn, A. . van Diepen, F. Kapteijn, *Appl. Catal. A Gen.* **2001**, *212*, 3–16.
[29] P. Salagre, J. L. G. Fierro, F. Medina, J. E. Sueiras, *J. Mol. Catal. A Chem.* **1996**, *106*, 125–134.

6.5. Appendix

Table A6.1. Results of N_2 physisorption and elementary analyses.

ICP-OES analyses				XRD Analyses				
Ni% (Actual)	Cu% (Actual)	Ni:Cu ratio (Actual)	Ni+Cu (Actual)	Ni Average size nm)	Cu Average size (nm)	BET Area (m^2/g)	Pore vol. (cm^3/g)	Average pore radius (nm)
-	-	-	-	-	-	227.2	0.81	6.8
0.0 (0.0)	35 (29.55)	0.0 (0.0)	35 (29.55)	-	150	152.9	0.58	7.6
12 (11.92)	23 (21.04)	0.52 (0.57)	35 (32.96)	10	>200	168.5	0.22	2.6
17.5 (15.85)	17.5 (12.99)	1.0 (1.20)	35 (28.84)	10	>200	178.3	0.21	2.4
23 (22.97)	12 (9.17)	1.91 (2.50)	35 (32.14)	10	>200	159.4	0.24	3.1
30 (29.25)	5 (4.12)	6.0 (7.10)	35 (33.37)	40	-	153.8	0.33	2.8
35 (36.10)	0.0 (0.0)	∞ (∞)	35 (36.10)	20	-	146.9	0.35	4.6

Leaching analysis of the optimal 23Ni-12Cu/Al_2O_3 catalyst in water and 2-PrOH were performed on the same device by analysing the concentration of Ni and Cu in the reaction liquid after 5 h experiments at 250 ºC. The results are shown in Table A6.2.

Table A6.2. Leaching experiment results for the 23Ni-12Cu/Al_2O_3 catalyst in H_2O and 2-PrOH.

Solvent	mg/L			Leaching %		
	Ni	Cu	Al	Ni	Cu	Al
H_2O	18.4	0.05	<0.03	1.85	0.009	<0.002
2-PrOH	0.35	<0.03	<0.04	0.019	<0.003	<0.002

Chapter 7

The role of the hydrogen source on the selective production of γ-valerolactone and 2-methyltetrahydrofuran from levulinic acid

The work contained in this chapter was published under the title “The Role of the Hydrogen Source on the Selective Production of γ-Valerolactone and 2-Methyltetrahydrofuran from Levulinic Acid” in *ChemSusChem* **2016**, 9, 2488-2495.

Table of contents

7.1. Introduction 117

7.2. Results under N_2 atmosphere 119

7.3. Results under H_2 atmosphere 122

7.4. Hydrogenation mechanism discussion 123

7.5. Conclusions 129

7.6. References 131

7.7. Appendix 132

7.1. Introduction

In this chapter a research about the influence of the hydrogen source on the reaction is presented. This mechanistic study was carried out in order to clarify the role of the solvent on the reaction which, as shown in the previous chapter, proved to be dominant. For this purpose, a set of three solvents and three catalysts with different activities towards Catalytic Transfer Hydrogenation (CTH) were selected and reactions performed under reactive (H_2) and inert (N_2) atmospheres in order to understand the influence of each variable.

The first step of the reaction, LA to GVL, is known to be achievable under a wide range of conditions. Despite the fact that the solvent may interfere to a certain extent[1], it seems not to play a determining role on this step of the reaction owing to the fact that the reaction proceeds up to high yields under H_2 atmosphere in different media such as water[2,3], 1,4-dioxane[1,4], THF[5], alcohols[6,7] or even under solvent-free conditions[1,8]. This reaction is also reported to occur *via* CTH over metal oxides or supported metal catalysts using alcohols[9] or formic acid[10,11] (FA) as hydrogen donor molecules.

The second step of the reaction, GVL to MTHF, is more challenging due to the high stability of GVL[12]. Hence, this step requires harsher reaction conditions. Previous investigations showed the paramount importance of the H_2 pressure on the GVL conversion. Hydrogen pressures below 80 bar (at room temperature, then heated up to 190 ºC) were insufficient for the solvent free hydrogenation of GVL over Ru/C[13], while 50 to 100 bar of H_2 were required to produce MTHF starting from LA when using homogenous Ru catalysts along with several additives[14–16]. Significant MTHF yields were also achieved over Pd(5%)/C under microwave conditions when LA was fed with a 170% excess of FA, a well known hydrogen donor[17]. Additionally, in the scarce literature dealing with this reaction, the important role of the solvent becomes evident. The most used solvent for this step is 1,4-dioxane, under 100 bar H_2[18] or in vapor phase[19]. GVL transformation is reported to be strongly inhibited by water[13,20], and the selectivity towards MTHF appears to be limited by still unclear mechanisms. Publications on the aqueous phase GVL dehydrogenation into AL[21] and LA[22] suggest the reversibility of these reactions as a factor in the water inhibition.

As shown in the previous chapters, MTHF yield significantly improved when alcohols were used as solvents instead of water. While the results in ethanol were similar to those in water (< 1% MTHF yield), 1-butanol (1-BuOH) allowed to reach up to 10% MTHF yield and 2-propanol (2-PrOH) allowed nearly complete GVL conversion along with 46% MTHF yield[21]. On the other hand, high PDO[23,24] and MTHF[25] yields were reported in aqueous phase reactions using noble metal based catalysts, emphasizing that further studies are required to fully understand this complex reaction.

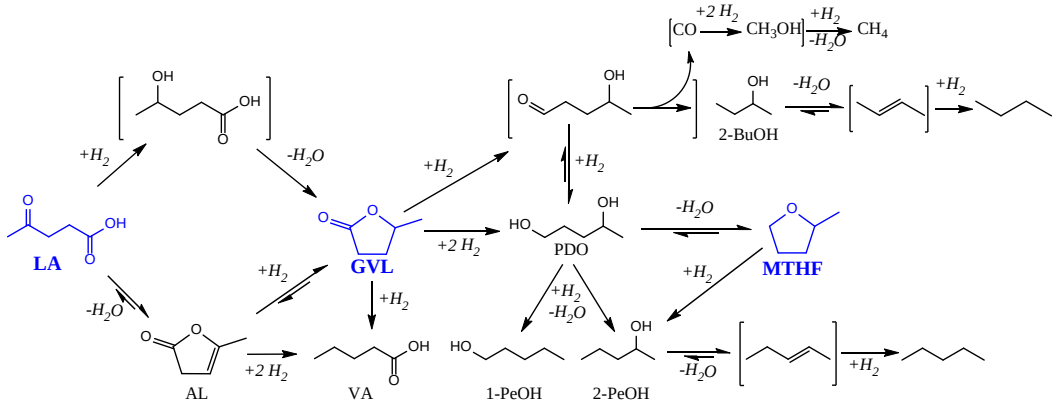

Figure 7.1. Reaction network for the production of MTHF from LA[13,15,21].

It is clear from the above cited works that the presence of a hydrogen donor in the reaction medium, either an alcohol or FA, enhances the MTHF yield. In order to investigate the effect of the two possible hydrogen sources (molecular hydrogen *vs.* CTH) on the hydrogenation of LA, this chapter presents a systematic study of the reaction with a set of three solvents (1,4-dioxane, 1-BuOH and 2-PrOH) and three catalysts (Ru(5%)/C, Ni(35%)/Al_2O_3 and Ni(23%)-Cu (12%)/Al_2O_3). These catalysts and solvents were selected according to their interest and reported use in the literature; either for hydrogenation using molecular hydrogen or for CTH reactions.

1,4-Dioxane, as an aprotic solvent, shows no ability to serve as hydrogen donor in the absence of degradation reactions. Nonetheless, the highest reported MTHF yields starting from LA were achieved using this solvent in gas phase reaction[19]. 1-BuOH is an interesting solvent for this reaction since recent literature showed a simple and effective method to separate LA from the aqueous phases where it is produced from biomass. In the presence of an acidic catalyst LA reacts with butene (and water) or butanol to yield butyl levulinate, causing a spontaneous aqueous-organic phase

separation[11,26]. Besides, these levulinic acid esters are known to show a similar reactivity towards GVL to that of neat levulinic acid[6,11]. Finally, 2-PrOH was selected as the third solvent due to its higher capacity for hydrogen donation compared to 1-BuOH[27,28] and, as shown in the previous chapter, it enables high MTHF yields using Ni-Cu based catalysts[21].

Regarding catalyst selection, a commercial Ru(5%)/C besides our previously used Ni(23%)-Cu(12%)/Al_2O_3 and Ni(35%)/Al_2O_3 catalysts were selected according to their reported use for these reactions and the significant MTHF yields previously achieved[13,21]. Ru/C showed to be an inadequate CTH catalyst due to the poor acidity of the catalyst[28]. On the other hand, Ni/Al_2O_3 was reported to be an active CTH catalyst but with tendency to C-C bond cleavage. The incorporation of Cu resulted in catalysts with similar activities and enhanced selectivities towards hydrogenation[21,29].

Two different atmospheres were chosen for the experiments, namely, N_2 and H_2. In the activity tests carried out under N_2 pressure, the CTH was the primary source of hydrogen for the reaction. In those performed under H_2 pressure, the required hydrogen could come from both molecular hydrogen and CTH.

The catalytic activities of the three catalysts in the aforementioned solvents and reaction atmospheres are summarised in Figure 7.2. For clearness, in this chapter the results of the experiments under N_2 will be discussed based on GVL yields, while the results under H_2 atmosphere will be examined based on MTHF yields. The reason for this consideration is that under H_2 atmosphere, the reaction of LA to GVL is very fast and reaches full conversion in all the cases, making activity comparisons impossible. Under N_2 atmosphere, as previously discussed, CTH reactions are the principal source of hydrogen for the transformation of LA into GVL. However, this *in-situ* generated hydrogen alone is insufficient to convert the highly stable GVL into MTHF. In the following sections these results are discussed in detail.

7.2. Results under N_2 atmosphere

Low hydrogen availability provided by a poor hydrogen donor (1,4-dioxane) and N_2 atmosphere resulted in relatively low LA conversions for the three tested catalysts. The Ru based catalyst allowed up to 20% LA conversion with GVL as the main product.

Interestingly, significantly higher LA conversions and GVL yields (up to 53%) were achieved with Ni and Ni-Cu based catalysts.

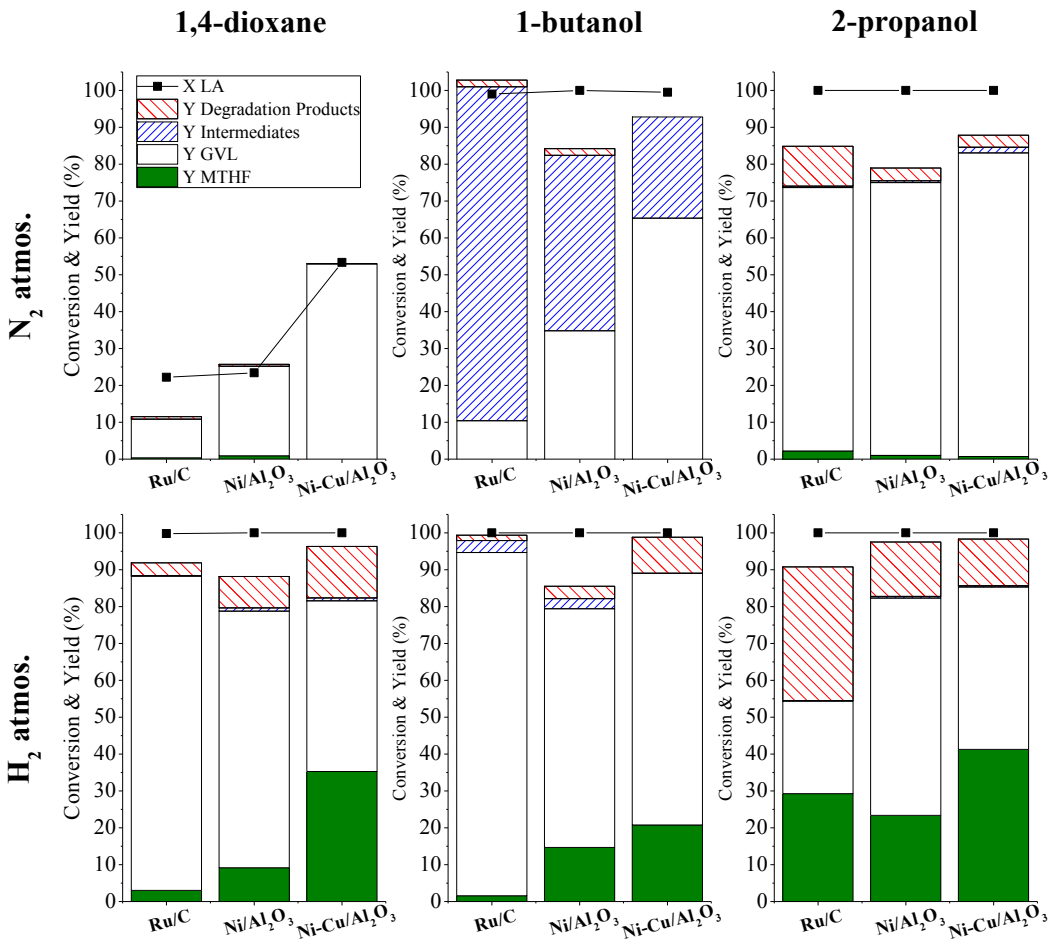

Figure 7.2. Levulinic acid conversion and product distribution for different catalysts, solvents and reaction atmospheres. Reaction conditions: 5 wt% LA in solvent, LA/Cat. 10 g/g, 250 ºC, 40 bar initial pressure and 5 h reaction time. The intermediates considered in this graph are: AL, PDO and LA esters. Quantified degradation products are: VA, 2-BuOH, 1- and 2-pentanol (PeOH). Other detected but not quantified degradation products: pentane, butane, methanol and methane.

The hydrogen required for LA to GVL transformation was most probably provided by solvent degradation. Indeed, 1,4-dioxane derivatives (ethanol, 2-ethoxy-ethanol, ethanol 2-ethoxy methoxy, *etc.*) were detected among the liquid reaction products by GC-MS. Additionally, neat 1,4-dioxane degradation experiments under N_2 atmosphere showed the presence of molecular hydrogen in the gas phase, confirming hydrogen production by solvent or solvent derivatives degradation. According to these data it is reasonable to argue that the low catalytic activity of Ru/C in the applied reaction conditions can be related to its lower activity for 1,4-dioxane degradation and for the use of the *in-situ* generated hydrogen in the LA conversion to GVL.

Using 1-BuOH, a moderate hydrogen-donor molecule[30], Ru/C reached a similar GVL yield as in 1,4-dioxane (up to 10%), while Ni-Cu/Al_2O_3 was able to produce GVL with up to 65% yield. In this solvent, full LA conversion was achieved over the three tested catalysts but with 27% to 90% yields of butyl levulinate, a by-product caused by esterification.

When using 2-PrOH, a well-known hydrogen donor[30], the performance of all the three catalysts improved. Complete conversion of LA was achieved with only trace amounts of 2-propyl levulinate detected in all cases. The most noticeable change concerned the Ru/C catalyst, which achieved up to 71% GVL yield. The GVL production with the non-noble metal catalysts also increased, delivering 74% to 82% GVL yields with VA as the main by-product (3%). VA yield is expressed as the sum of free VA and VA esters.

Noteworthy, none of the experiments carried out under N_2 atmosphere produced significant amounts of MTHF (< 2%). In order to confirm these results, additional experiments using GVL as substrate were carried out in 2-PrOH under N_2 atmosphere with the Ru/C and Ni-Cu/Al_2O_3 catalysts, respectively. The results were consistent showing, as well, low MTHF yields. As shown in Table 7.3, very low (≈ 10%) GVL conversions were achieved along with low MTHF yields (≈ 2%) for both catalysts. The main difference refers to the higher VA yield for Ni-Cu/Al_2O_3 and higher 2-BuOH yield achieved by Ru/C, in good agreement with the well known decarbonylation activity of Ru catalysts[13].

Overall, LA conversions and GVL yields were higher for each catalyst when a better hydrogen donor solvent was used, and, for each solvent by using a more CTH active catalyst. Besides, the results clearly indicate that under the applied reaction conditions *in-situ* generated hydrogen alone is insufficient to convert the highly stable GVL into MTHF even when operating with a high excess of active hydrogen donor molecules. In contrast with the presented results, significant MTHF yields were reported using FA as hydrogen donor molecule both under microwave irradiation and fixed bed reactor conditions; however, the tested catalyst lost its activity after a short reaction time[17].

7.3. Results under H_2 atmosphere

Using Ru/C in 1,4-dioxane, full LA conversion was achieved alongside a significant (85%) GVL and 3% of MTHF yields. When changing the solvent to 1-BuOH similar GVL and MTHF yields were observed. The use of 2-PrOH as solvent triggered the production of MTHF to 29% yield. The reaction system, however, produced 36% yield of degradation products (mainly 2-BuOH and VA) showing its lack of selectivity towards the desired product. The vast MTHF yield differences obtained with each solvent under H_2 atmosphere are in good agreement with the results under N_2 atmosphere. Besides, significant concentrations of solvent dehydrogenation products (acetone and butanal) were detected in the experiments under 100 bar H_2 (Table 7.1). Similarly to experiments under N_2, solvent dehydrogenation produced no measurable increases in the total reaction pressure, thus, keeping the dissolved H_2 concentration constant for each solvent.

Analogous conclusions were drawn from the results using non-noble metal catalysts. Similarly to the results under N_2 atmosphere, the general trend is as follows: for each catalyst, the better the hydrogen donating capacity of the solvent, the higher the MTHF yield; and, for each solvent, the higher the CTH activity of the catalyst, the higher the obtained MTHF yield. Under this atmosphere, however, two exceptions were found. First, a higher yield of MTHF was achieved using Ni-Cu/Al_2O_3 in 1,4-dioxane than in 1-BuOH. Second, a higher yield of MTHF was observed using Ru/C in comparsion to Ni/Al_2O_3 in 2-PrOH solvent. This different behaviour is indicative of more complex interactions and reaction mechanisms in the presence of a high H_2 pressure. Nevertheless, for all the catalysts the highest MTHF yields were obtained when the best hydrogen donor, 2-PrOH, was used as solvent.

Concerning the carbon balances of these experimensts those under nitrogen atmosphere showed a higher deviation (79.6-104.3) than the ones carried out under hydrogen atmosphere (88.6-99.3) as showed in Table A7.1 (see the Appendix). This difference can be associated to sufficient hydrogen availability that reduced secondary reactions.

7.4. Hydrogenation mechanism discussion

In view of the important role of the CTH in the reaction under N_2 and H_2 atmospheres, a direct correlation between the amount of solvent dehydrogenation products (acetone or butanal) and the yield of the desired product could be expected. Despite the fact that such trend could not be found in Figure 7.3 (left) some remarks are worth noting. As expected, under H_2 atmosphere acetone and butanal were present at lower concentrations than under N_2 atmosphere (Table 7.1).

Table 7.1. Butanal and acetone concentrations for the different catalysts and reaction atmospheres.

Entry	Product	Atmosphere	Concentration (mg/g of reaction media)			
			Ru/C	Ni/Al_2O_3	$Ni\text{-}Cu/Al_2O_3$	Equilibrium[a]
1	Butanal	N_2	15.6	29.5	30.4	49.6
2	Butanal	H_2	1.7	1.1	1.6	0.16
3	Acetone	N_2	179.5	135.3	128.1	159.5
4	Acetone	H_2	34.9	35.0	37.3	23.8

[a] Equilibrium concentrations (for pure alcohol dehydrogenation reactions) were calculated using Aspen Plus software (see Appendix).

Under H_2 pressure all the catalysts showed very similar concentrations of the dehydrogenated donor and near the thermodynamic equilibrium conditions, which indicates that the reaction $solv\text{-}H_2 \Leftrightarrow H_2 + Solv$ reached equilibrium. On the other hand, under N_2 atmosphere, different concentrations of dehydrogenation products were measured depending on the used catalysts. Considering the reaction atmosphere his fact may suggest a kinetic control in the solvent dehydrogenation reaction. Nevertheless, considerable differences in the product yields can be observed with similar solvent dehydrogenation products concentrations. This fact stresses the importance of the catalyst to effectively use the *in-situ* produced hydrogen atoms in the hydrogenation reactions, and to reduce their combination and desorption as H_2 molecules.

When plotting the hydrogenating performance (as MTHF yield) under H_2 atmosphere *vs.* CTH performance of the system (as GVL yield) under N_2, the linear trend shown in Figure 7.3 (right) can be observed. This linear trend suggests that the CTH mechanism (a good hydrogen donor solvent and an efficient catalyst) play an important role in the reaction even when operating under high H_2 pressures.

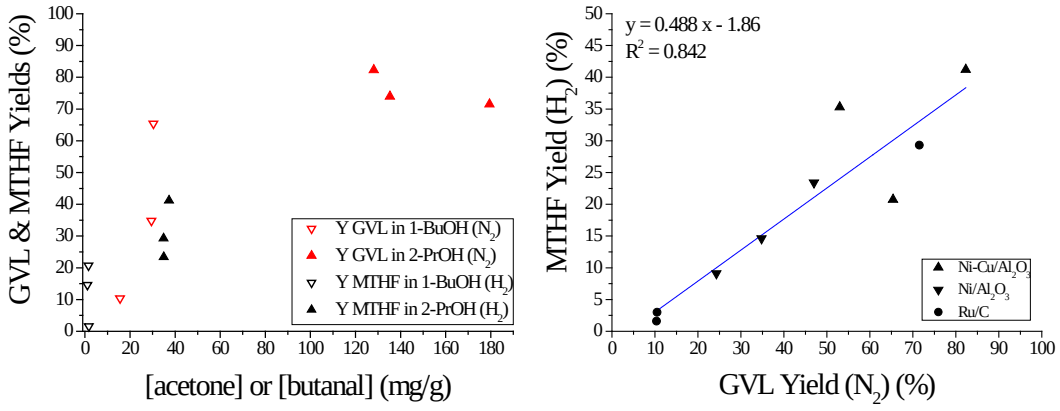

Figure 7.3. Correlation between the solvent dehydrogenation product concentration (mg/g of reaction media) and desired product yields (left) and correlation between GVL yields under N_2 and MTHF yield under H_2 atmosphere (right).

Based on these evidences it can be speculated that both hydrogen sources, molecular hydrogen and the hydrogen donor, play a significant and synergetic role in the reaction. The dynamic hydrogenation/dehydrogenation chemical equilibrium of the donor increases the amount of adsorbed hydrogen atoms on the catalyst surface. Meanwhile, a high molecular hydrogen pressure increases the H_2 dissolved in the reaction medium which, in turn, promotes the adsorption of hydrogen atoms and, hence, reduces their desorption rate.

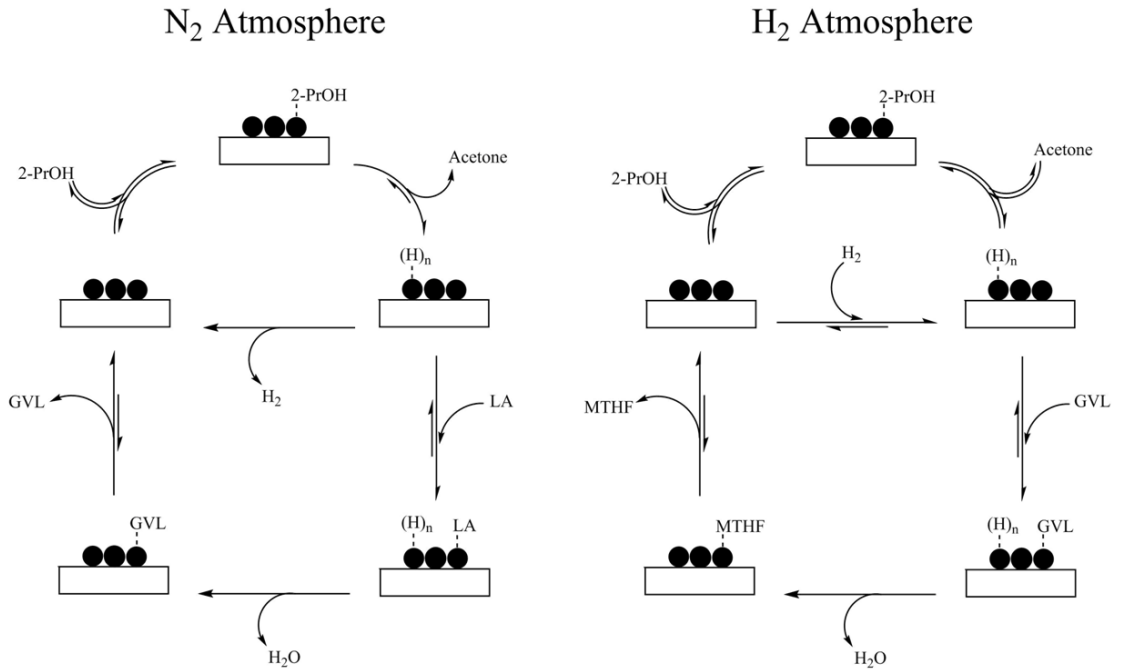

Figure 7.4. Proposed reaction mechanism hydrogen adsorption, 2-PrOH dehydrogenation and LA to GVL reaction under N_2 (left) and GVL to MTHF reaction under H_2 (right) atmosphere.

This improved hydrogen availability seems necessary for the slow and high hydrogen demanding GVL reaction (2 mol H_2 per mol GVL) to PDO and MTHF (Figure 7.1). In Figure 7.4 the two possible hydrogen sources are illustrated coupled with LA to GVL, and GVL to MTHF reactions under N_2 and H_2 atmospheres respectively.

Catalyst characterization was conducted in order to determine the origin of the observed catalyst activity differences. Considering that the reaction is composed of hydrogenation and dehydration steps, both hydrogenating and acidic functionalities are expected to play a role. Besides, it is well known that the CTH mechanism (the metal-hydride route) requires close proximity of both functionalities[30]. Therefore, the concentration of metal and acid sites on the catalysts surface was determined.

Table 7.2. Surface characterization of the fresh catalyst and Site Time Yields (STY).

Entry	Catalyst	μmol CO/ g	Acidity (mmol NH_3 / g)[a]			STY[c] (h^{-1})	
			Weak	Medium	Strong	GVL (N_2)	MTHF (H_2)
1	Ru/C	61.4	0.147 (310 ºC)	-[b]	-[b]	201	82
2	Ni/Al_2O_3	89.5	0.380 (325 ºC)	0.242 (564 ºC)	0.179 (785 ºC)	142	45
3	$Ni\text{-}Cu/Al_2O_3$	37.5	0.297 (364 ºC)	0.245 (537 ºC)	0.275 (742 ºC)	378	189

[a] The strength of the acidity was assessed by peak fitting. The maximum of the peaks are expressed in brackets. [b] Ru/C catalyst is decomposed during the TPD analysis for temperatures above 400 ºC, hence, its acidity cannot be determined above this temperatures [c] STYs are calculated by dividing the produced GVL or MTHF mol by the amount of metallic active sites (g Cat. *x* CO mol/g) and reaction time (5 h).

It appears likely that a higher concentration of metal active sites in the catalyst could be the reason for the improved catalytic performance of $Ni\text{-}Cu/Al_2O_3$. Therefore, CO chemisorption measurements of the three fresh catalysts were carried out (Table 7.2). The results showed that Ni/Al_2O_3 contained the largest amount of metallic active sites, followed by Ru/C; surprisingly $Ni\text{-}Cu/Al_2O_3$ showed the least, two times less than Ni/Al_2O_3. These results showed the significant activity differences related to the metal active sites of each catalyst. For comparison purposes, STYs with 2-PrOH as solvent under N_2 and H_2 atmospheres were selected. Under N_2 atmosphere Ru metal sites were

1.4 times more active than Ni sites, while the active sites in the Ni-Cu catalyst were 2.6 times more active. These differences increased under H_2 atmosphere, with Ru sites being twice as active as Ni ones and the sites on the Ni-Cu catalyst exhibiting 4.2 times higher activity as the ones of the Ni catalyst.

The superior performance of the active sites on Ni-Cu/Al_2O_3, as compared to Ni/Al_2O_3, is indicative of a noteworthy promotion effect by Cu addition, considering that Cu was found to be a less active metal than Ni for this reaction[21]. The lower metal sites concentration on the surface of Ni-Cu/Al_2O_3 reveals that Cu promotion effect was not caused by metal dispersion enhancement, but rather by a bimetallic effect producing an especially active Ni-Cu mixed phase. This bimetallic effect was previously detected in this catalyst showing Cu incorporation to Ni crystal structures[21].The presented evidences are consistent with literature data showing the improved CTH activity of Ni-Cu bimetallic catalyst compared to Ni or Cu monometallic catalysts[29,31].

Acidity measurements revealed that Ni/Al_2O_3 and Ni-Cu/Al_2O_3 presented a similar total acidity (around 0.8 mmol/g). On the other hand, the NH_3-TPD profiles showed Ni to have a higher amount of weak acid sites while the Ni-Cu catalyst has more strong acid sites (Table 7.2). The TPD profile of Ru/C is difficult to analyze since further contributions (including decomposition of the support) cannot be excluded. The profile (see Figure A7.1 in the Appendix) showed some weak acidity on this catalyst but, for temperatures above 400 ºC, carbon is expected to decompose and, hence, the measurements allow no direct interpretation.

The low acidity of Ru/C catalysts was emphasized in CTH studies were partial oxidation of Ru was necessary in order to provide the required acidity for the reaction mechanism. This catalyst was partially deactivated by *in-situ* reduction[28], showing both metallic and acid sites, and their proximity for interaction, to be necessary for CTH reactions[30]. Therefore, the better performance of the Ni-Cu/Al_2O_3 catalyst as compared to Ru/C under the applied reaction conditions can be ascribed to its balanced amount of adjacent acidic and especially active metal sites.

Additionally, the reactivity of PDO, GVL and MTHF in 2-PrOH was checked to gain a deeper insight into the reaction mechanism. PDO was found to be stable in the absence of a catalyst. When using a catalyst, however, full conversion to MTHF was

achieved in less than 90 min with trace amounts of 2-BuOH, 1-PeOH, 2-PeOH and GVL.

Table 7.3. PDO, GVL and MTHF conversion and product distribution in 2-PrOH for different catalysts.

Entry	Catalyst	Conv. (%)	Yields (%)						CB (%)
		PDO	MTHF	VA	2-BuOH	1-PeOH	2-PeOH	Others	
1	-	2.3	1.5	0.0	0.0	traces	0.0	0.0	99.2
2	Ni-Cu/Al_2O_3	99.4	99.0	0.0	0.0	0.4	0.0	0.8	100.8
		GVL	MTHF	VA	2-BuOH	1-PeOH	2-PeOH	Others	
3[a]	Ru/C	12.6	1.9	3.3	3.0	0.0	0.4	0.7	96.7
4[a]	Ni-Cu/Al_2O_3	5.4	2.5	4.6	0.5	0.1	0.0	0.0	102.3
5	Ru/C	97.4	14.9	1.8	37.3	0.0	18.9	9.2	84.7
6	Ni-Cu/Al_2O_3	44.1	30.3	8.5	2.5	1.1	0.5	0.5	99.3
		MTHF		VA	2-BuOH	1-PeOH	2-PeOH	Others	
7	Ru/C	98.5		0.0	5.4	0.0	51.8	15.8	74.5
8	Ni-Cu/Al_2O_3	10.3		0.0	1.0	0.1	3.8	0.3	94.9

All experiments were carried out under H_2 atmosphere except for those marked with [a]. [a] experiments under N_2 atmosphere. CBs over 100% are probably caused by experimental or analytical errors.

As shown in Table 7.3, Ru/C showed a high activity for GVL conversion in 2-PrOH, approaching full conversion with 15% MTHF, 37% 2-BuOH and 19% 2-PeOH yields as the main products. Similarly, MTHF was fully converted over Ru/C in 2-PrOH with 2-PeOH as the main product along small 2-BuOH quantities. These experiments (Table 7.3, entries 5 and 7) clearly differentiate the origin of the degradation products when Ru/C is used: the high 2-BuOH yields observed in LA hydrogenation experiments (Table A7.1) were mainly produced from GVL conversion rather than from MTHF degradation; since MTHF degradation produced mainly 2-PeOH. On the other hand, using Ni-Cu/Al_2O_3 in 2-PrOH, 44% GVL conversion was achieved with 30% MTHF yield and VA as the main by-product (8%). Under the same conditions, in the presence of this catalyst MTHF conversion only reached 10% with 2-PeOH as the main product. This catalyst, which showed a significant activity for the challenging GVL conversion, also showed high selectivity towards MTHF. Besides, its low activity for MTHF degradation makes it a suitable catalyst for selective MTHF production. Meanwhile, Ru/C is also a very active catalyst for the conversion of GVL in the presence of 2-PrOH. However, the selectivity towards MTHF is considerably lower, due to 2-BuOH formation from GVL, and the high activity of this catalyst for MTHF degradation (mainly to 2-PeOH).

Taking into consideration the presented activity results and the features of the studied catalysts and solvents, the most active and selective system was chosen for a more in-depth analysis. Ni-Cu/Al_2O_3 was found to produce the highest MTHF yields

(35 - 40%) over 5 h reaction time in both 2-PrOH and 1,4-dioxane under H_2 atmosphere. As discussed above, these superior results are derived from a high efficiency of the catalyst for CTH alongside high selectivity in GVL conversion to MTHF and a very low activity for MTHF degradation. 2-PrOH was selected as a green solvent alternative to 1,4-dioxane[32] which, in addition, was not stable under the applied reaction conditions.

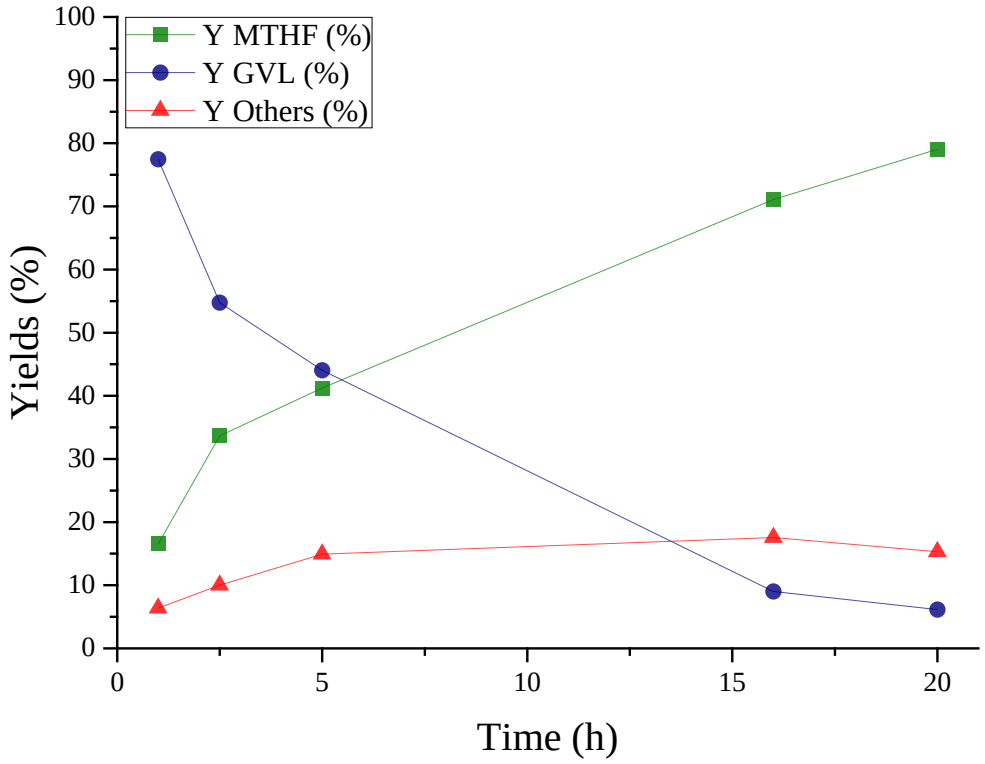

Figure 7.5. Time evolution profile of the reaction in 2-PrOH with Ni-Cu/Al_2O_3. Reaction conditions5 wt% LA in 2-PrOH, LA/Cat. 10 g/g, 250 ºC, 40 bar H_2 initial pressure. The term "others" include VA (up to 9.9% yield), 2-BuOH (up to 2.3%) and 1-PeOH (up to 2.9%).

The time evolution profile in Figure 7.5 showed complete LA conversion in less than one hour reaction time. The MTHF yield continuously increased from 16% in the first hour of reaction to 80% after 20 h reaction time. To the best of our knowledge, this is the highest reported MTHF yield starting from LA over non-noble metal catalysts in green solvents. GVL was the main product at short reaction times and steadily decreased from 77% after 1 h to 6% after 20 h reaction. The main detected by-product was VA, which reached 10% yield at the end of the reaction. Minor amounts of 2-BuOH and 1-PeOH were also detected, reaching 2% and 3%, respectively, at the end of the test.

Additional experiments were carried out to show the potential applicability of this reaction system. As 2-PrOH readily dehydrogenates to acetone as part of the CTH mechanism, the activity of the system may decrease when acetone builds up in the reaction mixture. This fact was checked by carrying out an activity test with 5 wt% LA in a mixture of 2-PrOH and acetone (up to 4:1 weight ratio).

The results showed that even this high initial acetone loading produced no decrease of the activity of the system, still reaching complete LA conversion with 40% MTHF, 39% GVL and 6% VA yields after 5 h of reaction with 91% carbon balance. Besides, acetone concentration in the reaction mixture decreased from 190 to 55 mg/g at the end of the reaction, only slightly above the concentration in the experiment without acetone addition (37 mg/g). This fact, along with comparable LA hydrogenation results, indicates that the *2-PrOH* $\Leftrightarrow$ *acetone* + H_2 reaction occurs much faster than the conversion of LA to GVL and MTHF. Conseqeuntly, the kinetics of 2-PrOH transformation do not affect LA conversion. This would be an important advantage for a possible scale-up of the process since no *ex-situ* acetone hydrogenation would be required for solvent recycling into the reactor.

On the other hand, the use of more concentrated solutions would be of paramount importance for a possible industrial application. Hence, an experiment feeding a 30 wt% LA solution in 2-PrOH was carried out keeping the LA-to-catalysts weight ratio constant at 10. The results showed a good agreement to the results of 5 wt% feed facilitating full LA conversion after 5 h of reaction time with 47% MTHF, 43% GVL and 6% VA yields at 98% carbon balance.

7.5. Conclusions

The two possible sources of hydrogen (CTH and molecular hydrogen) for the conversion of levulinic acid to MTHF were studied with three different catalysts and discussed in this chapter. While hydrogenation through CTH or molecular H_2 alone were able to produce up to 82 - 93% GVL yields, only trace amounts of MTHF (< 3%) were detected under these conditions. The combination of both sources of hydrogen was indispensible to achieve significant yields. Furthermore, the linear relationship found between the results under N_2 and H_2 atmospheres points to the important role of CTH in

the hydrogenation of LA to MTHF even when operating under high H_2 pressure. Hydrogen pressure is considered to contribute to the reaction by increasing the hydrogen dissolved in the reaction medium and, as a consequence, by reducing hydrogen desorption from the catalyst surface. This enhanced hydrogen availability allows an efficient conversion of GVL and high yield of MTHF.

Provided a good enough hydrogen donor solvent, Ru/C proved to be a very active catalyst for the conversion of LA and GVL. However, its selectivity towards MTHF from GVL is low and it is further hampered due to the high activity of Ru/C for MTHF degradation. Ni-Cu/Al_2O_3, on the contrary, showed the best results, even when using hydrogen donors as poor as 1,4-dioxane. Besides, this catalyst was very active to convert the highly stable GVL into MTHF while showing very low activity for further transformations of MTHF, resulting in high MTHF selectivity. Noticeably, this bimetallic catalyst, which produced the highest MTHF yields, has the lowest active site concentration among the tested catalysts. This fact stresses the bimetallic promotion effect of the catalyst, producing lower amounts of active sites but with much higher activity, rather than improving metal dispersion. Overall, Ni-Cu/Al_2O_3 enabled MTHF yields as high as 80% using a good hydrogen donor, 2-PrOH, as solvent under H_2 atmosphere after 20 h reaction time.

7.6. References

[1] W. Luo, U. Deka, A. M. Beale, E. R. H. van Eck, P. C. A. Bruijnincx, B. M. Weckhuysen, *J. Catal.* **2013**, *301*, 175–186.

[2] I. Obregón, E. Corro, U. Izquierdo, J. Requies, P. L. Arias, *Chinese J. Catal.* **2014**, *35*, 656–662.

[3] J. C. Serrano-Ruiz, D. Wang, J. A. Dumesic, *Green Chem.* **2010**, *12*, 574–577.

[4] L. E. Manzer, K. W. Hutchenson, *Preparation of 5-Methyl-Dihydro-Furan-2-One from Levilinic Acid in Supercritical Media*, **2004**, US 2004254384 A1.

[5] C. Ortiz-Cervantes, J. J. García, *Inorganica Chim. Acta* **2013**, *397*, 124–128.

[6] M. G. Al-Shaal, W. R. H. Wright, R. Palkovits, *Green Chem.* **2012**, *14*, 1260–1263.

[7] Y. Gong, L. Lin, Z. Yan, *BioResources* **2011**, *6*, 686–699.

[8] J.-P. Lange, R. Price, P. M. Ayoub, J. Louis, L. Petrus, L. Clarke, H. Gosselink, *Angew. Chemie Int. Ed.* **2010**, *49*, 4479–4483.

[9] M. Chia, J. a. Dumesic, *Chem. Commun.* **2011**, *47*, 12233–12235.

[10] L. Deng, Y. Zhao, J. Li, Y. Fu, B. Liao, Q.-X. X. Guo, *ChemSusChem* **2010**, *3*, 1172–1175.

[11] X. L. Du, Q. Y. Bi, Y. M. Liu, Y. Cao, K. N. Fan, *ChemSusChem* **2011**, *4*, 1838–1843.

[12] O. A. Abdelrahman, A. Heyden, J. Q. Bond, *ACS Catal.* **2014**, *4*, 2–9.

[13] M. G. Al-Shaal, A. Dzierbinski, R. Palkovits, *Green Chem.* **2014**, *16*, 1358–1364.

[14] H. Mehdi, V. Fábos, R. Tuba, A. Bodor, L. T. Mika, I. T. Horváth, *Top. Catal.* **2008**, *48*, 49.

[15] F. M. A. Geilen, B. B. Engendahl, A. Harwardt, W. Marquardt, J. Klankermayer, W. Leitner, *Angew. Chemie - Int. Ed.* **2010**, *49*, 5510–5514.

[16] A. Phanopoulos, A. J. P. White, N. J. Long, P. W. Miller, *ACS Catal.* **2015**, *5*, 2500–2512.

[17] J. M. Bermudez, J. A. Menendez, A. A. Romero, E. Serrano, J. Garcia-Martinez, R. Luque, *Green Chem.* **2013**, *15*, 2786–2792.

[18] D. C. Elliott, J. G. Frye, *Hydrogenated 5C Compound and Method of Making*, **1999**, US 5883266.

[19] P. P. Upare, J.-M. Lee, Y. K. Hwang, D. W. Hwang, J.-H. Lee, S. B. Halligudi, J.-S. Hwang, J.-S. Chang, *ChemSusChem* **2011**, *4*, 1749–1752.

[20] M. G. Al-Shaal, P. J. C. Hausoul, R. Palkovits, *Chem. Commun.* **2014**, *50*, 10206–10209.

[21] I. Obregón, I. Gandarias, N. Miletić, A. Ocio, P. L. Arias, *ChemSusChem* **2015**, *8*, 3483–3488.

[22] J. Deng, Y. Wang, T. Pan, Q. Xu, Q.-X. Guo, Y. Fu, *ChemSusChem* **2013**, *6*, 1163–1167.

[23] M. Li, G. Li, N. Li, A. Wang, W. Dong, X. Wang, Y. Cong, *Chem. Commun.* **2014**, *50*, 1414–1416.

[24] T. Mizugaki, Y. Nagatsu, K. Togo, Z. Maeno, T. Mitsudome, K. Jitsukawa, K. Kaneda, *Green Chem.* **2015**, *17*, 5136–5139.

[25] T. Mizugaki, K. Togo, Z. Maeno, T. Mitsudome, K. Jitsukawa, K. Kaneda, *ACS Sustain. Chem. Eng.* **2016**, *4*, 682–685.

[26] E. I. Gürbüz, D. M. Alonso, J. Q. Bond, J. a. Dumesic, *ChemSusChem* **2011**, *4*, 357–361.

[27] J. C. van der Waal, P. J. Kunkeler, K. Tan, H. van Bekkum, *J. Catal.* **1998**, *173*, 74–83.

[28] P. Panagiotopoulou, N. Martin, D. G. Vlachos, *J. Mol. Catal. A Chem.* **2014**, *392*, 223–228.

[29] I. Gandarias, J. Requies, P. L. Arias, U. Armbruster, A. Martin, *J. Catal.* **2012**, *290*, 79–89.

[30] M. J. Gilkey, B. Xu, *ACS Catal.* **2016**, *5*, 1420–1436.

[31] I. Gandarias, P. L. Arias, S. G. Fernández, J. Requies, M. El Doukkali, M. B. Güemez, *Catal. Today* **2012**, *195*, 22–31.

[32] P. G. Jessop, *Green Chem.* **2011**, *13*, 1391.

[33] D. W. Gree, R. H. Perry, *Perry´s Chemical Engineers´ Handbook*, Mc Graw Hill, New York, **2008**.

7.7. Appendix

Table A7.1. LA conversion and product distribution for different catalysts, solvents and reaction atmospheres. Data used for Figure 7.2.

Entry	Solvent	Catalyst	Products of LA transformation (%)								Solvent derived (mg/g)[a]	
			Conversion	Yields						CB (%)	Acetone	Butanal
			LA	GVL	MTHF	VA	2-BuOH	LA Ester	Others			
N_2 Atmosphere												
1	1,4-dioxane	Ru/C	22.2	10.5	0.4	0.3	0.3	0.0	0.9	89.3	-	-
2	1,4-dioxane	Ni/Al_2O_3	23.4	24.3	0.9	0.5	0.0	0.0	0.0	102.3	-	-
3	1,4-dioxane	Ni-Cu/Al_2O_3	53.4	53.0	0.0	0.0	0.0	0.0	3.3	102.9	-	-
4	1-BuOH	Ru/C	99.0	10.4	0.0	0.0	1.7	90.6	0.6	104.3	-	15.6
5	1-BuOH	Ni/Al_2O_3	100.0	34.8	0.0	0.0	1.8	47.6	4.5	88.7	-	29.5
6	1-BuOH	Ni-Cu/Al_2O_3	99.5	65.4	0.0	0.0	0.0	27.4	4.3	97.6	-	30.4
7	2-PrOH	Ru/C	100.0	71.5	2.2	4.6	5.4	0.4	9.5	93.6	179.5	-
8	2-PrOH	Ni/Al_2O_3	100.0	74.0	1.0	3.0	0.4	0.5	0.7	79.6	135.3	-
9	2-PrOH	Ni-Cu/Al_2O_3	100.0	82.3	0.7	3.1	0.1	1.3	0.7	88.2	128.1	-
H_2 Atmosphere												
10	1,4-dioxane	Ru/C	99.8	85.3	3.0	1.1	1.9	0.0	2.4	93.9	-	-
11	1,4-dioxane	Ni/Al_2O_3	100.0	69.6	9.1	6.8	1.3	0.0	1.8	88.6	-	-
12	1,4-dioxane	Ni-Cu/Al_2O_3	100.0	46.3	35.3	9.2	3.3	0.0	2.2	96.3	-	-
13	1-BuOH	Ru/C	100.0	93.1	1.6	0.5	0.5	3.2	0.4	99.3	-	1.7
14	1-BuOH	Ni/Al_2O_3	100.0	64.8	14.6	10.1	1.0	2.4	0.0	92.9	-	1.1
15	1-BuOH	Ni-Cu/Al_2O_3	100.0	68.3	20.7	9.7	0.0	0.0	0.3	99.0	-	1.6
16	2-PrOH	Ru/C	100.0	25.1	29.3	3.4	25.1	0.0	8.1	91.0	34.9	-
17	2-PrOH	Ni/Al_2O_3	100.0	58.9	23.4	10.4	1.8	0.1	2.9	97.5	35.0	-
18	2-PrOH	Ni-Cu/Al_2O_3	100.0	44.1	41.2	6.5	5.0	0.0	1.7	98.5	37.3	-

Carbon balances over 100%, are probably caused by experimental or analytical errors. [a] Dehydrogenation product concentration is given as mg of product per gram of reaction mixture

Thermodynamic calculations

Solvent dehydrogenation equilibriums were calculated using Aspen Plus software and the NRTL activity coefficient method. A "RGIBBS" equilibrium reactor was fed with the pure solvents and the corresponding gas at the used experimental conditions (250 ºC and 100 bar). The only considered products in this simulations were the gases (H_2 and N_2), the two solvents (2-PrOH and 1-BuOH) and their dehydrogenation products (acetone and butanal).

Table A7.3. Dehydrogenation potentials of the used solvents

Entry	Solvent	ΔG^0_{Red} (kJ mol^{-1})[a]
1	2-propanol	23.9
2	1-butanol	34.4

[a] ΔG^0_{Red} defined as the difference between the formation Gibbs´ free energies of the ketone or aldehyde and the corresponding alcohol. Data taken from the Chemical Engineer´s Handbook[33].

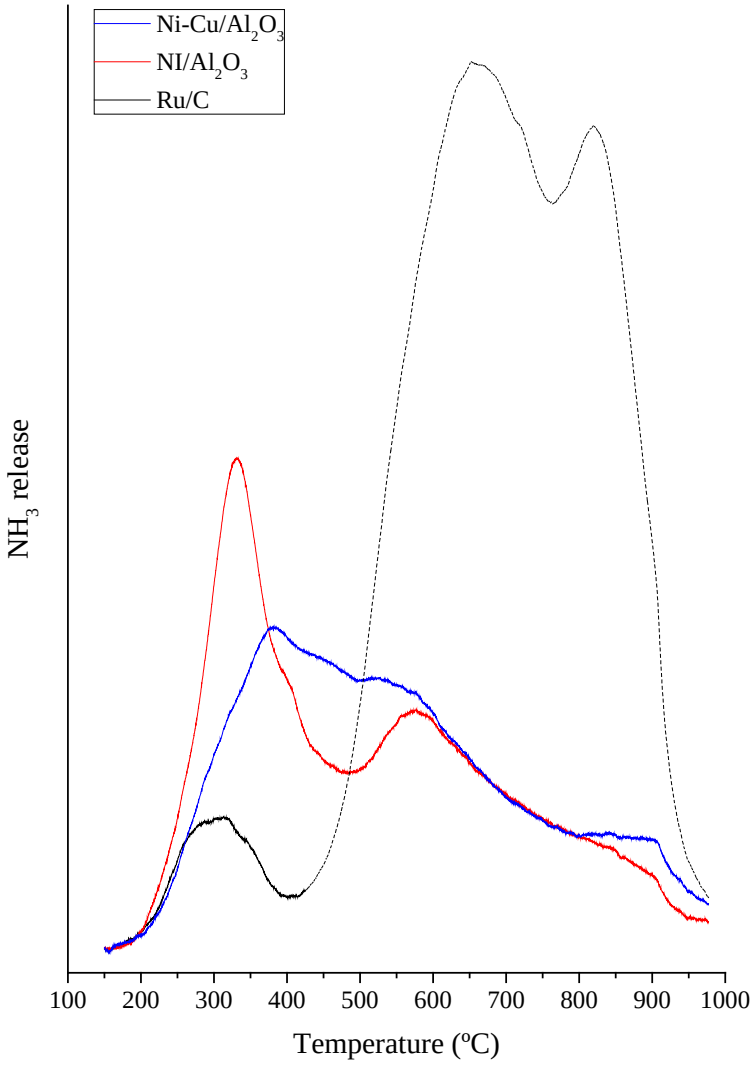

Figure A7.1. NH_3-TPD profiles of the three fresh catalysts.

Chapter 8

Structure-activity relationships of Ni-Cu/Al_2O_3 catalysts for γ-valerolactone conversion to 2-methyltetrahydrofuran

The work contained in this chapter was submitted under the title “Structure-activity relationships of Ni-Cu/Al_2O_3 catalysts for γ-valerolactone conversion to 2-methyltetrahydrofuran” to *Applied Catalysis B: Environmental*.

Table of contents

8.1. Abstract 139

8.2. Effect or the metal content 139

8.3.1. Sequential impregnation catalysts 144

8.3.2. Co-precipitatied catalysts 148

8.3. Catalyst stability and reusability 150

8.4. Conclusions 156

8.5. References 158

8.6. Appendix 159

8.1. Abstract

In this chapter the study was focused on the catalyst and the properties that make it active for the GVL to MTHF reaction. In this case, instead of starting from LA, only the last step of the reaction - the most challenging step - was studied in order to simplify the discussion.

Based on the previously presented research, Ni-Cu/Al_2O_3 catalysts were found to be especially active, owing to its particular ability to activate the CTH mechanism and use the *in-situ* generated hydrogen for the conversion of LA and GVL with high selectivities. In the previous chapters this activity was correlated with the presence of a Ni-Cu mixed phase, which promoted the aforementioned effects. Hence, the aim of this chapter is to prove this hypothesis by understanding the structure-activity relationships *i.e*. the role of the metal sites, the relevance of the Ni-Cu interactions and the effect of the catalyst acidity.

To achieve this goal, the effect of both the total metal content and the catalyst preparation technique were analyzed and their properties thoroughly characterized. By doing so, the catalyst formulation and the used preparation method were optimized and also the stability and reusability of the catalysts were assessed. This last point is of great importance for catalysts devoted to the industrial production of high volumes of price competitive biofuels.

In this case, 2-BuOH was the selected solvent owing to the fact that it is a well known hydrogen donor molecule; it is partially immiscible with water and is currently used as gasoline additive[1]. The temperature was set to 230 ºC instead of the previously used 250 ºC in order to limit the side reactions. In addition, the lower conversions and yields achieved under these conditions allow for a clear discrimination of each catalysts activity.

8.2. Effect or the metal content

In order to study the effect of the metal content, a series of catalysts with the optimized Ni:Cu weight ratio (2:1) determined in Chapter 6, and different total metal

loadings were prepared by a *Wet Impregnation* (WI) method and their activity was tested. The results displayed in Figure 8.1 showed, as expected, the negligible activity of the bare γ-Al_2O_3 support for this reaction, owing to the lack of hydrogenating active sites. For metal loads up to 35% the activity of the catalysts increased with the metal content, reaching a maximum 48% MTHF yield. Further increase on the metal loading to 50% showed no significant differences compared to the 35% catalyst. Carbon balances (CB) were typically above 90% and the selectivity of the catalysts increased with the metal loading, from 66% for the 10WI catalyst up to 80% on the 50WI. In addition to the substrate, GVL, and MTHF, other detected reaction products were valeric acid and its butyl ester (2-3%), 1- and 2-pentanol (1-1.5%) and PDO (< 1.5%).

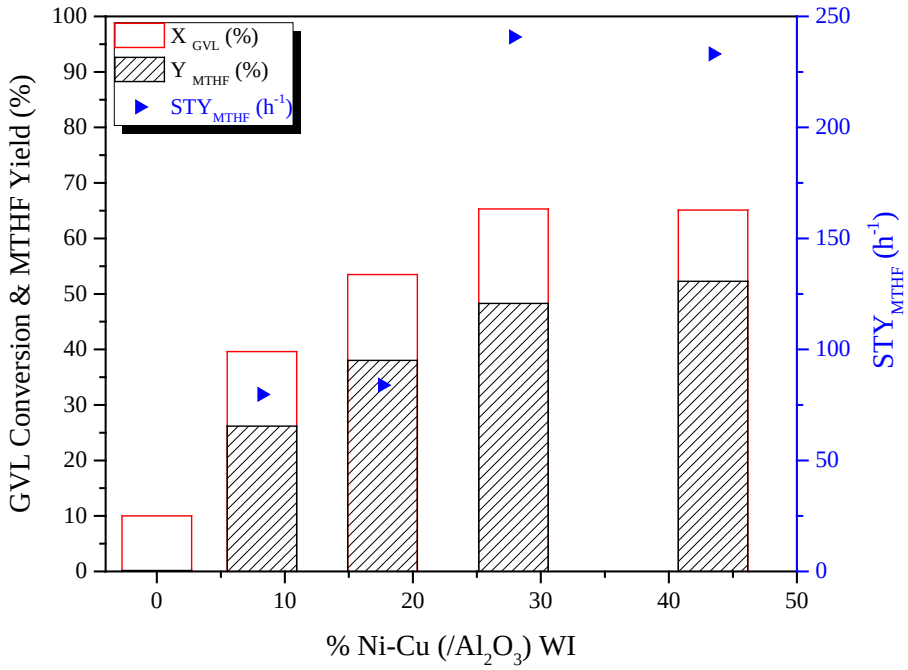

Figure 8.1. GVL conversions, MTHF yields and Site Time Yield (h^{-1}) for 2:1 Ni-Cu catalysts with different total metal loadings. Reaction conditions: 230 ºC, 50 bar H_2 pressure (@room T), GVL-to-Cat. weight ratio of 10, 5 wt% GVL in 2-butanol, 500 rpm stirring and 5 h reaction time. STY is calculated as the MTHF mol produced per metal active site (CO chemisorption) and reaction time.

Catalyst characterization was conducted in order to determine the origin of the activity differences. Since the reaction consists of hydrogenation and dehydration steps, both metallic and acidic active sites would be required. Therefore, NH_3-TPD and CO chemisorption experiments were performed on freshly reduced catalysts (see Table 8.1).

Interestingly, the 10WI catalyst showed higher acidity than the bare γ-Al_2O_3 support, suggesting that a part of the added metals was not reduced during the activation, probably leading to Ni oxide phases which can act as Lewis acid sites[2].

Further increases in the metal loading led to a steady decrease in the total acidity of the material from 0.91 to 0.73 mmol NH_3/g (see Table 8.1).

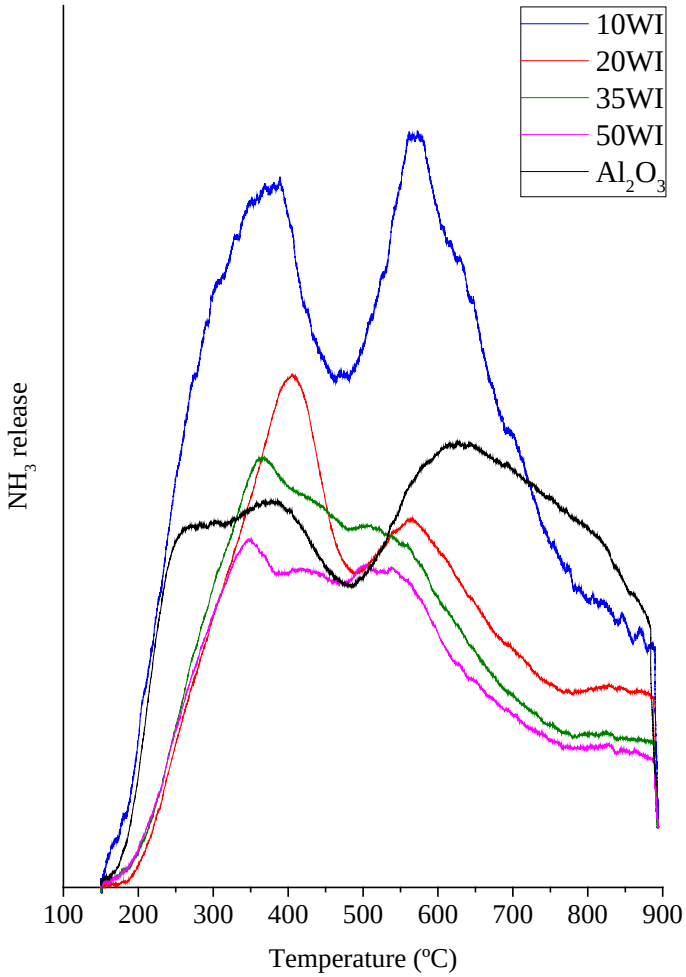

Figure 8.2. NH_3-TPD profiles of the fresh WI catalysts with different metal contents. The signals are normalized by the weight of sample used for the analysis.

CO chemisorption showed an increasing amount of metallic active sites with metal loadings up to 20% (see Table 8.1). Further increases in the metal loading led to a sharp decrease in the metallic sites amount. These measurements are consistent with XRD patterns of the reduced catalysts, which showed no Ni or Cu diffraction peaks for loadings below 35% and important metal related peaks for the higher metal loads (see Figure 8.3). These two techniques consistently indicated that the catalysts with lower metal contents contained small and dispersed metal particles while the highly loaded ones showed larger particles.

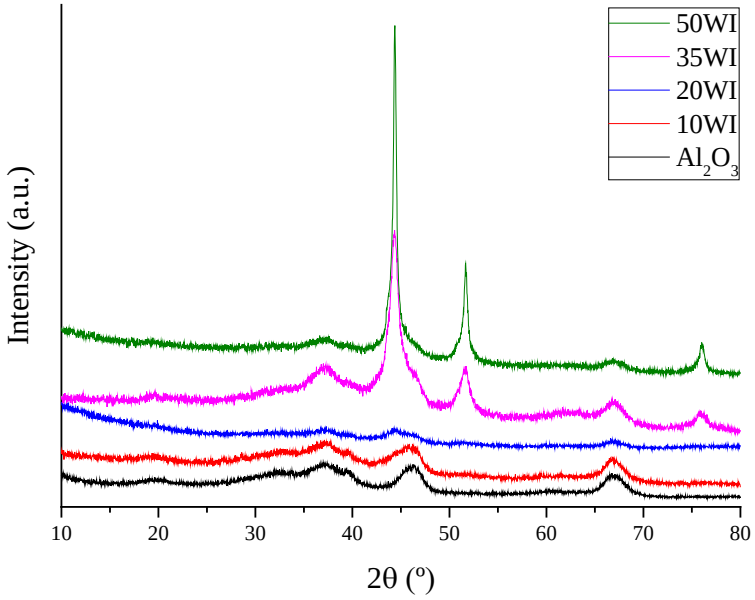

Figure 8.3. XRD profiles of the fresh WI catalysts with different metal contents.

TPR profiles of the catalysts (Figure 8.4) showed three differentiated peaks which can be related to the different metal species *i.e.* Cu (peaks centered at 216 - 227 ºC)[3,4], Ni in high interaction with the Al_2O_3 support (peaks centered at 377 - 417 ºC)[3,5] and a Ni-Cu mixed phase (shoulder-peak centered at 262 - 271 ºC)[4]. The profile of the 10WI catalyst is considerably different from the others, showing two reduction peaks at 316 and 555 ºC. The high T reduction peak can be ascribed to Ni aluminate species whereas the low T peak can be ascribed to Cu species[3].

Table 8.1. Peak area percentage from fitting of the TPR profiles in Figure 8.4, acidity quantification from the profiles in Figure 8.2 and CO chemisorption results for the impregnation catalysts with different metal loading.

	TPR			NH_3-TPD (mmol NH_3/g)			CO
Catalyst	% Peak 1[a]	% Peak 2[a]	% Peak 3[a]	150-525 ºC	525-900 ºC	Total	(μmol/g)
10WI	77 *(312)*	-	23 *(558)*	0.84	0.79	1.63	65.6
20WI	65 *(216)*	7 *(280)*	28 *(416)*	0.48	0.44	0.91	90.5
35WI	60 *(226)*	26 *(278)*	14 *(405)*	0.48	0.37	0.85	37.5
50WI	64 *(218)*	30 *(251)*	6 *(384)*	0.41	0.33	0.73	44.8

[a] The figures in brackets indicate the temperature (ºC) of the reduction peaks maximum. TPR fitting are shown in Figure A8.15 in the Appendix.

A comparison of the profiles evidenced increasing Ni-Cu interactions with increasing metal loadings, which enhanced the reducibility of the metal species[3,6] as indicated by the shift towards lower temperatures of all the reduction peaks (100 ºC for the low T peak and up to 180 ºC for the high T peak, see Table 8.1). TPR profiles also confirmed the hypothesis of incomplete metal reduction, with reduction peaks at temperatures above the catalyst activation temperature (450 ºC). The unreduced metal fraction was the largest for the 10WI catalyst, and decreased to minimal amounts with

the increment of the metal loading. As described in a previous publication[4], the presence of a mixed Ni-Cu phase can be observed in the second reduction peak located around 280 ºC. This peaks contribution was the highest for the 50WI catalyst and decreased with the metal content until it was not detected on the 10WI catalyst.

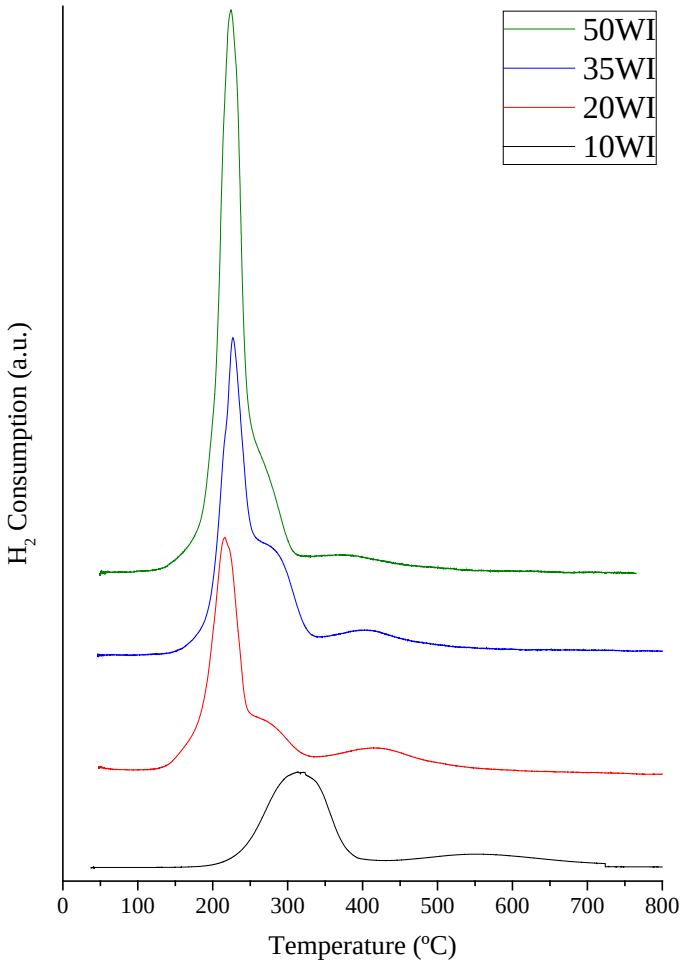

Figure 8.4. TPR profiles of the calcined WI catalysts with different metal contents. The signals are normalized by the weight of sample used for the analysis.

All the described characterization along with the activity results suggest that the total amount of metal sites or acidic sites is not as influential for the activity of this catalyst series as the "specific activity" of the sites, as shown by the *Site Time Yield* (STY) in Figure 8.1. Interestingly the STYs of the metallic sites in the small particle containing catalysts, 10WI and 20WI, were almost equal and three times lower than the STY of the sites of the catalysts containing larger metal particles, *i.e.* 35WI and 50WI.

These results suggest that a stepwise change occurs in this catalysts surface chemistry when moving from small particles to larger clusters. Apparently, according to the presented activity and characterization data, particle agglomeration triggers the

formation of the Ni-Cu mixed phase, whose active sites showed much higher activity than isolated Ni and Cu particles. However, the 50WI catalyst showed similar activity to the 35WI catalyst despite of the fact that the mixed phase was more abundant in the 50WI and the amount of metal sites was larger (see Table 8.1).

Considering that the acidity was the only parameter that decreased from the 35WI to the 50WI catalyst it can be speculated that the catalyst acidity plays a role on the adsorption and activation of the GVL molecule aside from the dehydration of PDO to MTHF. The fact that only trace amounts of PDO were detected in the reaction media suggests that the PDO dehydration to MTHF is not the rate controlling step; hence, providing further evidence that the observed effect of the acidity is more strongly related to the conversion of GVL, the rate limiting step of the reaction, than it is for the dehydration of PDO.

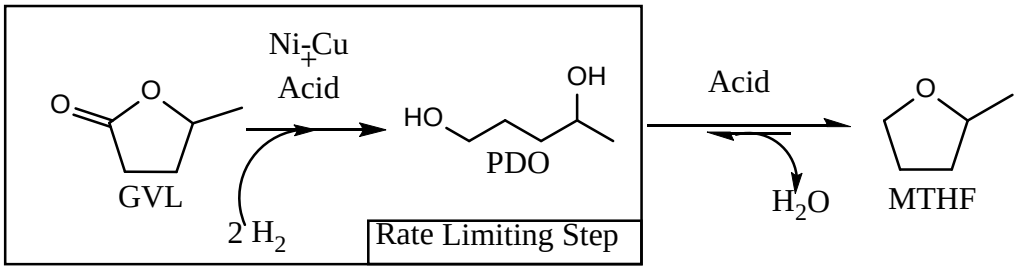

Figure 8.5. GVL reaction mechanism and limiting step identification.

According to these findings, it is reasonable to suggest that GVL may adsorb on an acid site and, due to this interaction, the GVL ring may lose some stability and as a result the addition of dissociated hydrogen atoms from an adjacent metal (Ni-Cu) sites becomes an easier process. This reaction mechanism, which is reported for other hydrogenolysis reactions[5,7], requires close proximity of metallic and acidic sites so that the GVL molecule can interact with both functionalities. A control experiment adding γ-Al_2O_3 to a reaction with the 50WI catalyst demonstrated this point, since no activity differences were observed de*spite the increased total acidity on the reaction medium.

8.3.1. Sequential impregnation catalysts

In view of the importance of the Ni-Cu phase, the acidity and their proximity, different impregnation procedures were applied trying to promote the formation of the Ni-Cu mixed phase along with higher surface acidity. Based on the previously presented results the 35% metal content was selected (keeping the Ni-Cu weight ratio at 2)

because it showed significant amounts of the Ni-Cu phase and it showed higher acidity than the 50WI catalyst. Contrary to the simultaneous impregnation used to prepare the WI catalysts, sequential impregnation was used, alternating the order of the impregnation of Ni and Cu. The catalysts will be denoted as 35Ni+Cu, when Ni was the second impregnated metal, and 35Cu+Ni, when the second metal to be impregnated was Cu. The activity results for these catalysts are summarized in Figure 8.6.

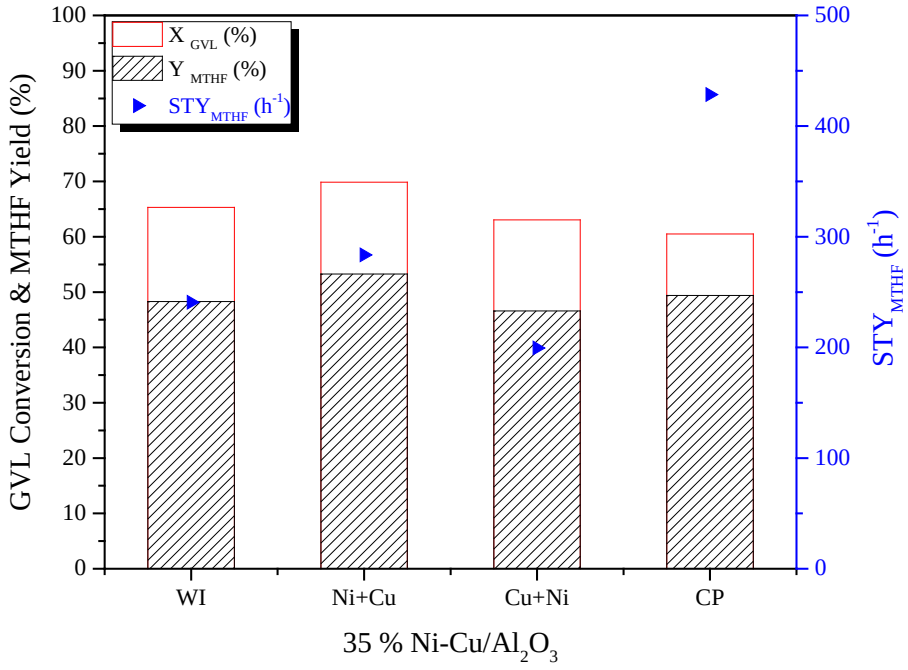

Figure 8.6. GVL conversions, MTHF yields and Site Time Yield (h^{-1}) of 35% Ni-Cu/Al_2O_3 catalysts prepared by different methods.

The activity data showed similar results for the three impregnation methods. The 35Ni+Cu catalyst showed a slight increase in the MTHF yield (53 *vs.* 48%) compared to the 35WI catalyst whereas the 35Cu+Ni showed similar values (47 *vs.* 48%) to those of the 35WI catalyst. As all the catalysts showed similar selectivity (≈ 75%), the same trend was observed regarding GVL conversion. In view of the slightly superior activity of the 35Ni+Cu catalyst, a metal content screening was carried out using this preparation method. The results, displayed in Figure A8.16 (left), showed the 35% metal content to provide the highest activity and STY.

TPR analysis of the different 35% impregnation catalysts showed similar profiles. Nevertheless, a shift towards higher reduction temperatures (from 225 to 258 ºC in the low T peak and from 400 to 442 ºC in the high T peak, see Table 8.2) was noticed for the sequential impregnation catalysts, indicating stronger metal support interactions[6]

and, hence, lower bimetallic interaction (Figure 8.7). These results are consistent with the two calcination steps involved in the preparation method. Nonetheless, all the profiles showed the shoulder-peak on the low temperature peak, ascribed to the Ni-Cu mixed phase. In the sequential impregnation samples the Ni-Cu related peak was centered at 322 - 327 ºC while on the 35WI it was centered at 278 ºC.

TPR profile fitting showed that the highest amounts of the Ni-Cu phase were present in the 35WI catalyst, followed by the 25Ni+Cu and the 35Cu+Ni showed the lowest amount (see Table 8.2). These results showed that no improvement was achieved by this impregnation procedure regarding the Ni-Cu phase formation.

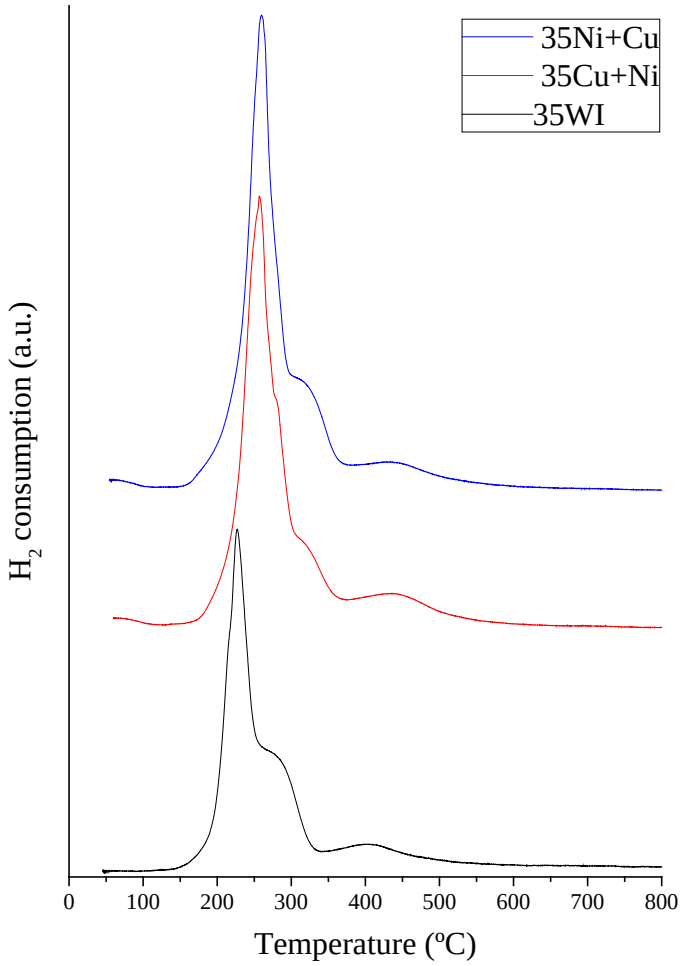

Figure 8.7. TPR profiles of the three impregnation method catalysts. The signals are normalized by the weight of sample used for the analysis.

XRD patterns showed (Figure 8.9), similarly to the 35WI catalyst, large Ni and Cu related peaks. In the case of the sequential catalysts, however, sharper Cu peaks were detected, indicating the presence of larger metal crystals. This fact is, again, consistent with the two calcination step procedure which promotes particle sintering. A

closer look to the XRD patterns of the sequential impregnation catalysts revealed a meaningful asymmetry in the peak related to Cu (43.3°, Figure 8.9). High resolution XRD measurements of these samples allowed the detection of the Ni-Cu solid solution diffraction peak, which was estimated to contain 9 - 14% Ni in Cu (Figure A8.19). Considering the *reference intensity ratio* (RIR) corrected areas of the peaks ascribed to Ni, Cu and Ni-Cu respectively it was estimated that the Ni-Cu solid solution was twice as abundant as the Cu phase in the 35Ni+Cu catalysts, whereas the opposite results were obtained for the 35Cu+Ni catalyst. The smaller particle sizes found in the 35WI catalyst resulted in broader diffraction peaks that overlapped and, hence, phase analysis was not possible for this catgalyst.

Table 8.2. Peak area percentage from fitting of the TPR profiles in Figure 8.7, acidity quantification from the profiles in Figure 8.8 and CO chemisorption results for the 35% impregnation catalysts.

	TPR			NH_3-TPD (mmol NH_3/g)			CO
Catalyst	% Peak 1[a]	% Peak 2[a]	% Peak 3[a]	150-525 ºC	525-900 ºC	Total	(μmol/g)
35WI	60 *(226)*	26 *(278)*	14 *(405)*	0.48	0.37	0.85	37.5
35Ni+Cu	71 *(258)*	19 *(319)*	10 *(420)*	0.44	0.41	0.85	40.1
35Cu+Ni	66 *(253)*	17 *(303)*	17 *(434)*	0.49	0.36	0.85	46.7
20CP	45 *(233)*	23 *(263)*	33 *(515)*	0.69	0.49	1.18	23.0

[a] The figures in brackets indicate the temperature (ºC) of the reduction peaks maximum. TPR fitting are shown in Figure A8.17 in the Appendix.

The NH_3-TPD profiles of this catalyst series showed a similar total acidity, around 0.85 mmol NH_3/g, but with differences regarding the strength distribution (Figure 8.8). Despite the similar values observed in Table 8.2, the TPD profile showed the sequential impregnation catalysts to exhibit a larger acidity peak at low temperatures (400 ºC) while the WI (co-impregnated) catalyst showed higher amount of stronger acid sites (450 – 600 ºC). These results suggest that, in this catalyst series, the acidity might be the activity limiting factor; owing to the fact that a series of catalysts with similar acidity and lower, yet high, Ni-Cu proportion and similar surface metal sites concentration (see Table 8.2) showed similar activity results.

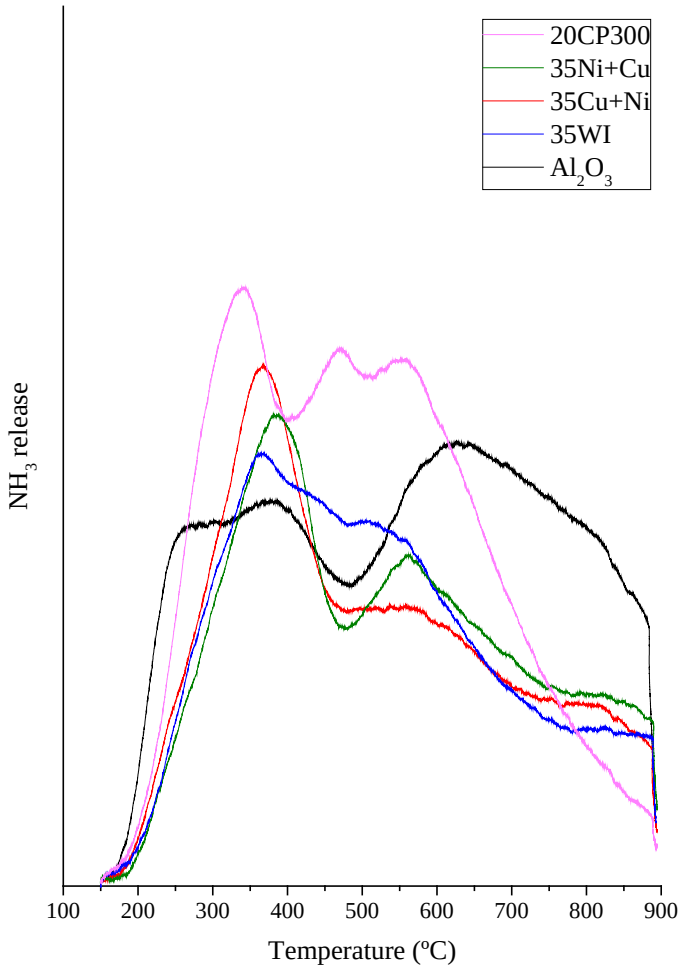

Figure 8.8. NH_3-TPD profiles of the fresh impregnation and co-precipitation catalysts. The signals are normalized by the weight of sample used for the analysis.

8.3.2. Co-precipitatied catalysts

Considering the presented results, increased activity could be expected from catalysts with higher proportions of the Ni-Cu phase along with higher surface acidity. Besides, the proximity of those two functionalities was found necessary for the conversion of GVL. Therefore, attempting to fulfill the mentioned requirements, another method was used to prepare a catalyst with the same Ni-Cu ratio and metal content. The actual metal content of this catalyst, prepared by a co-precipitation (CP) method was 20%, and it will be denoted as 20CP300 according to the used calcination temperature (in order to differentiate from other catalyst that will be presented later in the text). This catalyst showed similar conversion and MTHF yield results compared to the 35% impregnated catalysts but with a noticeably higher STY (1.8 times higher, Figure 8.6). In addition, this catalyst also showed higher selectivity than the impregnated ones (81 *vs.* 75%). Similarly to the procedure applied to the Ni+Cu

sequentially impregnated catalysts, a metal load screening was also carried out using the CP method (see Figure A8.16) and the 20% metal load (20CP300) showed the highest activity.

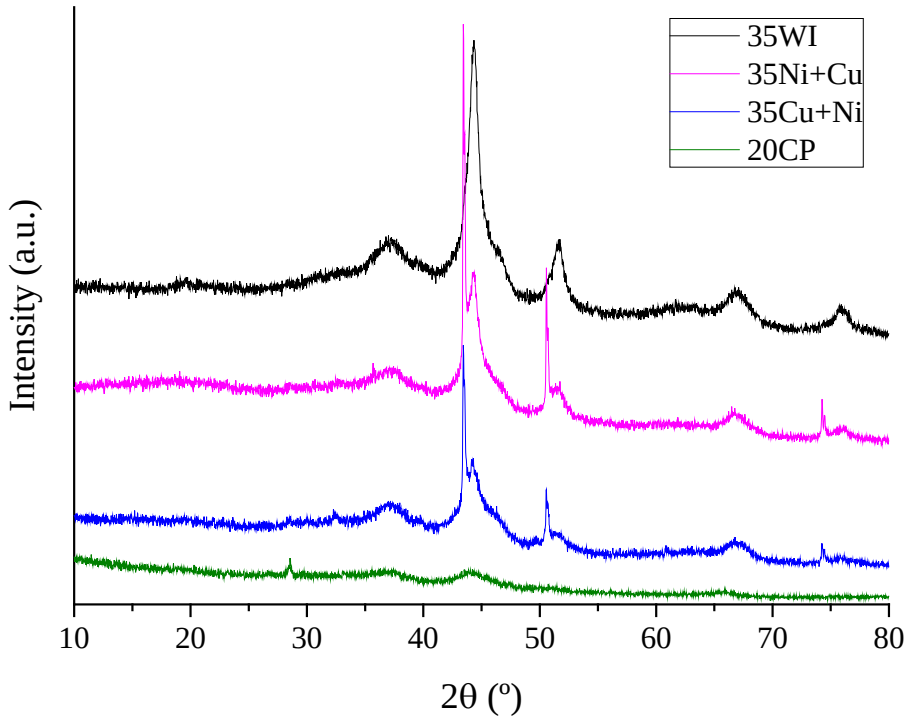

Figure 8.9. XRD patterns of the 35% impregnation catalysts and the 20CP catalyst.

XRD profiles of the 20CP300 catalyst showed no diffraction peaks related to Ni or Cu phases and only small and broad γ-Al_2O_3 related peaks (see Figure 8.9). The small particle size along with the low surface active sites concentration (Table 8.2) can be attributed to the preparation method. The co-precipitation procedure generates a material with an intimate contact between the metals and between the metals and the support, thus, promoting the dispersion of small particles (see Figure 8.13). However, this preparation method also leaves unexposed Ni and Cu atoms in the bulk of the material. The close contact this method promotes is considered responsible for the superior activity of this catalyst; producing a balanced amount of acid and metallic active sites in close proximity from each other. As previously explained this sites proximity is required for hydrogenolysis reactions[5,7] and for *catalytic transfer hydrogenation* (CTH) reactions[8], which were reported to be important in this reaction system[9].

The NH_3-TPD profile of the 20CP300 catalyst showed a significantly higher surface acid site concentration in the low temperature range but most noticeably, in the

high temperature region (see Figure 8.8). The TPR profile of the 20CP300 catalyst differs in shape from the previously presented ones: instead of a low temperature peak with a shoulder-peak, this profile shows a single peak with a tailing on the low temperature region. Peak fitting of the profile showed the presence of the aforementioned Cu, Ni-Cu and Ni phases (see Figure A8.17). In this case, high proportions of the Ni-Cu and the Ni aluminate phases were detected (see Table 8.2), which fits the previously discussed preparation method effect of enhancing bimetallic and metal-support interactions. These observations were further evidenced by the shift in the *Binding Energy* (BE) of Ni and Cu by XPS measurements.

Table 8.3. Surface atomic ratios and peak positions of fresh, used and regenerated 20CP samples calcined at different temperatures determined by XPS.

Catalyst	Sample	C/Al	Ni/Cu	Ni $2p_{3/2}$ (eV)	Cu $2p_{3/2}$ (eV)
20CP300	Fresh	0.26	2.76	855.7	933.3
20CP450[a]	Fresh	0.29	3.07	855,6	933,5
	Used	0.44	3.31	855,6	933,5
	Solvent	0.35	2.94	854,9	933,2
	Regenerated	0.26	2.19	855,9	934,3
20CP600[b]	Fresh	0.32	2.72	855,0	933,2
	Used	0.53	2.05	855,1	933,6
	Regenerated	0.15	2.48	854,6	933,5

[a] This sample was calcined at 450 ºC, and this was also the regeneration temperature. [b] This sample was calcined at 600 ºC, and this was also the regeneration temperature. For reference purposes, the positions of the $2p_{3/2}$ peaks of Ni and Cu in impregnated Al_2O_3 catalysts were 854.8 and 933.0 eV respectively.

As shown in Table 8.3, the BE of both Ni and Cu were consistently higher than the values observed for Ni/Al_2O_3 and Cu/Al_2O_3 samples respectively. The BE of Cu in Ni-Cu alloys is reported to increase by up to 0.3 eV[10,11], which is in good agreement with the results in Table 8.3. Consequently the BE of Ni in Ni-Cu alloys is reported to decrease by up to 0.5 eV[10,11]. Nevertheless, Ni interaction with the Al_2O_3 support increases the BE of Ni by about 1.0 eV[12]. Considering those effects and the fact that the 20CP300 catalyst showed high amounts of Ni aluminate species (reduction peaks > 400 °C), the increase in the Ni BE can be explained as the effect of the second interaction ($Ni\text{-}Al_2O_3$) is more important on the Ni species than the first one (electronic interactions between Ni and Cu).

8.3. Catalyst stability and reusability

Reusability experiments were carried out with the most promising catalysts, *i.e.* 20CP300 and 35Ni+Cu, in order to assess the catalysts stability. As depicted in Figure

8.10 a), direct reuse of the catalyst led to a progressive activity decrease. Four reasons were speculated to be possible deactivation causes: *i)* metal leaching, *ii)* metal oxidation between runs, *iii)* poisoning by carbon deposition and *iv)* metal sintering.

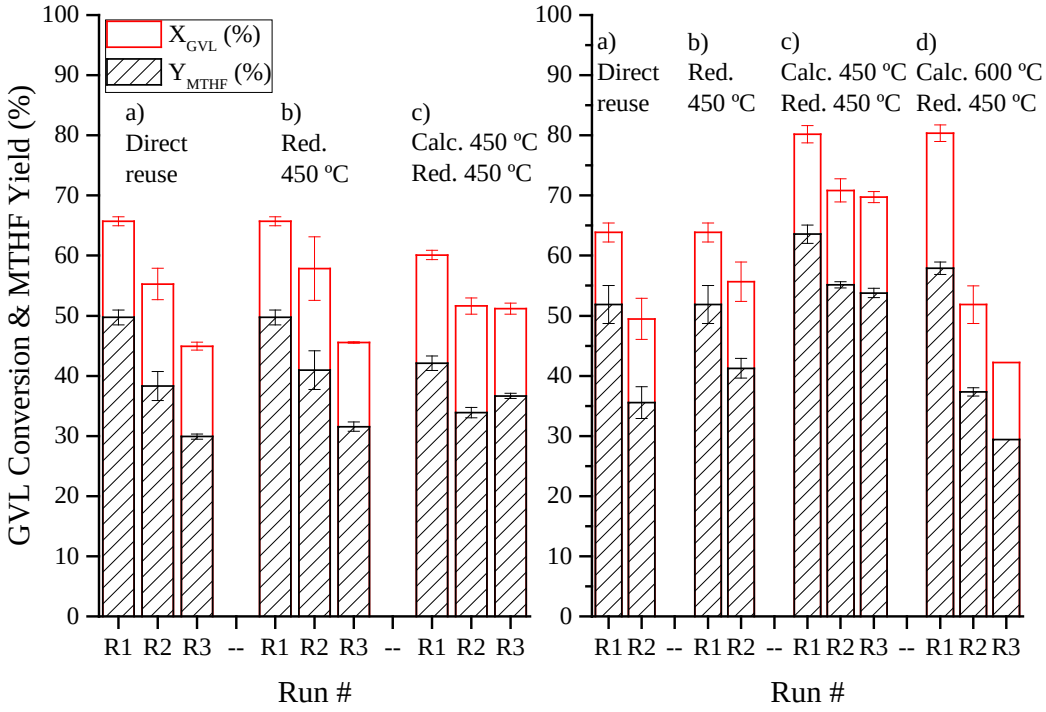

Figure 8.10. Results from reusability experiments. Left graph corresponds to the 35Ni+Cu catalyst and the right graph to the 20CP catalyst.

Metal leaching was checked by measuring Ni, Cu and Al concentrations in the reaction mixture and they were found to be negligible (leached amount after 2 runs < 0.2% in all cases, see Table A8.5). After discarding this deactivation route, the influence of catalyst oxidation was tested by reducing the used catalysts between runs. As shown in Figure 8.10 b), no significant stability improvements were achieved with this strategy, suggesting that other deactivation mechanisms were more important under the applied conditions.

Next, the presence of carbon deposits was checked by XPS analysis of used catalysts, finding higher carbon contents on the used catalysts compared to the fresh samples (see Table 8.3).

In order to eliminate the possible carbon deposits through calcination a higher temperature than the one used for the original calcination step (300 ºC) is required. According to previous reports showing carbon combustion on catalysts used under similar reaction conditions[13–17], 450 ºC was chosen as the calcination temperature for

catalyst regeneration. Consequently, fresh (uncalcined) catalyst samples were calcined at 450 ºC to avoid structural changes upon regeneration and the activities of these catalysts are displayed in Figure 8.10 c).

For the purpose of establishing whether the deposited carbon was produced out of the substrate (or reaction intermediates), from the solvent or from both sources, a control experiment was carried out exposing the 20CP450 catalyst, the 20CP catalyst calcined at 450 ºC, to the reaction conditions but in the absence of substrate (GVL) and then, reusing it for GVL conversion without any treatment. The results were significantly below of those achieved by the fresh catalyst (60 *vs.* 80% GVL conversion), suggesting that the carbonaceous deposit on the catalyst might be produced from the solvent as well as from the substrate or the reaction intermediates. This hypothesis was also confirmed by the increase in the carbon content of the catalyst determined by XPS (see Table 8.3).

In order to confirm and overcome catalyst deactivation *via* carbon deposition, spent catalysts were calcined and reduced (regenerated) between runs. As already explained, the calcination was carried out at 450 ºC and the reduction step was identical to the original activation step (450 ºC). This strategy, as highlighted in Figure 8.10 c), provided catalyst stability but with important differences between the two catalysts. The 35Ni+Cu450 catalyst, calcined at 450 ºC, showed lower activity than the 35Ni+Cu catalyst calcined at 300 ºC (60 *vs.* 65% GVL conversion) and it further deactivated after the first use (51 *vs.* 60% GVL conversion). The third run of this catalyst, however, showed the same results as the second one. On the other hand, for the 20CP450 catalyst an improved activity was achieved with the new thermal treatment (77 *vs.* 61% GVL conversion). The second and third run of this catalyst showed lower but stable activity with 70% GVL conversion and 54% MTHF yields (Figure 8.10 c) right).

Similarly to the 35Ni+Cu450 catalyst, some deactivation took place from the first to the second runs of the 20CP450 catalyst and XPS analysis indicated that it was not related to remaining carbon deposits on the catalyst surface (see Table 8.3); thus, the observed deactivation must be related to structural or surfaces properties changes on the catalyst. Therefore, a calcination temperature of 600 ºC was tested for the 20CP catalyst looking for a higher structural stability. The freshly prepared 20CP600 showed to be as active as the fresh 20CP450, in good agreement with the similar acidity and metal sites

concentration (Table 8.4) these catalysts presented. However, a sharp and continuous activity decrease occurred in the second and third runs of this catalyst (Figure 8.10 d)).

Table 8.4. Summary of the NH_3-TPD and CO chemisorption characterization of the CP samples.

Catalyst	Sample	NH_3 (mmol/g) 150-525 °C	NH_3 (mmol/g) 525-900 °C	NH_3 (mmol/g) Total	CO (μmol/g)
CP450	Fresh	0.92	0.20	1.12	52.1
	Used	0.86	0.40	1.26	57.3
	Regenerated	0.95	0.47	1.42	53.3
CP600	Fresh	0.97	0.32	1.29	42.6
	Used	1.03	0.64	1.67	62.8
	Regenerated	0.38	0.05	0.43	47.8

NH_3-TPD results were divided into two temperature ranges for in order to provide further detail on the acidity variations.

XRD analysis of the used and regenerated 20CP450 and 20CP600 samples showed no difference, indicating that both catalysts were structurally stable under the applied conditions. None of the patterns showed Ni or Cu related diffraction peaks, indicating that only small metal particles are present, and only broad Al_2O_3 related peaks were detected.

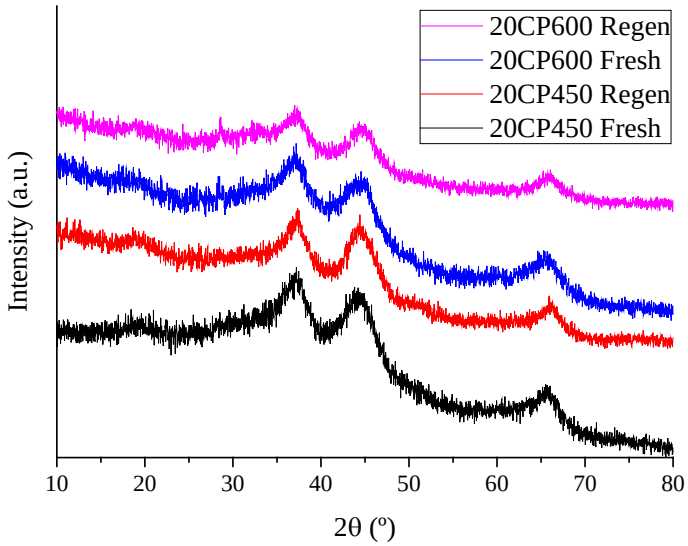

Figure 8.11. XRD patterns of the fresh and regenerated 20CP450 and 20CP600 catalysts.

CO chemisorption analysis of the fresh, used and regenerated catalysts samples evidenced a similar behavior between the two catalysts (20CP450 and 20CP600). The used samples chemisorbed higher amounts of CO than the fresh samples, a fact previously reported in the literature[18–20]. The CO uptake of the regenerated samples decreased to values similar to that of the fresh sample in the case of 20CP450 and slightly higher in the case of the 20CP600 sample. These results suggest that the total

metal sites concentration remained essentially constant, thus, showing the stability of the metal phase.

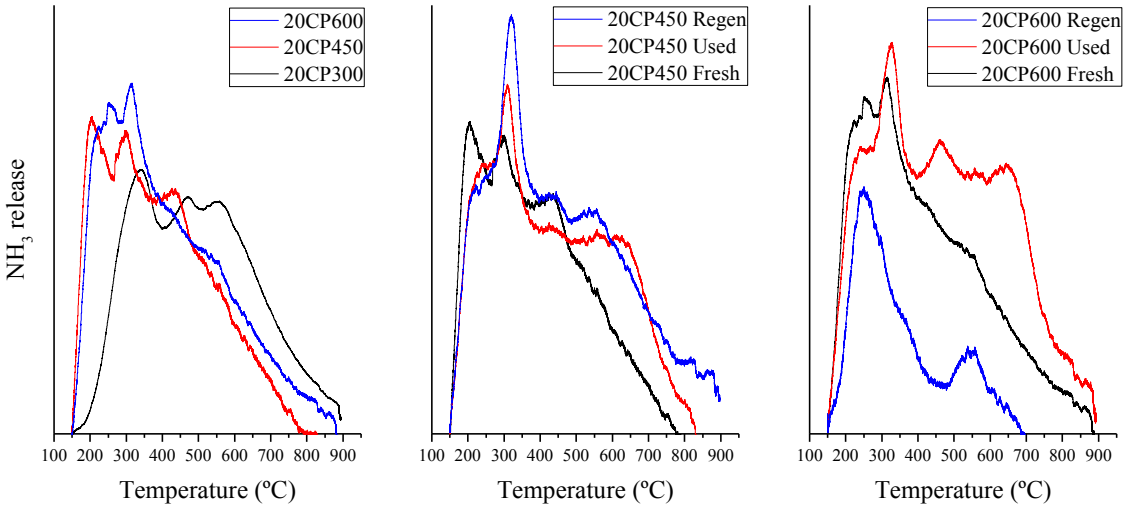

Figure 8.12. NH_3-TPD profiles. Fresh 20CP300, 20CP450 and 20CP600 catalysts (left graph). Center (20CP450) and right (20CP600) graphs show the profiles of fresh (black), used (red) and regenerated (blue) samples.

Regarding acidity measurement, NH_3-TPD characterization of the used 20CP450 catalyst showed a similar profile to that of the fresh sample, but with an increased amount of high temperature sites (see Figure 8.12). This increased acidity might be attributed to the adsorption of reaction intermediates or the presence of carbonaceous species[21]. However, the fact that those high temperature acid sites were also present in the regenerated sample (used, calcined and reduced) suggest that those strong acid site might be related to unreduced Ni species (oxides or aluminates), which are more abundant due to the repeated thermal treatment (Figure 8.14), that can act as Lewis acid sites[2]. Similarly, on the 20CP600 used sample the overall profile remained close to the fresh one, except for the increase in the high temperature acidity. When the used 20CP600 sample was regenerated the acidity drastically dropped across all the temperature range but more acutely in the high temperature range (see Table 8.4). This dramatic decrease in the acidity of the catalyst is most probably caused by a structural change[22] leading to a less hydroxylated surface with a much lower acidity.

According to the previous discussion, balanced amounts of adjacent metallic and acid sites are required for the reaction. Therefore, considering that the amount of metallic active sites remains basically stable (Table 8.4) and the metallic species do not vary drastically (see Figure 8.14), the drop on acidity would damage the metallic - acid

site relation and their distribution. In addition, electronic microscopy images showed Ni agglomeration on the regenerated 20CP600 catalyst, which would also be detrimental for the catalytic activity.

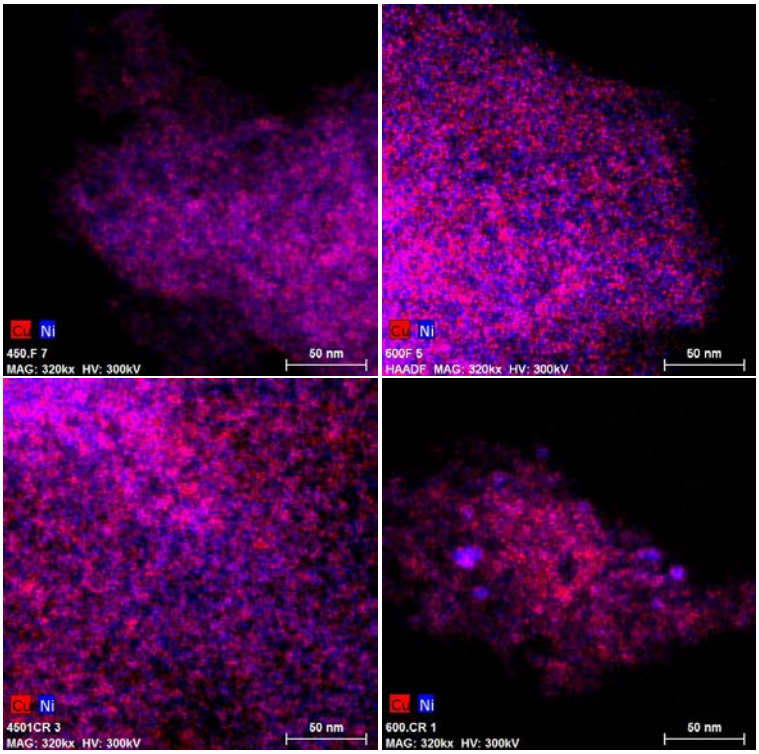

Figure 8.13. STEM images of fresh (upper row) and regenerated (lower row) CP450 (left) and CP 600 (right) catalysts.

In good agreement with the other presented characterization techniques, microscopy images showed no meaningful modifications on the regenerated 20CP450 catalyst compared with the fresh sample (Figure 8.13). However, as depicted in Figure 8.10 some deactivation takes place on the 20CP450 catalyst between the first and the second run. The reason for this behavior can be found on the TPR profile showed in Figure 8.14. The variation on the profile, provably caused by the increased metal support interactions promoted during the repeated calcination processes, suggests modifications on the metal particles or their interaction, which could be the reason for the activity decrease evidenced in Figure 8.10 b). Besides, these processes also trigger the formation of hardly reducible $NiAl_2O_4$ species[23], as observed in the TPR profiles of both 20CP450 and 20CP600 catalysts.

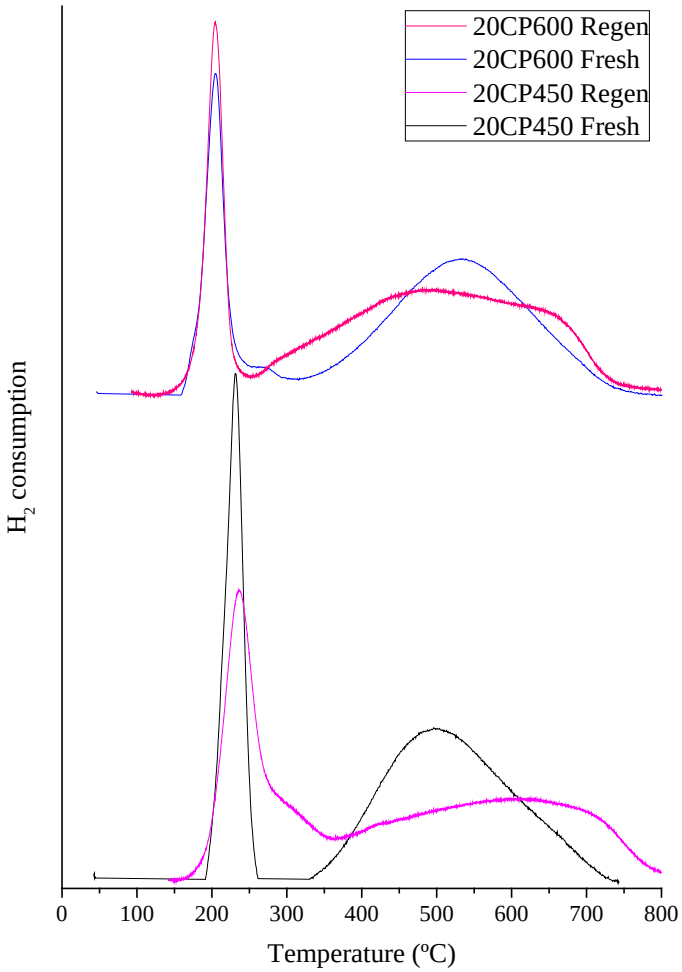

Figure 8.14. TPR profiles of fresh and regenerated 20CP450 and 20CP600 samples.

8.4. Conclusions

The Ni-Cu-Al_2O_3 catalytic system was thoroughly studied for the conversion of GVL into MTHF, finding mayor activity differences related to both the total metal content and the catalyst preparation method. Wet impregnation catalysts evidenced the controlling role of the metal active sites nature over the active sites concentration. In this catalysts series the higher activity (overall and as STY) was shown by the catalysts with the lowest total concentration of metal active sites. The reason for that lies on the higher concentrations of Ni-Cu mixed phase related active sites that were promoted when high metal loadings were incorporated. In addition to this effect, catalyst acidity was found to play an important role; the activity of catalysts with the highest amounts of the active Ni-Cu phase was limited by the lower acidity of these samples. Enhanced activities were achieved by using a co-precipitation preparation method, which further promotes Ni-Cu interactions, produces a more acidic material and enables a closer

proximity between both functionalities on the catalytic surface. Additional activity improvements were achieved by increasing the calcination temperature of the catalyst, reaching up to 64% MTHF yield after 5 h reaction time. The stability of these catalysts was evaluated and deactivation was found due to carbon deposition taking place which can be partially mitigated by calcination between runs. This strategy allowed for a steady > 54% MTHF yield after 3 runs for the most active catalysts, prepared by co-precipitation, while stable < 36% MTHF yields were achieved for the impregnated catalyst.

8.5. References

[1] J. Yanowitz, E. Christensen, R. McCormick, *Utilization of Renewable Oxygenates as Gasoline Blending Components*, **2011**.
[2] Z. Si, D. Weng, X. Wu, Z. Ma, J. Ma, R. Ran, *Catal. Today* **2013**, *201*, 122–130.
[3] J. Ashok, M. Subrahmanyam, A. Venugopal, *Int. J. Hydrogen Energy* **2008**, *33*, 2704–2713.
[4] I. Obregón, I. Gandarias, N. Miletić, A. Ocio, P. L. Arias, *ChemSusChem* **2015**, *8*, 3483–3488.
[5] I. Gandarias, J. Requies, P. L. Arias, U. Armbruster, A. Martin, *J. Catal.* **2012**, *290*, 79–89.
[6] E. T. Saw, U. Oemar, X. R. Tan, Y. Du, A. Borgna, K. Hidajat, S. Kawi, *J. Catal.* **2014**, *314*, 32–46.
[7] A. Martin, U. Armbruster, I. Gandarias, P. L. Arias, *Eur. J. Lipid Sci. Technol.* **2013**, *115*, 9–27.
[8] M. J. Gilkey, B. Xu, *ACS Catal.* **2016**, *5*, 1420–1436.
[9] I. Obregón, I. Gandarias, M. G. Al-Shaal, C. Mevissen, P. L. Arias, R. Palkovits, *ChemSusChem* **2016**, *9*, 2488–2495.
[10] P. . Barbieri, A. de Siervo, M. . Carazzolle, R. Landers, G. . Kleiman, *J. Electron Spectros. Relat. Phenomena* **2004**, *135*, 113–118.
[11] A. Yin, C. Wen, X. Guo, W.-L. Dai, K. Fan, *J. Catal.* **2011**, *280*, 77–88.
[12] A. R. Naghash, T. H. Etsell, S. Xu, *Chem. Mater.* **2006**, *18*, 2480–2488.
[13] W. Luo, U. Deka, A. M. Beale, E. R. H. van Eck, P. C. A. Bruijnincx, B. M. Weckhuysen, *J. Catal.* **2013**, *301*, 175–186.
[14] I. Obregón, E. Corro, U. Izquierdo, J. Requies, P. L. Arias, *Chinese J. Catal.* **2014**, *35*, 656–662.
[15] V. V. Kumar, G. Naresh, M. Sudhakar, C. Anjaneyulu, S. K. Bhargava, J. Tardio, V. K. Reddy, A. H. Padmasri, A. Venugopal, *RSC Adv.* **2016**, *6*, 9872–9879.
[16] X. Tang, H. Chen, L. Hu, W. Hao, Y. Sun, X. Zeng, L. Lin, S. Liu, *Appl. Catal. B Environ.* **2014**, *147*, 827–834.
[17] J. Wang, S. Jaenicke, G.-K. Chuah, *RSC Adv.* **2014**, *4*, 13481–13489.
[18] S. G. Wettstein, J. Q. Bond, D. M. Alonso, H. N. Pham, A. K. Datye, J. A. Dumesic, *Appl. Catal. B Environ.* **2012**, *117–118*, 321–329.
[19] S. T. Oyama, X. Wang, Y.-K. Lee, W.-J. Chun, *J. Catal.* **2004**, *221*, 263–273.
[20] I. Simakova, O. Simakova, P. Mäki-Arvela, A. Simakov, M. Estrada, D. Y. Murzin, *Appl. Catal. A Gen.* **2009**, *355*, 100–108.
[21] X. Tang, Z. Li, X. Zeng, Y. Jiang, S. Liu, T. Lei, Y. Sun, L. Lin, *ChemSusChem* **2015**, *8*, 1601–1607.
[22] L. A. O'Dell, S. L. P. Savin, A. V. Chadwick, M. E. Smith, *Solid State Nucl. Magn. Reson.* **2007**, *31*, 169–173.
[23] F. Mariño, G. Baronetti, M. Jobbagy, M. Laborde, *Appl. Catal. A Gen.* **2003**, *238*, 41–54.

8.6. Appendix

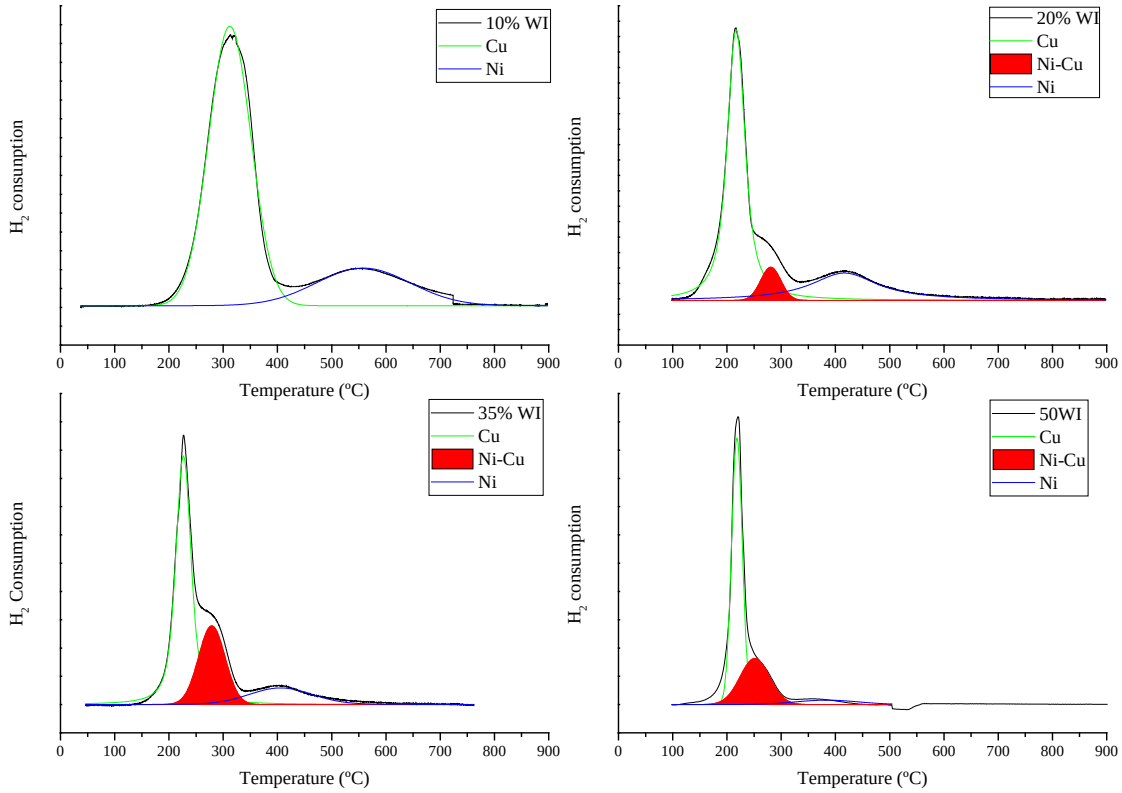

Figure A8.15. TPR profiles and peak fitting for the WI catalyst series with different metal loadings.

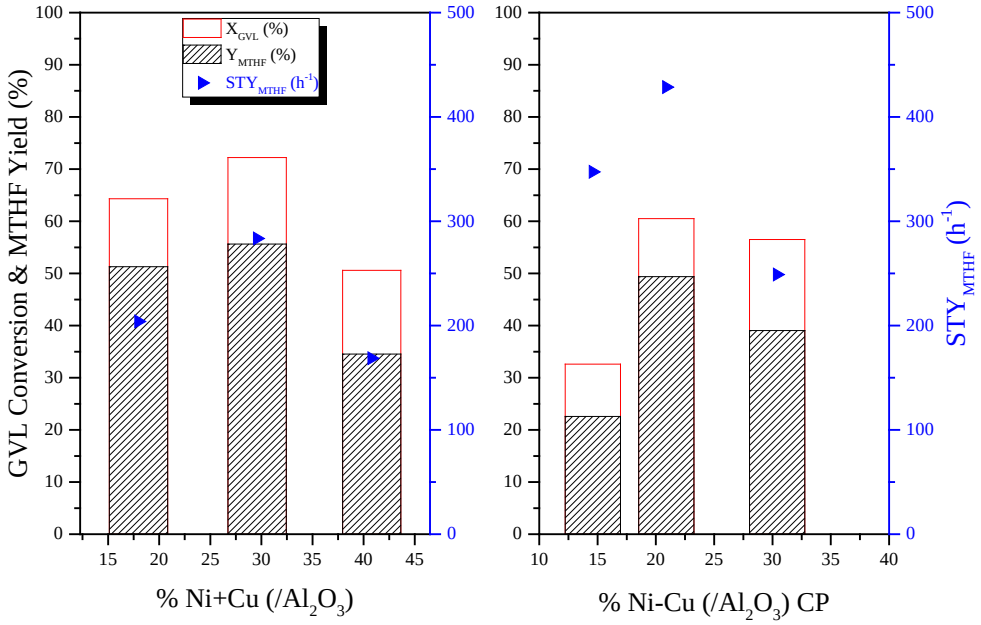

Figure A8.16. Metal content screening for the Ni+Cu sequential impregnation and the CP methods.

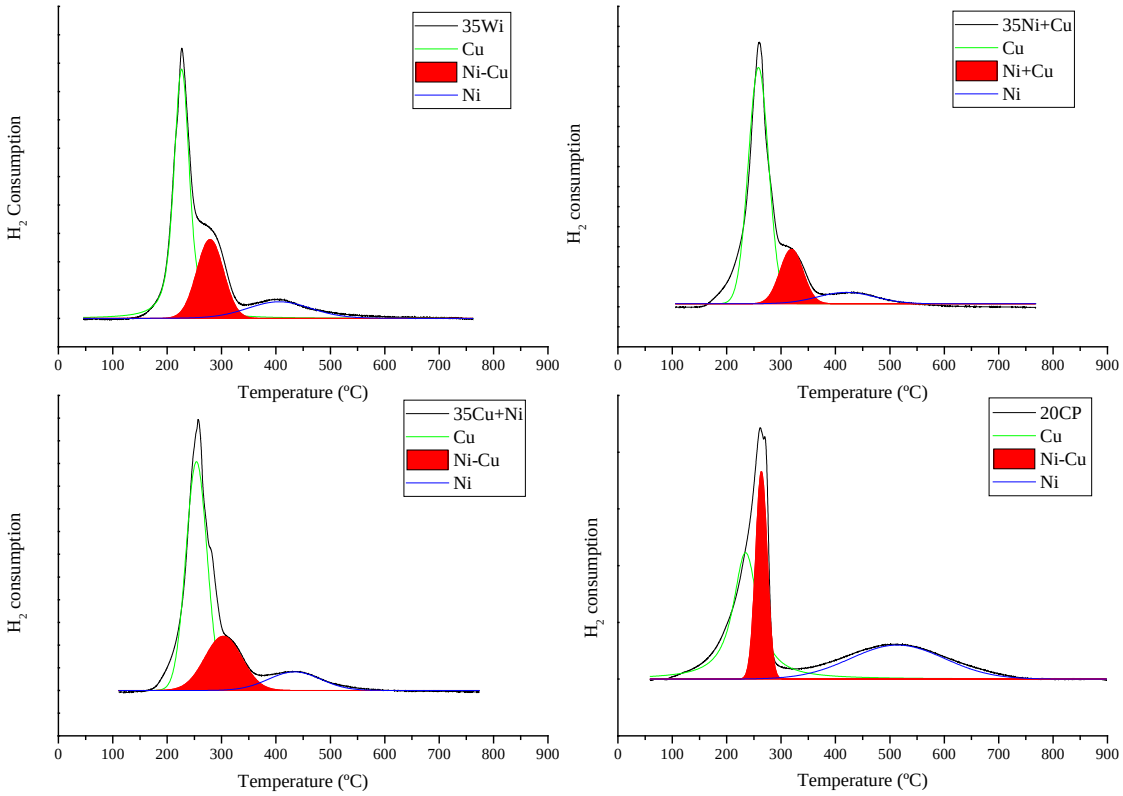

Figure A8.17. TPR profiles and peak fitting for the 35% impregnation catalyst and the 20CP catalyst.

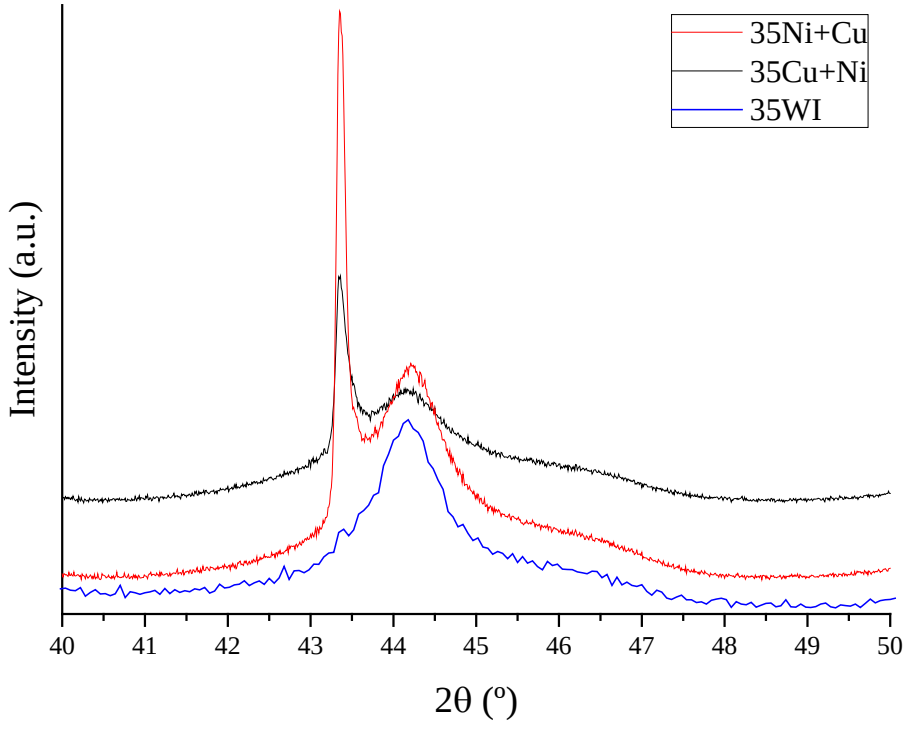

Figure A8.18. High resolution XRD profiles of the three 35% impregnation catalysts.

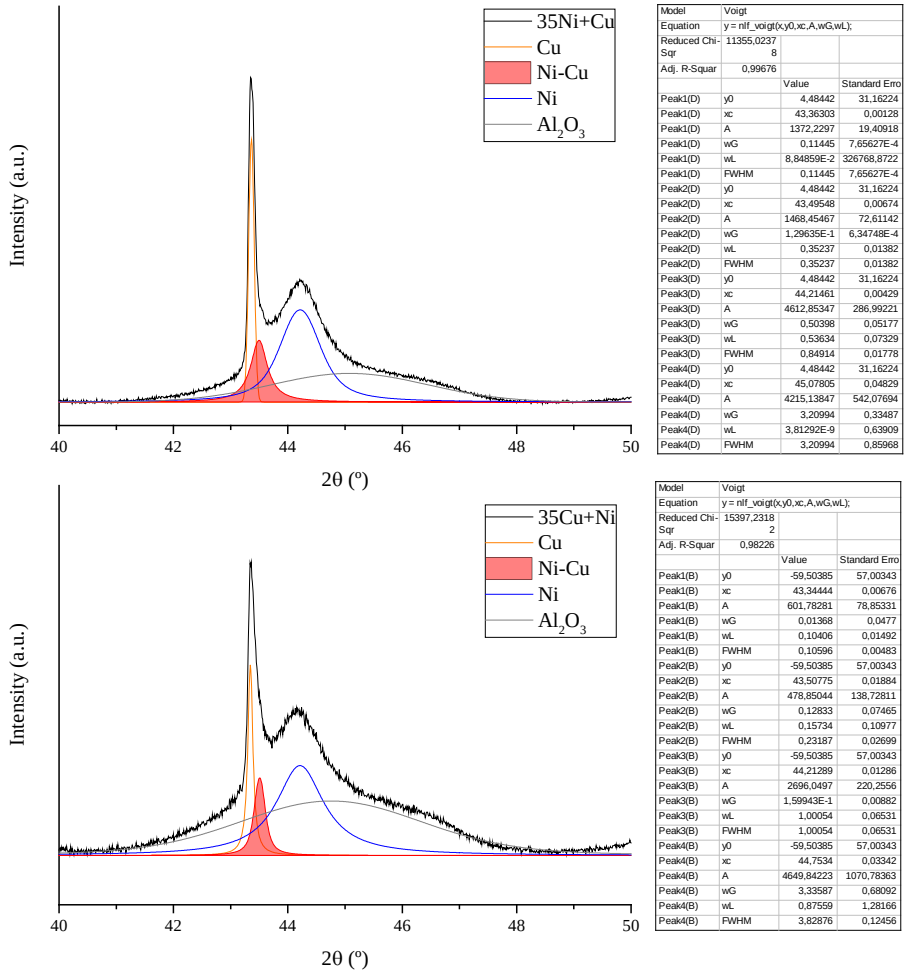

Model	Voigt		
Equation	y = nlf_voigt(x,y0,xc,A,wG,wL);		
Reduced Chi-Sqr	11355,02378		
Adj. R-Squar	0,99676		
		Value	Standard Erro
Peak1(D)	y0	4,48442	31,16224
Peak1(D)	xc	43,36303	0,00128
Peak1(D)	A	1372,2297	19,40918
Peak1(D)	wG	0,11445	7,65627E-4
Peak1(D)	wL	8,84859E-2	326768,8722
Peak1(D)	FWHM	0,11445	7,65627E-4
Peak2(D)	y0	4,48442	31,16224
Peak2(D)	xc	43,49548	0,00674
Peak2(D)	A	1468,45467	72,61142
Peak2(D)	wG	1,29635E-1	6,34748E-4
Peak2(D)	wL	0,35237	0,01382
Peak2(D)	FWHM	0,35237	0,01382
Peak3(D)	y0	4,48442	31,16224
Peak3(D)	xc	44,21461	0,00429
Peak3(D)	A	4612,85347	286,99221
Peak3(D)	wG	0,50398	0,05177
Peak3(D)	wL	0,53634	0,07329
Peak3(D)	FWHM	0,84914	0,01778
Peak4(D)	y0	4,48442	31,16224
Peak4(D)	xc	45,07805	0,04829
Peak4(D)	A	4215,13847	542,07694
Peak4(D)	wG	3,20994	0,33487
Peak4(D)	wL	3,81292E-9	0,63909
Peak4(D)	FWHM	3,20994	0,85968

Model	Voigt		
Equation	y = nlf_voigt(x,y0,xc,A,wG,wL);		
Reduced Chi-Sqr	15397,23182		
Adj. R-Squar	0,98226		
		Value	Standard Erro
Peak1(B)	y0	-59,50385	57,00343
Peak1(B)	xc	43,34444	0,00676
Peak1(B)	A	601,78281	78,85331
Peak1(B)	wG	0,01368	0,0477
Peak1(B)	wL	0,10406	0,01492
Peak1(B)	FWHM	0,10596	0,00483
Peak2(B)	y0	-59,50385	57,00343
Peak2(B)	xc	43,50775	0,01884
Peak2(B)	A	478,85044	138,72811
Peak2(B)	wG	0,12833	0,07465
Peak2(B)	wL	0,15734	0,10977
Peak2(B)	FWHM	0,23187	0,02699
Peak3(B)	y0	-59,50385	57,00343
Peak3(B)	xc	44,21289	0,01286
Peak3(B)	A	2696,0497	220,2556
Peak3(B)	wG	1,59943E-1	0,00882
Peak3(B)	wL	1,00054	0,06531
Peak3(B)	FWHM	1,00054	0,06531
Peak4(B)	y0	-59,50385	57,00343
Peak4(B)	xc	44,7534	0,03342
Peak4(B)	A	4649,84223	1070,78363
Peak4(B)	wG	3,33587	0,68092
Peak4(B)	wL	0,87559	1,28166
Peak4(B)	FWHM	3,82876	0,12456

Figure A8.19. High resolution XRD profile fitting of the 35Ni+Cu and 35Cu+Ni catalysts.

Table A8.5. Leaching metal analysis on the liquid media.

Cat	Run #	Conc. Liq. (mg/L)			Leached %		
		Al	Ni	Cu	Al	Ni	Cu
35 Ni+Cu	1	2,25	0,56	0,34	0,03	0,02	0,01
	2	0,85	1,78	0,78	0,01	0,07	0,04
				Cumulative (%)	**0,04**	**0,09**	**0,05**
20 CP	1	2,10	0,86	0,46	0,03	0,03	0,03
	2	0,52	0,69	0,83	0,01	0,03	0,09
				Cumulative (%)	**0,04**	**0,06**	**0,12**

Chapter 9

Global conclusions and future work

This presented Ph.D. thesis presents a detailed study of the LA transformation into MTHF using Ni-Cu/Al_2O_3 catalysts. The accomplishment of the initially established partial goals has led to a better understanding of this reaction, the main parameters governing the activity of the developed catalysts and, as a consequence, the achievement of some of the highest MTHF yields reported in the literature.

In this final chapter the main conclusions of each chapter are summarized and interesting ideas for future research on the topic are suggested.

Levulinic acid hydrogenolysis on Al_2O_3 supported Ni-Cu bimetallic catalysts

- Aqueous solutions demonstrated not to be a suitable medium for MTHF conversion. In water, LA rapidly reacted to GVL but its further reaction to MTHF was greatly inhibited. The main reason for this behavior was found on the significant AL production under the used reaction conditions. This molecule, AL, is prone to polymerization over acidic surfaces leading to catalyst deactivation by carbon deposition.
- Cu showed to be a less active metal than Ni. However, Ni-Cu bimetallic catalysts showed similar activity to monometallic Ni ones.

One pot 2-methyltetrahydrofuran production from levulinic acid in green solvents

- A solvent screening using a 35% Ni/Al_2O_3 catalyst showed alcohols to be a more suitable reaction medium for GVL conversion than water. In ethanol the reaction showed similar results as in water; in 1-butanol, the MTHF yield improved up to 10% and in 2-porpanol the MTHF yield reached 46%. These activity differences evidenced a strong influence of the solvent on the catalytic activity. It was speculated that the hydrogen donation capacity of 2-propanol was responsible for the high activity on this solvent.
- A catalyst composition screening, with equal total metal contents, showed important Ni-Cu bimetallic promotion effects. This effect produced an especially active catalyst (23Ni-12Cu/Al_2O_3) with similar activity for GVL conversion as Ni/Al_2O_3 but with significantly lower activity for MTHF degradation.

  • The different behavior of this catalyst was also made evident by the different MTHF ring-opening mechanism. While Ni preferentially opened the MTHF ring on the non-substituted side (producing 2-pentanol), the monometallic Cu and the 23Ni-12Cu catalyst favored the opening on the methyl substituted side (producing 1-pentanol).
- Catalyst characterization by TPR and XRD pointed to the presence of a Ni-Cu mixed phase as the active hydrogenating phase responsible for the observed high activities.

The role of the hydrogen source on the selective production of γ-valerolactone and 2-methyltetrahydrofuran from levulinic acid

- The activity of Ru(5%)/C, Ni(35%)/Al_2O_3 and Ni(23%)-Cu(12%)/Al_2O_3 catalysts was tested using three different solvents with different hydrogen donation capacities *i.e.* 1,4-dioxane, 1-butanol and 2-propanol and under inert (N_2) and reactive (H_2) atmospheres.
- Under pure CTH conditions (N_2 atmosphere) only trace amounts of MTHF were achieved with all the catalysts, indicating that higher hydrogen availabilities are required for the transformation of the stable GVL molecule. Under H_2 atmosphere MTHF yields sharply increased but with important differences among catalyst-solvent combinations.
- For the two tested atmospheres the results consistently indicated the catalyst activity order Ru/C < Ni/Al_2O_3 < Ni-Cu/Al_2O_3. In addition, the highest activities were achieved in 2-propanol followed by 1-butanol and, last, in 1,4-dioxane.
- Comparison of the results under CTH conditions (N_2 atmosphere) and under H_2 atmosphere (CTH + H_2) nicely correlated. This fact suggested that, under the applied reaction conditions, the CTH mechanism is important even under high H_2 pressures and both hydrogenation mechanisms cooperate for the conversion of GVL.
- Further experiments using 2-propanol and the Ni-Cu/Al_2O_3 catalyst showed that the solvent dehydrogenation reaction (for the CTH mechanism) did not interfere with the GVL conversion reaction. Besides, the suitability of the catalyst-solvent system to convert 5 to 30 wt% LA solutions was stated. Finally, the highest reported MTHF yield over non-noble metal catalysts (Ni(23%)-Cu(12%)/Al_2O_3) using green solvents was achieved (80%) at 250 ºC under 100 bar H_2 after 20 h of reaction.

Structure-activity relationships of Ni-Cu/Al_2O_3 catalysts for γ-valerolactone conversion to 2-methyltetrahydrofuran

- A series of impregnated catalysts with equal Ni-Cu ratios and different total metal loading showed the strong dependency of the catalyst activity on the hydrogenating and acidic active phases.
- The mixed Ni-Cu phase was found to be the most active hydrogenating phase (3 times higher STY than isolated Ni or Cu phases). Its activity, however, is heavily dependent on the presence of adjacent acid sites.
- This finding suggests that the hydrogenation mechanism of the GVL molecules requires the simultaneous interaction of this molecule with an acid and a hydrogenating site. It is suggested that GVL may adsorb on an acid site and, due to this interaction, the stability of the GVL ring is reduced facilitating, hence, the addition of the dissociated hydrogen atoms from the adjacent metal site(s).

- Co-precipitated catalysts proved to be more active than the impregnated ones due to the similar amounts of the active Ni-Cu phase present, their higher dispersion and their increased surface acidity. The combination of these factors allowed for a higher amount of adjacent active metal and acidic sites, resulting in an enhanced STY, 1.8 times higher than that of the most active impregnated catalysts.
- Reusability experiments showed progressive deactivation by carbon deposition, which could be mitigated by calcination and re-activation (reduction) of the catalyst. This strategy allowed for up to 64% MTHF yield on the first run and stable 54% after three runs.
- When the regeneration step was set at 450 ºC minor structural modifications account for the slight catalyst deactivation. When the regeneration was carried out at 600 ºC the surface acidity loss was extensive and, in accordance, so was the activity decrease.

According to the conclusions of this thesis, the following ideas are considered interesting for future research work in this topic:

- Enhancing the stability of the catalyst against carbon deposition through support modification. The tune of the acidity (Brönsted *vs.* Lewis, and the relative strength) is considered a promising way to enhance the catalyst stability. By doing so, the direct reutilization of the catalyst or its use in continuous flow reactors would be closer to potential real applications.
- Mechanistic studies in order to confirm the proposed reaction mechanism would be interesting.
- Explore the substitution of noble metals by cheaper hydrogenating phases for the aqueous phase production of MTHF. As shown by both the literature review as well as the experiments on this thesis, the conversion of GVL in aqueous media seems to require the cooperation of an active hydrogenation functionality and an oxophilic promoter. Therefore, Ni-*M*/Al_2O_3 catalyst systems (where *M* stands for W, Mo, V, *etc*.) are considered to be very promising candidates for this reaction.

List of acronyms

1-BuOH	1-butanol
1-PeOH	1-pentanol
2-PeOH	2-pentanol
2-PrOH	2-propanol
AIP	Aluminum isopropoxyde
AL	α-angelica lactone
BE	Binding energy
BET	Brunauer-Emmett-Teller
BJH	Barrett-Joyner- Halenda
boe	Barrels of oil equivalent
C	Carbon
CB	Carbon balance
CMF	5-(chloromethyl) furfural
CNT	Carbon nanotubes
CP	Co-precipitation
CTH	Catalytic transfer hydrogenation
ΔG	Gibb´s free energy variation
EDS	Energy dispersive electron spectroscopy
eq.	Equivalent
Et_3N	Triethylamine
EtLA	Ethyl levulinate
FA	Formic acid
FID	Flame ionization detector
GC	Gas chromatography
GVL	γ-valerolactone
HAADF	High angle annular dark field
HAP	Hydroxyapatite
HMF	Hydroxymethylfurfural
HTOf	Trifluoromethylsulfonic acid
HVA	Hydroxyvaleric acid
LA	Levulinic acid
LD50	Lethal dose that kills 50% of a test sample
MeLA	Methyl levulinate
MPV	Meerewein-Ponndorf-Verley
MS	Mass spectrometry
MTHF	2-methyl tetrahydrofuran
NH_3-TPD	Amonnia temperature programmed desorption
OMC	Ordered mesoporous carbon
PDO	1,4-pentanediol
RON	Research octane number
SG	Sol-gel

STEM	Scanning transmission electron microscopy
STY	Site time yield
TCD	Thermal conductivity detector
TGA	Thermogravimetric analysis
THF	Tetrahydrofuran
toe	Tons of oil equivalent
TOF	Turnover frequency
TPR	Temperature programmed reduction
U.S.	United States of America
U.S. EPA	U.S. Environment Protection Agency
VA	Valeric acid
vol%	Percentage by volume
WHSV	Weight Hour Space Velocity
WI	Wet impregnation
wt%	Percentage by weight
X	Conversion
XPS	X-ray photoelectron spectroscopy
XRD	X-ray diffraction
Y	Yield

Publications derived from the PhD Thesis:

- Obregón, I., Gandarias, I., Ocio, A., García-García, I., Alvarez de Eulate, N., Arias, P.L. *Structure-activity relationship of Ni-Cu/Al_2O_3 catalysts for γ-valerolactone conversion to 2-methyltetrahydrofuran.* Under review by Applied Catalysis B: Environmental.

- Obregón, I., Gandarias, I., Al-Shaal, M.G., Mevissen, C., Arias, P.L., Palkovits, R. *The Role of the Hydrogen Source on the Selective Production of γ-Valerolactone and 2-Methyltetrahydrofuran from Levulinic Acid.* ChemSusChem 9, 2488-2495 (2016).

- Obregón, I., Gandarias, I., Miletić, N., Ocio, A. & Arias, P.L. *One-Pot 2-Methyltetrahydrofuran Productionn from Levulinic Acid in Green Solvents Using Ni-Cu/Al_2O_3 Catalysts*. ChemSusChem 8, 3483-3488 (2015).

- Obregón, I., Corro, E., Izquierdo, U., Requies, J. & Arias, P.L. *Levulinic acid hydrogenolysis on Al_2O_3-based Ni-Cu bimetallic catalysts*. Chinese J. Catal. 35, 656-662 (2014).

Contributions to conferences derived from the PhD Thesis:

- 3rd International Symposium on Catalysis for Clean Energy and Sustainable Chemistry (Madrid, Spain, 2016)
  Poster: *Influence of the hydrogen source, molecular H_2 and in-situ generated hydrogen, in the selective production of gamma-valerolactone and 2-methyltetrahydrofuran from levulinic acid.*
  Obregón, I., Gandarias, I., Al-Shaal, M.G., Mevissen, C., Arias, P.L., Palkovits, R.

- 3rd International conference on catalysis for biorefineries (Rio de Janeiro, Brazil, 2015)
  Poster: *Reviewing the influence of the dolvent on biorefinery catalystic hydrogenation processes.*
  Arias, P.L., Gandarias, I., García-Fernandez, S., Obregón, I., Aguirrezabal-Telleria, I.

- 3rd international conference on Green chemistry (La Rochelle, France, 2015)
  Oral presentation: *2-methyltetrahydrofuran production from levulinic acid using non-noble Metal catalysts and green solvents*
  Obregón, I., Gandarias, I., Arias, P.L.